U.PORTO

FEUP FACULDADE DE ENGENHARIA
UNIVERSIDADE DO PORTO

M 2019

USE OF QUIKCAST ON THE DESIGN AND OPTIMIZATION OF A GATING AND FEEDING SYSTEM FOR A PATTERN PLATE

ANASTASIYA TSELIKOVA
DISSERTAÇÃO DE MESTRADO APRESENTADA
À FACULDADE DE ENGENHARIA DA UNIVERSIDADE DO PORTO EM JULHO DE 2019

PROF. CARLOS ALBERTO SILVA RIBEIRO

Candidato	Anastasiya Tselikova	*Código*	201407824
Título	USE OF *QUIKCAST* ON THE DESIGN AND OPTIMIZATION OF A GATING AND FEEDING SYSTEM FOR A PATTERN PLATE		
Data	23 de julho de 2019		
Local	Faculdade de Engenharia da Universidade do Porto – Sala F106 - 10:30h		

Júri	*Presidente*	Prof. Luís Filipe Malheiros de Freitas Ferreira	DEMM/FEUP
	Arguente	Prof. Hélder Jesus Fernandes Puga	DEM/UMinho
	Orientador	Prof. Carlos Alberto Silva Ribeiro	DEMM/FEUP

ABSTRACT

The present master thesis of Metallurgical and Materials Engineering was carried out with the collaboration of SAKTHI Portugal, ESI Europe, and *Análisis y Simulación*. The work was implemented in the context of development by SAKTHI Portugal of a pattern plate of a new component and its expressed interest to develop *QuikCAST* functionalities not only in the mold filling and solidification simulations, already worked by me at *Seminário* but also in core blowing simulations. The primary purposes were the development of a gating system for two and three mold cavities pattern plate of an automotive engine component as well as the optimization of the feeding system for two mold cavities pattern plate in order to decrease the predicted porosity. Beyond that, was proposed to analyze the effect of shooting pressure, nozzle dimensions and vents proportion on the predicted core defects.

In order to meet the proposed requirements, the gating system calculations were based on the continuity law and *Torricelli's* theorem. The 3D modeling of the gating system and feeding systems were made in *SolidWorks*. The mold filling and solidification simulations, as well as core blowing simulations, were done in *QuikCAST* 2018.0.

In conclusion, the porosity obtained in practice for two mold cavities was removed in simulation by using three internal chills and one extra side feeder, which reduce the yield of 59%, obtained in practice, up to 58%. Nevertheless, an increase in 10% of porosity C was predicted. In the design of the pattern plate with three mold cavities was achieved 69% of system yield. However, due to a lack of space in the pattern plate, a porosity of around 40% at the hot spot was predicted. In core blowing simulations, the nozzle dimensions, the shooting pressure and the vents proportions interfere with the density of the predicted void.

KEYWORDS

QuikCAST; Filling simulation; Solidification simulation; Core blowing simulation; Shrinkage porosity; Gating system design; Sand Casting

RESUMO

A presente dissertação de Mestrado Integrado em Engenharia Metalúrgica e de Materiais foi realizada em colaboração com o grupo SAKTHI Portugal, ESI Europa e *Análisis y Simulación*. Esta foi realizada no âmbito do desenvolvimento, pelo grupo SAKTHI Portugal, do projeto da placa molde de uma nova referência e seu interesse manifestado em aprofundar o conhecimento sobre as funcionalidades do *QuikCAST* tanto como ferramenta de simulação dos processos de enchimento e solidificação, trabalhado por mim em Seminário, como do enchimento da caixa de machos. Os objetivos iniciais foram o desenvolvimento de um sistema de gitagem para uma placa molde com duas e três cavidades moldantes do componente de motor automóvel assim como a otimização do sistema de alimentação para uma placa molde com duas cavidades moldantes com o intuito de diminuir a quantidade de porosidade prevista. Pretendeu-se verificar, adicionalmente, a influência da pressão, dimensões dos injetores e da proporção de respiros nos defeitos previstos no macho.

O projeto do sistema de gitagem foi baseado na lei da continuidade e no teorema de *Torricelli*. O *SolidWorks* foi a ferramenta de modelação 3D dos sistemas de gitagem e alimentação. As simulações de enchimento e solidificação, bem como do enchimento da caixa de machos foram realizadas no *QuikCAST* 2018.0.

Em conclusão, foi conseguido eliminar, em simulação, a porosidade obtida na prática através do uso de três arrefecedores internos e a adição de um alimentador lateral, diminuindo o rendimento de 59%, obtido na prática, para 58%. No entanto, foi previsto um aumento de 10% de porosidade C. No projeto de três cavidades moldantes, foi conseguido um rendimento de 69%. Contudo, devido à falta de espaço na placa molde, foi prevista uma porosidade de 40% no ponto quente. Nas simulações de enchimento da caixa de machos, a pressão utilizada, as dimensões dos bicos injetores e a proporção de respiros utilizados interfere com a densidade de *voids* prevista.

PALAVRAS-CHAVE

QuikCAST; simulação de enchimento, simulação de solidificação; simulação de enchimento da caixa de machos; porosidade; projeto do sistema de gitagem; fundição em areia verde

AGRADECIMENTOS

Em primeiro lugar, gostaria de agradecer ao Prof. Carlos A. Silva Ribeiro pela orientação incondicional prestada ao longo de todo a realização da dissertação, através da qual me foi fornecido todo o apoio, o saber, conselhos e críticas necessárias para a sua realização.

Um agradecimento à SAKTHI Portugal pelo voto de confiança, proporcionando-me a possibilidade de realização desta dissertação. Particularmente, aos meus orientadores empresariais, Engª Cristina Monteiro e Engº Carlos Silva. Ao Engº Carlos Silva pelo acompanhamento constante ao longo de todo o trabalho e todas as sugestões fornecidas para tal. À Engª Cristina Monteiro pela sua disponibilidade e apoio prestado. À Cristiana Maia por tratar de todas as questões burocráticas relacionadas com a dissertação.

À minha família, especialmente à minha mãe, por me proporcionarem sempre as condições necessárias e todo o apoio desde o ínico do percurso académico.

Ao Lino pelo encorajamento constante, apoio e todo a paciência prestada ao longo de todo o percurso académico.

CONTENTS

LIST OF FIGURES

LIST OF TABLES

1. INTRODUCTION

This master thesis was developed in English in order to enable its reading by ESI Group, supplier of *QuikCAST* software.

1.1. CONTEXT

Cast iron, especially spheroidal graphite cast iron is used more and more in most countries of the world due to its excellent mechanical properties and castability. Spheroidal graphite cast iron presents higher tensile strength as well as toughness when compared with malleable or grey cast irons, which become a significant advantage in structural applications.

To produce a sound casting component, the gating, and the feeding systems, which have two entirely different roles, are crucial. Gating system fills the casting, which is completed quickly. Here, several rules should be considered. Perhaps, the most complex one to fulfill, when dealing with gravity systems, is to avoid the turbulence of the surface of molten alloy. So, process parameters such as pouring time, pouring temperature, and many others should be correctly defined in order to achieve a sound casting.

On the other hand, the feeding system feeds the generated shrinkage during solidification, taking a much longer time than required by casting to solidify. Feeding is a long and slow process that is needed during the contraction of the liquid during its solidification. It is necessary due to the less volume occupation of solid than the liquid, so the difference should be provided from the feeder. Solidification contraction is the contraction where the volume deficit of the alloy can cause problems for the casting, such as porosity.

An essential aid to many foundrymen in casting defects prediction is the computer simulation of the mold filling and solidification processes. It is essential towards the design of an optimum manufacturing cycle in order to ensure the life of the final part within a prescribed accuracy. *QuikCAST* is an ESI Group software, commercialized by *Análisis y Simulación* company in the Iberian Peninsula. This software is a finite difference code able to simulate sand and die casting, being a fast solution for a full evaluation of the process. However, comparing with a finite element method (FEM), the finite differences method (FDM) as *QuikCAST* may not represent geometry quite accurately. Thus, to reach the right prediction of the solidification and porosity formation, the calculation should describe the casting phenomena in a particularly correct way. A selection of accurate parameters, as well as boundary conditions, are required in order to acquire reliable results.

Nevertheless, this task might be not so easy to achieve, especially in spheroidal graphite cast iron, which has the expansion associated with graphite precipitation. Shrinkage and porosity formation in spheroidal graphite cast iron depends on several important factors, classified in two groups: metallurgical and process conditions. The first ones play a crucial role in shrinkage formation, which in spheroidal graphite cast iron includes chemical composition and inoculation. These two factors may be included in a comprehensive factor called the degree of graphite precipitation. The process conditions affecting the shrinkage generation include molding material and mold wall dilatation. Other factors, such as pouring temperature and pouring time, have a significant influence on the shrinkage generation in spheroidal graphite cast iron.

The sand core's production is a complex process that can usually delay production, generate scrap and rework, and increase the overall cost of the casting finishing process. In order to foundries stay profitable, it is essential to optimize the core making process to keep the process control tighter while eliminating sources of wasted time and money. Therefore, the simulation of the core making process aids in understanding the causes of defects in cores. Here, *QuikCAST* has also a core blowing simulation, which predicts some core defects like voids, representing the last filled portions, that can be detected and evaluated in order to eliminate them with design changes and process parameters. These parameters, including the pressure applied during shooting, recommended areas of shooting and venting holes, the complexity of the core shape and total shot time can affect core blowing. Process modeling also requires the consideration of parameters related to the used equipment, such as the way how the pressure build-up is accomplished inside the shot cylinder. Thus, many factors must be considered in the simulation of core blowing since they affect the core blowing process itself and, afterwards, the soundness of the core.

1.2. GOALS

The present master thesis was carried out with the collaboration of SAKTHI Portugal, a Portuguese foundry which produces exclusively spheroidal graphite cast iron. The studied part is a hollow thin-walled engine component. This work was undertaken in the context of development, by SAKTHI Portugal, of a pattern plate design of a new component and its expressed interest to develop *QuikCAST* functionalities as a casting process simulation tool not only in the solidification and filling processes, but also to explore its functionalities in the core blowing simulations. Therefore, the main purposes of this thesis were:

- Development of a gating system as well as the optimization of the feeding system for two mold cavities pattern plate of a hollow thin-walled engine component, in order to decrease the experimentally observed shrinkage porosity;
- Development of the gating system for three mold cavities pattern plate for the same component;
- Analysis of the effect of the imposed shooting pressure, nozzle dimensions as well as the used vents proportion in the predicted core defects after core blowing simulation.

1.3. METHODOLOGIES

In order to meet the purposed requirements, the development of the gating system for this component was done by using the continuity law and *Torricelli's* theorem and, later, modeled in *SolidWorks*. All the improvements that were done in the gating and feeding system were also carried out in *SolidWorks.* The mold filling and solidification simulations, as well as core blowing simulations, were done in *QuikCAST* 2018.0, an ESI Group simulation software of casting processes.

1.4. DISSERTATION STRUCTURE

This dissertation is structured in five chapters: 1- *Introduction*, 2- *Literature Review*, 3- *Experimental Methods*, 4- *Results and Discussion,* and 5- *Conclusions and future developments*.

After the current chapter, comes Chapter 2- *Literature Review*, where are introduced the solidification processes of the spheroidal graphite cast iron and its influence on the formation of as-cast defects. Then, is discussed all the considerations that should be taken into account in mold filling and solidification simulations, from the preprocessing to the postprocessing parameters. For gating and feeding system, are presented the requirements that must be considered in their design. Finally, it is introduced the core blowing process and the parameters that affect it and must be considered forward in the core blowing simulation.

In Chapter 3 – *Experimental Methods*, are presented the used material and the implemented methodologies on the developed work. The carried out experimental work was based on three steps: (1) gating system design, (2) CAD modeling in *SolidWorks,* (3) use of *QuikCAST for* mold filling and solidification simulations, and (4) core blowing simulations.

In Chapter 4 – *Results and Discussion*, is present and discussed the development and optimization of the whole carried out work. In the first instance, the development and improvement of the gating and feeding system, for two and three mold cavities pattern plate are presented and discussed, according to the results obtained in the mold filling and solidification simulations in *QuikCAST*. Further ahead, are presented and discussed the results of core blowing simulations and the influence of the used shooting pressure, the nozzle's dimensions and the vents proportion on the resulted voids density in the core.

Finally, the last chapter, Chapter 5 – *Conclusions and future developments* contains the main conclusions of this work as well as some future work proposals.

2. LITERATURE REVIEW

In this initial chapter is presented, in the first instance, the solidification processes of the spheroidal graphite cast iron and its influence on the formation of as-cast defects. Then, is discussed all the considerations that should be taken into account in mold filling and solidification simulations, from the preprocessing to the postprocessing parameters. These parameters must be more detailed when spheroidal graphite cast iron is used since graphite precipitation must be assumed in order to obtain the most accurate results as possible when compared with practice. In terms of gating and feeding system design, are presented the requirements that must be considered, from the pouring time and pouring temperature to the turbulent effect that should be avoided. Finally, are introduced the core blowing process and the parameters that affect it and, therefore, must be considered in the core blowing simulation.

2.1. SPHEROIDAL GRAPHITE CAST IRON

In typical commercial cast irons, the graphite may be present in different configurations, from lamellar to spheroidal. In spheroidal graphite cast iron, graphite precipitates as spheroidal shape during the solidification of molten iron. During the transformation from liquid to solid, the structure of cast iron presents a significant effect on the formation of the solidification structure and, therefore, generation of defects [1]. Cast iron, especially spheroidal graphite cast iron is used more and more in most countries of the world due to its excellent mechanical properties and castability [2].
Due to the nodular shape of the graphite, the cutting effect of stress concentration is reduced in comparison with the flake graphite present in grey cast iron. Thus, the spheroidal graphite cast iron presents a higher tensile strength as well as toughness, when compared with malleable or grey cast irons, which become a significant advantage in structural applications [1, 3].

2.1.1. GRAPHITE NUCLEATION

The formation of spheroidal graphite takes place in two steps: nucleation and growth. The nucleation is the first step of spheroidal graphite formation [1].

2.1.2. INOCULATION

After nodularization but without inoculation, if poured, the cast iron presents a smaller number of graphite nodules. Inoculation boosts the number of graphite nuclei. Therefore, it is required in order to decrease the tendency to carbide precipitation and achieve more graphite nodules. Furthermore, it promotes the sphericity as well as the nodularity of graphite, apart from being the crucial way to increase the number of graphite nodules and improve the mechanical properties of spheroidal graphite cast iron. Figure 1 shows that inoculation influences the undercooling of the spheroidal graphite cast iron due to the presence of the remaining magnesium (Mg) in the liquid iron. Undercooling, in its turn, affects the number of graphite nodules [1].

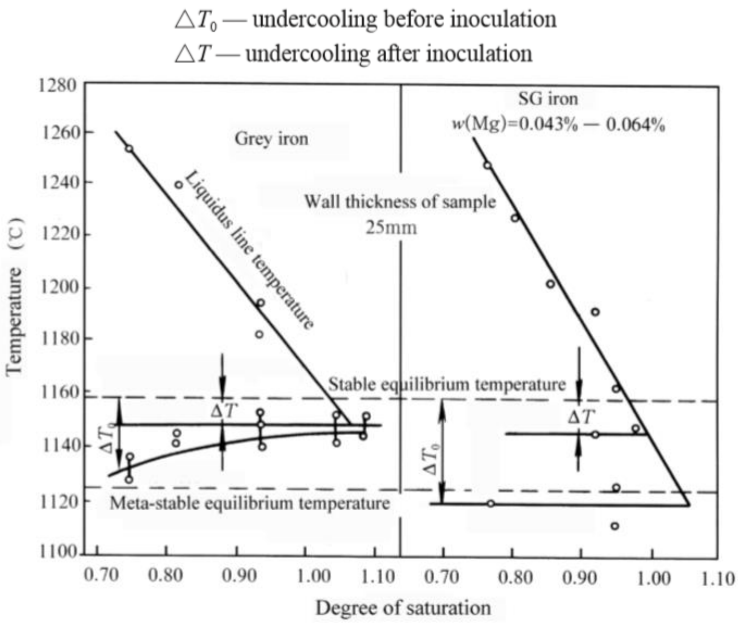

Figure 1: Influence of inoculation on undercooling of spheroidal graphite cast iron and grey iron [3]

2.1.3. GRAPHITE GROWTH

After inoculation, graphite starts to precipitate in the exogenous substrate supplied by inoculants. Its final shape depends on the growth way, which is influenced by process conditions. Therefore, its control is essential in order to obtain a high-quality cast iron [4].

2.1.4. FORMATION AND GROWTH OF AUSTENITE MATRIX

During the solidification, it is believed that at the first stage of eutectic reaction, the austenite and spheroidal graphite nucleate and growth independently of each other (divorced eutectic). Later, the graphite nodules are surrounded by austenite dendrites [1].

Primary austenite precipitation involves two stages. In the first step, austenite is growing in the melt in the heat extraction direction, either forming columnar or equiaxed dendrites. When these dendrites collide, the second stage starts, where secondary dendrites grow, perpendicularly to the first ones. Thus, the network is developed [2]. Dendrite coherency does not co-occur throughout the whole macrostructure of the casting [5]. Dendrites form a coherent structure, which prevents the melt flow between dendritic arms, increasing the risk of microshrinkage developing [6].

The austenite dendrites precipitation during the spheroidal graphite cast iron solidification plays an important role in shrinkage formation mechanism type. The macroshrinkage occurs, commonly, in gaps between the dendrite clusters, while microshrinkage often occurs between dendritic arms. It is pointed out that macroshrinkage is formed at an early stage of eutectic solidification, after the formation of dendrite frames and it is a result of solidification contraction in other regions, which draw liquid from the hot spot. On the other hand, microshrinkage is formed at the final solidification stage due to the solidification contraction of the last isolated liquid between dendrites that is not able to be fed [1].

2.1.5. Solidification morphology

The solidification morphology refers to the description of the change, distribution, and correlation of the solidification structures such as graphite and austenite. This morphology is essential because interferes with the internal quality of the casting. Through measurement of the contraction, expansion, and cooling curves of cast iron, it was studied the correlation between the solidification morphology and the shrinkage cavities, represented in figure 2. The spheroidal graphite cast iron contracts substantially in the first steps of eutectic solidification, predominantly, due to the growth of austenite dendrites. In the latest steps, it expands quickly due to the quite significant growth of graphite nodules between dendrites. Thus, through figure 3, it is deduced that shrinkage is formed during the first stages of eutectic solidification, i.e., during the austenite precipitation period. If at that moment, the compensatory liquid is provided by the feeder, a sound casting may be produced [1].

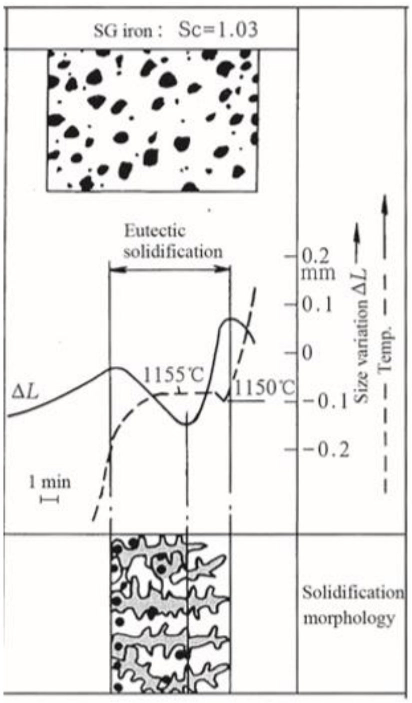

Figure 2: Relationship of solidification morphology, cooling curve and size variation curve for spheroidal graphite cast iron [3]

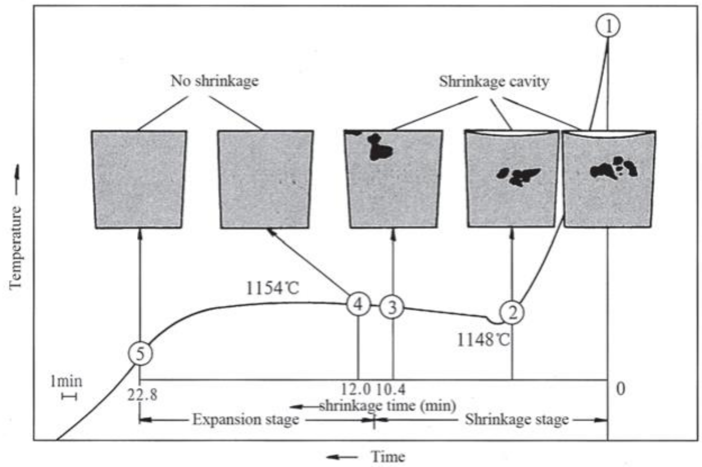

Figure 3: Formation sequence of a shrinkage cavity in spheroidal graphite cast iron [3]

2.2. COMPUTATION SIMULATION

The computer simulation of mold filling and solidification of casting has achieved a sophisticated and speed, which makes it an essential aid to many foundrymen [7].

Most of the problems in casting parts are caused by an incorrect filling of some regions or an excessive shrinkage during solidification and cooling. These factors can also introduce appreciable residual stresses, which can negatively influence the performance in service of the part [7].

The main troubles of simulating the flow of molten metal are the modeling of the turbulence character (described in section 2.3.1.). Most of the numerical approaches to these problems have been restricted to simple geometry, due to the high computational cost of this simulation. Thus, these numerical models have been mainly based on finite difference techniques, such as *QuikCAST* [7].

2.2.1. *QUIKCAST*

The *QuikCAST* is an ESI Group software, commercialized by Análisis y Simulacion company in the Iberian Peninsula. This software is finite difference code, able to simulate most casting processes ranging from gravity sand casting to high and low-pressure die casting. Initially, it has been created by a foundry professional from Aluminum Pechiney in 1985 as *SIMULOR*. This software is an easy and fast solution to approach the principles of any casting process [8]. Although being fast, in comparison with finite elements method (FEM), finite differences method (FDM) might represent the geometry not very accurately [9].

2.2.2. OPERATIVE MODE

Simulation software based on Finite Differences Method (FDM) presents the advantage of being easy to use. Once the mesh consists of simple rectangular cells, the meshing process becomes a simple task. Nevertheless, the geometry is not represented very accurately, especially when the casting has complex thin walls. Commonly, uniform cell size is used, which can result in many cells if the casting includes both thin and thick sections [9].

Computer simulation of casting consists of three steps. The first one is preprocessing, followed by running the simulation and, finally, postprocessing.
Preprocessing is the most critical step to achieve success in a simulation because this is the step where computer modeling is built for a given casting process. This stage consists of multiple steps: building geometry, meshing process, defining material properties, specifying initial and boundary conditions, choosing simulation control parameters, and many more.

Running simulation involves carrying out the calculations done in the first step as well as monitoring the results.

The final step, postprocessing, is the step of recovering and processing of the simulation results [9].

2.2.2.1. PREPROCESSING

To reach the right prediction of the solidification and porosity formation, the observed phenomena should be described in a particularly correct way [2].

A selection of accurate parameters, as well as boundary conditions, are required in order to acquire reliable results. Nevertheless, this task might be not so easy to achieve, especially in spheroidal graphite cast iron, which has the expansion associated with graphite growth effect. This graphite expansion is an outcome from precipitation, and it is directly connected to inoculation practice, which is very difficult to keep constant along the production process. Although this effect occurs, it is difficult to predict it [9,10]. In the simulation of the solidification process of spheroidal graphite cast iron, it is assumed that eutectic grains are formed under eutectic temperature and their growth rate is controlled by carbon diffusion through the already formed austenite shell. This effect may be not correct since there are elements that influence the undercooling and partition coefficient of most critical elements sulfur (S), magnesium (Mg) and silicon (Si) so the definition of chemical composition and inoculation practice are crucial [2].

Shrinkage and porosity formation in spheroidal graphite cast iron depends on several important factors, classified in two groups: metallurgical and process conditions. The first ones play a crucial role in shrinkage formation, which in spheroidal graphite cast iron includes chemical composition and inoculation. These two factors may be included in a comprehensive factor called the degree of graphite precipitation. The definition of the chemical composition is essential because the segregation of the alloying elements is calculated by the lever rule or by modifying the *back diffusion* model, depending on the diffusion rate of the atoms in austenite. As the primary and eutectic austenite precipitation is calculated, the undercooling is influenced and, consequently, the nucleation rate of graphite is influenced as well [2]. In the simulation preprocessing, the inoculation is defined as a graphite precipitation degree, explained further in section 2.2.2.2.

Process conditions that affect shrinkage generation include molding material and mold wall dilatation. Other factors such as pouring temperature and pouring time have a significant influence on the shrinkage generation in spheroidal graphite cast iron. Although being complicated, there are many ways that directly or indirectly allow measuring the graphite precipitation degree, like metallographic analysis or thermal analysis [10].

In spheroidal graphite cast iron, the effect of mold material and expansion of mold walls are more appreciable than in other alloys. So, it is crucial to consider it while assigning the postprocessing conditions in the simulation. The mold walls dilatation depends, among several factors, on the molding material itself. Except for the static pressure of liquid metal, the expansion forces due to the precipitation of graphite act on the molding sand. If the molding sand is weak, as in some low-pressure green sand molds, and the expansion is high enough, the mold wall may move. This volume increase during the solidification of spheroidal graphite cast irons is inevitable and increase the probability of shrinkage in casting [4].

Due to the solidification characteristics of spheroidal graphite cast iron, for early stages of solidification, the metal wall is weak, and the expansion force caused by the graphite precipitation is appreciable. If the mold is tough enough, the casting cannot expand and, therefore, the liquid metal could be transported to the existing porosity, obtaining a sound cast. The high-density green sand, such as from DISA machines, are typical of high strength green sand. On the other hand, if the mold material is soft enough, like the green sand, the casting will expand and, thus, the already existing porosity cannot be filled again . Thus, it is necessary to design a feeding system able to form a sound cast, without shrinkage presence [4].

I. BUILDING GEOMETRY

The geometries for the casting process include the casting, gating and feeding system, mold and solidification aid (if applicable). All the element, except the mold, are all modeled in CAD software and imported in *QuikCAST* as *.igs* or *.stl* model. The mold can be defined in *QuikCAST* itself by using a basic shape, which is a parallelepiped [9]. First of all, it is crucial to check the imported geometry in order to detect some CAD defects. It is essential to point out that the imported geometry must be as simple as possible. For instance, several numbers or letters present in the CAD model must be removed in the 3D model before being imported to *QuikCAST*, since they may produce some intersection and defects on it. After checking the imported geometry, there is a way to *auto-correct* all the detected defects and intersections. However, sometimes, this option may not be enough to get rid of all of them. Thus, in advanced options, there is a manual way to rectify some of them. Nevertheless, even doing so, the problem may be not fixed. In this case, the removal of all detected defect must be done directly in the CAD modeling software like *SolidWorks*.

II. MESHING

Commonly, the casting has complex geometry. Meshing such a part should be correctly done since the quality of the mesh affects not only the accuracy of the result obtained afterwards in postprocessing parameters, but also the stability and convergence of the calculated solution. Commonly, the higher the mesh density (more elements and nodes for a given volume), the higher is the simulation accuracy. However, this also means a significant increase in CPU time, memory and storage space. Therefore, the establishing of a minimum mesh density, required to ensure a reliable and stable numerical solution is crucial [9].

Once the meshing is done, its checking is required (using a coarse *mesh* scheme) in order to evaluate its integrity. If some mesh problems are detected, there is a simple way to correct them, by using the *auto-correct* option. However, sometimes, this is not enough to correct them. So, in advanced options, there is a manual way to do so. Nevertheless, when this option cannot delete the mesh defects, an increase of mesh size may be used in order not to allow the *QuikCAST* to detect them and, thus, proceed with the simulation.

III. ASSIGNING MATERIAL PROPERTIES

The properties of the materials can be individually defined for each element. The materials properties related to fluid and heat transfer include thermophysical properties, such as density, specific heat, thermal conductivity, viscosity, thermal expansion coefficient, surface tension coefficient and latent heat of fusion. These properties, in a conventional way, are temperature and chemical-dependent. The simulation software database includes several types of materials, where some properties can be modified [9].

IV. SPECIFYING INITIAL CONDITIONS

In this stage, several conditions are defined, such as initial metal position and initial temperature [9]. In *QuikCAST* are assigned different initial temperatures to different elements.

V. SPECIFYING BOUNDARY CONDITIONS

The boundary conditions are, usually, more complicated than the initial conditions. In the solidification simulation, only thermal conditions should be defined. However, when a mold filling and solidification simulation is required, both thermal and fluid flow conditions should be assigned. The difference between both simulation types will be explained later in this chapter. By using *QuikCAST* for simulating a gravity sand casting process, the most critical conditions to be assigned in thermal conditions is the mold exterior walls. For fluid flow conditions, the most important ones are the inlet position, permeability, and region roughness [9].

The mold exterior walls may be defined by a constant temperature (in temperature conditions) or a constant heat flux (in heat exchange conditions). The inlet position should be defined on the top of the pouring cup. Here there is the possibility to specify the mass flow rate from a given fill time and temperature, as shown in section 3.3. The permeability condition is defined by all the element in contact with the mold by choosing the used sand or by introducing the permeability factor. For all the same elements is assigned the region roughness condition, which depends on the mold material as well [9].

VI. SELECTING SIMULATION CONTROL PARAMETERS

Simulation control parameters include, among others, total simulation time, time step size control variables, convergence criteria, frequency of results output. These parameters influence the solution accuracy, stability, and computational efficiency. It is essential to point out that the total simulation time does not represent the computer CPU time spent in the simulation, but the operation time in the casting process spent in real practice for mold filling and solidification processes. [9].

2.2.2.2. GRAPHITE PRECIPITATION DEGREE

According to section 2.2.1., the graphite precipitation degree and, consequently, its expansion depends on the chemical composition and inoculation. As in this work, the used alloy is spheroidal graphite cast iron, the inoculation is the parameter that will be changed by modifying the graphite precipitation parameter (P), available in preprocessing parameters of *QuikCAST*. This parameter allows considering the expansion caused by graphite precipitation in the solidification simulations. It changes from 0 to 1, where 0 represents the lowest graphite precipitation, and 1 represents the maximum expansion caused by the graphite precipitation. Therefore, the density prediction curve, calculated by the software, will be continuously changed in order to allow higher (values close to 1) or lower (values close to 0) expansion [4, 11].

By default, *QuikCAST* imposes a solid diffusion model as *scheil*. This approach is close to equilibrium solidification and considers that the solidification of different liquid portions, with temperature decrease, occurs with distinct chemical compositions. Nevertheless, the solidification of spheroidal graphite cast iron is not so uniform as in other alloys due to graphite precipitation [12]. Furthermore, phase transformation in cast iron is highly dependent on the kinetics and, thus, also strongly influenced by the cooling rate [2]. Therefore, it is required the use of another solid diffusion model in order to consider this effect. *Back diffusion* model plays a vital role in solidification kinetics, which influences, e.g. the final solidification temperature. This model is fundamental to use in spheroidal graphite cast iron simulations, because this model consider the expansion caused by graphite growth. *Back diffusion* model is present in *QuikCAST* and allows the consideration of the present graphite precipitation degree by changing the graphite precipitation parameter (P) described above [13].

2.2.2.3. MICROSTRUCTURE EVOLUTION

Castings may be produced with a considerable variety of dimensions, from a few millimetres up to some meters in length. As the microstructure of the casting determines its properties, it is crucial to analyze it [9].

A simulation where only heat transfers are calculated is called solidification simulation. Here it is assumed that the mold cavity is initially filled with liquid metal at a constant temperature [9]. This simulation type does not incorporate fluid flow and assumes that once the mold is full, the temperature is uniform across the whole mold cavity. In this case, lower cooling rates are predicted when the flow is not taked into account. This assumption is a source of a significant error, particularly for casting with great variations in section size, as well as for several mold cavities. Therefore, a simulation where the filling of the mold cavities is involved is required. This simulation type is called mold filling and solidification simulation. Here, the position of the liquid metal, imposed in the initial conditions, is defined as being zero since mold cavities are empty before pouring. In *QuikCAST,* this is easily achieved by assigning the metal position, in terms of percentage, of a given element [9]. So, to generate the most accurate defects prediction, a mold filling and solidification simulation are required because this type of simulations considers not only mold filling phenomenon but also generates the most accurate and comprehensive information about the casting process [9].

Once solidification is the process of moving individual atoms from the liquid to a more stable position in the alloy lattice, the solidification on the casting must be analyzed at three different levels: macroscale, microscale, and nanoscale. These simulations can easily encompass macroscopic models such as a turbulent flow and mass transportation, as well as microscopic models, such as solidification kinetics by using the *back diffusion* as a solid diffusion model [9].

2.2.2.4. POSTPROCESSING

This step includes in the first instance, the visualization of the simulation results and, later, their analysis in order to provide a better understanding of a given casting process and predict defects formation [9].

2.3. GATING SYSTEM DESIGN

The gating system design plays a crucial role to produce a sound casting. Therefore, in the present section are represented several factors to consider when the desired pouring rate for a given gating system is decided [14]. The calculation methodologies to gating system design are presented, forward, in section 3.1.

2.3.1. TURBULENCE

Perhaps, the most complicated rule to fulfil when dealing with gravity systems is to avoid the turbulence of the free flow surface of the molten filling alloy. This rule is the requirement to liquid metal front goes not too fast, with a maximum velocity of around 0.5 $m.s^{-1}$ at the entrance of the mold cavity. However, this velocity may be increased up to 1.0 $m.s^{-1}$ when the casting presents thin sections [6]. Another reason to hold the velocity limit below the critical value is to ensure that in green sand systems, the sand resists erosion when the gating system is filled [14].

Gating systems usually incorporate the use of large runners in order to decrease the metal velocity and afford time for the slag to be separated from the molten metal before entering the mold cavity. This reduction in turbulence will ensure that separation of the nonmetallic inclusions occurs in the gating system [14].

The velocity reduction may also be achieved by the progressive enlargement of the area of the flow channels at each stage (unpressurized system), which progressively reduces the flow rate. Nevertheless, this section reduction may not be able to fill the whole mold cavity [6]. Therefore, a naturally pressurized system (with a gating ratio to choke area: runners: gates of 1: 1.1: 1.2) is an option between pressurized (1: 0.8: 0.6) and unpressurized (1: 2: 4) systems. Comparing with the pressurized system, the natural one is better because it keeps the velocity below critical 0.5 $m.s^{-1}$. On the other hand, comparing with an unpressurized system, the naturally pressurized one ensures that the system is filled [6].

2.3.2. POURING TEMPERATURE

Pouring temperature is critical since it influences the solidification processes, and it depends on several factors. The ability of the molten metal to continue to flow while it loses temperature and even during the start of solidification is a valuable feature of the casting process [6]. Increasing pouring temperature may directly benefit fluidity if no oxidation occurs but may increase the problem of sand burn. All fluidity investigations have confirmed that the fluidity increases linearly with the superheat (defined as the excess of casting temperature over liquidus temperature), as shown in figure 4. The effect of superheat is, therefore, valuable. In terms of casting alloys, the fluidity is defined as the maximum distance to which the metal will flow in a standard mold [6].

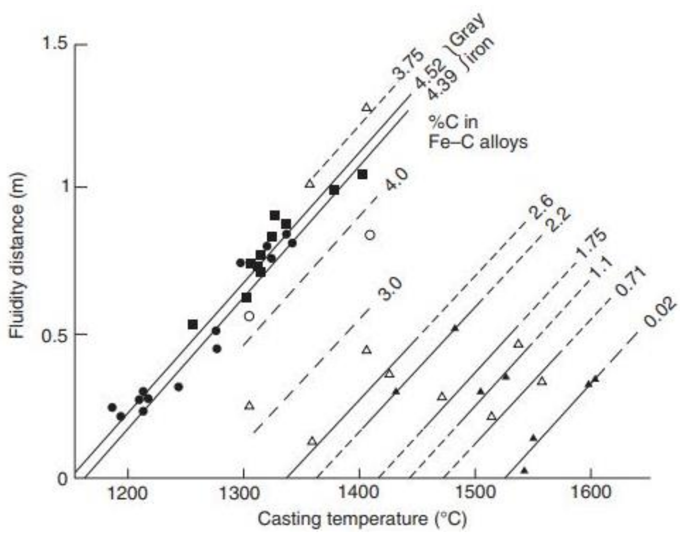

Figure 4: Effect of temperature and carbon content on the fluidity of Fe-C alloys [4]

Fluidity depends not only on the temperature but also on %CE (equivalent carbon content), and another present element like phosphorous. For cast iron, according to figure 5, the fluidity reaches its maximum for eutectic composition [6]. Furthermore, for spheroidal graphite cast iron, increasing pouring temperature, the solidification time increases, which increases the specific contraction of the alloy. This parameter increases the porosity generation [15, 16].

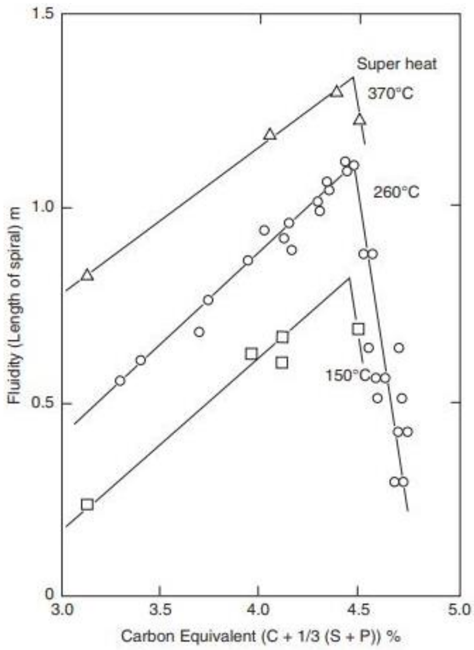

Figure 5: Effect of composition of Fe-C alloys and superheat on its fluidity [4]

2.3.3. POURING TIME

Perhaps, the most crucial factor to consider in the gating system design is the pouring time. Low pouring time causes an excessive velocity of the molten metal. On the other hand, such a long time produces premature solidifications [17].

Pouring time should be established considering that it is necessary to fill the mold before solidification starts in its thinnest section and that the ingate velocity of 0.5 $m.s^{-1}$ should be assured to avoid turbulence [17].

2.3.4. SPRUE GEOMETRY

In gravity filled, to reduce bubbles in the liquid stream during the filling of the molding cavities in the gating system, the sprue should be tapered in order to avoid the entrainment of air [6].

2.3.5. EFFECT OF CHILLS

The action of chills increases localized cooling of the casting in order to aid directional solidification towards the feeder, which may lead to porosity reduction in spots where they are placed at [6].

Usually, the used chills in sand castings are made of iron, which has a higher density and thermal conductivity than the mold material. Chills can be made of several different materials, such as iron, aluminum, copper, bronze, and many others.

There are external and internal chills. External chills are placed on the edge of the mold cavity, while internal chills are placed inside the mold cavity. When the cavity is filled, a chill portion melts and becomes part of the casting, an important factor to consider in the moment of material selection [6].

2.4. FEEDING SYSTEM DESIGN

Commonly, the gating system, in comparison to the feeding system, is not required to provide any significant feeding. These two ones have two entirely different roles. The gating system fills the casting, which is completed quickly. On the other hand, the feeding system feeds the shrinkage during solidification, taking a much longer time that the casting requires to solidify [6].

Feeding is a long and slow process that is needed during the contraction of the molten metal during its solidification. It is necessary due to the less volume occupation of solid than the liquid, so the difference should be provided from the feeder. This contraction on solidification is a consequence of liquid being a structure resembling a random close-packed array of atoms in comparison with the solid, presenting a denser regular close packing in a structure, called crystal lattice [6].

Three separate stages of contraction occur during the solidification down of liquid metal to room temperature, as represented in figure 6. Nevertheless, in section 2.1.5 was explained that this behavior is typical for all alloys, except the spheroidal graphite cast iron, which has a distinct solidification process, according to figure 2. The solidification contraction should be considered, once being the contraction where the volume deficit can cause problems for the casting such as porosity. If for some reason, the molten metal to feed cannot be supplied quickly, the contraction starts occurring in casting on the surrounding solid [6].

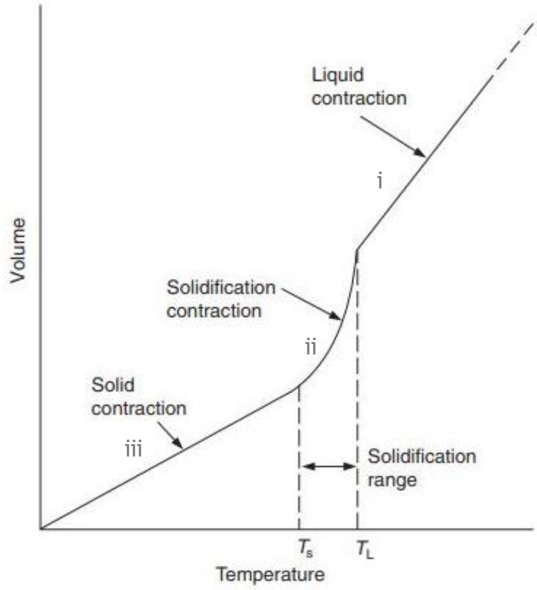

Figure 6: Illustration of three shrinkage stages in the most alloys:
(i) in the liquid; (ii) during solidification and (iii) in the solid [4]

Many requirements should be fulfilled at the feeding system design to prevent porosity formation in the casting. In the first instance, the feeder should be placed on a chunky casting that requires the feed metal in order to avoid some significant shrinkage problems. Beyond that, feeder's height should be enough in order to enable enough metallostatic pressure to prevent subsequent pore formation in the casting [18]. Thus, increasing the feeder size in proportion to the casting may decrease the resulting porosity and, at the same time, results in a decrease of system yield, which in practice is a drawback that is considered. Although there are concerns about the overfeeding of the casting. Figure 7 illustrates that an oversize feeder is far less damaging than an undersized feeder and, beyond that, shows that if no feeder is used, then 7% of shrinkage may be expected.

Nevertheless, as the feeder size increase in proportion to the casting, the resulting porosity decrease and reach the minimum at feeder-to-casting modulus ratio at around 1.25. The porosity at this minimum depends on the gas content. At zero gas, is expecting a sound casting. However, at higher gas levels, the porosity increases, but not in such high proportions as for feeder-to-casting modulus ratio below 1.25 [6].

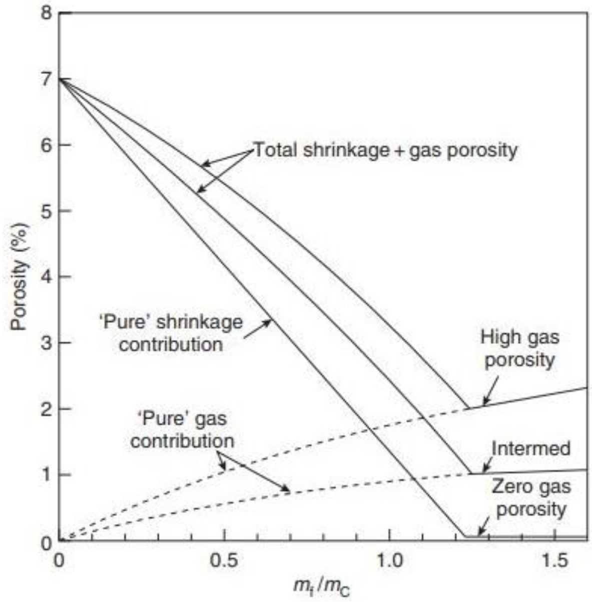

Figure 7: Generalized relationship between gas and shrinkage with increasing of feeder mass (mf) in relation to the casting mass (mc) [4]

2.4.1. THERMAL MODULUS

Thermal modulus, defined as the ratio 'volume/area cooling rate' of a casting part, is used as a conventional method for feeder system design. Thermal modulus can be reached through the solidification simulation of the casting isolated in the mold. Here, the larger values of thermal modulus, so-called hot spots, consist in the last sections to be solidified and, therefore, the possible obtained porosity will be located there. So, the feeders should be placed close to these spots [6].

2.4.2. HEAT-TRANSFER REQUIREMENT

The *Chvorinov*'s heat transfer requirement for an efficient feeding system may be announced as "the feeder must solidify at the same time as, or later than, the casting itself". Therefore, to ensure this rule, it is essential to the feeder has a larger modulus than the casting [6].

2.4.3. VOLUME REQUIREMENT

The volume rule states that the feeder must contain enough liquid to meet the liquid volume-contraction condition of the casting. This rule can be confused with the previous one. However, when ensuring the higher modulus in the feeder, it is not assured that its size is suitable to compensate the shrinkage, and do not enable it to diffuse at the casting itself. Furthermore, the macroshrinkage cannot pass from the feeder neck, in order to ensure a sound casting [6].

2.5. CORES PRODUCTION AND ITS SIMULATION

In order to foundries stay profitable, it is essential to optimize the core making process in order to keep the process control tighter while eliminating sources of wasted time and money [19]. The sand core's production is a complex process that can usually delay production, produce scrap and rework, and increase the overall cost of the casting finishing process [19]. Generally, the manufacturing of sand cores is made using chemically bonded sands in two stages. Firstly, sand is blown into a core box at high pressure and speed. The blowing process is driven by the release of a high-pressured air cartridge. A catalyst or hardening gas is then passed through the core box to harden and cure the sand [20].

The core production optimization process consists of the selection of working parameters of filling the core-making machine, compaction of molding sands as well as methods of sands hardening [21]. Process parameters, including the pressure applied during shooting, recommended areas of shooting and venting holes, the complexity of the core shape and total shot time may affect the core blowing process [19, 21].
Some defects on the core, such as poor sand compaction, low strength, and poor surface finish may be produced after the core manufacturing process. These common core defects may form a large proportion of scrap rates in the casting industry. Thus, numerical simulation solutions provide reliable information in order to improve core blowing process parameters and achieve a cost-effective quality core production [20]. The flow behavior of a granular solid is quite different from a liquid. Thus, the physical-mathematical models required to simulate the core shooting process are distinct from those used to simulate the flow of a liquid [19].

Many factors must be considered in the simulation of core blowing since they affect the core blowing process itself and, afterwards, the defects present in the core. The vents allow the evacuation of air during blowing and of gas during gassing, so they are essential to consider in order to obtain reliable results [20]. In core blowing simulation, voids inside the core, representing the last filled portions, can be detected and evaluated. Once identified, they can then be eliminated with design changes and process parameters [19]. Therefore, the simulation of the core making process aids in understanding the causes of defects in cores and provide information in order to improve the setup core box layout and process parameters that impact quality cores. As a result, for foundries, the core production simulation improves casting quality and reduce overall production costs.

Process modeling also requires the consideration of parameters related to the used equipment, such as the way how the pressure build-up is accomplished inside the shot cylinder. The nozzles connect the toll of core making with the core shooting equipment. Commonly, a multitude of nozzle geometries may be used. Small changes in the nozzle locations may have a significant impact on the dynamics of the core shooting process and expected core quality. Beyond that, distinct nozzle geometries lead to distinct flow characteristics, such as sand velocities and efficiency of shot sand masses. Wherefore, nozzle configuration and gas pressure influence gas flow through the core sand [22].

3. EXPERIMENTAL METHODS

In this chapter are presented the used material, and the implemented methodologies during the work. The used material for mold filling and solidification simulations was a hollow thin-walled engine component as-cast spheroidal graphite cast iron EN-GJS-500-7. For the core blowing simulations, was used sand core, which is implemented in practice to produce the hollow section of this engine component. The implemented experimental work was based on three steps: (1) gating system design, (2) CAD modeling in *SolidWorks*, use of *QuikCAST* in (3) mold filling and solidification simulations and (4) core blowing simulations.

The developed methodologies for calculating the design of the gating system were based on Torricelli's law and continuity law. The design of the gating system in *SolidWorks*, as well as the correct way to do it before importing the model to the QuikCAST, are also described in this chapter. All the defined preprocessing parameters used in all the mold filling and solidification simulations, and all the core blowing simulations are also listed.

The analyzed hollow thin-walled engine component, represented in figure 8, is as-cast spheroidal graphite cast iron EN-GJS-500-7, whose chemical composition is represented in table 1. The minimum thickness of the casting is 4.5 mm. The pouring temperature, in practice, varies between 1375°C and 1400°C.

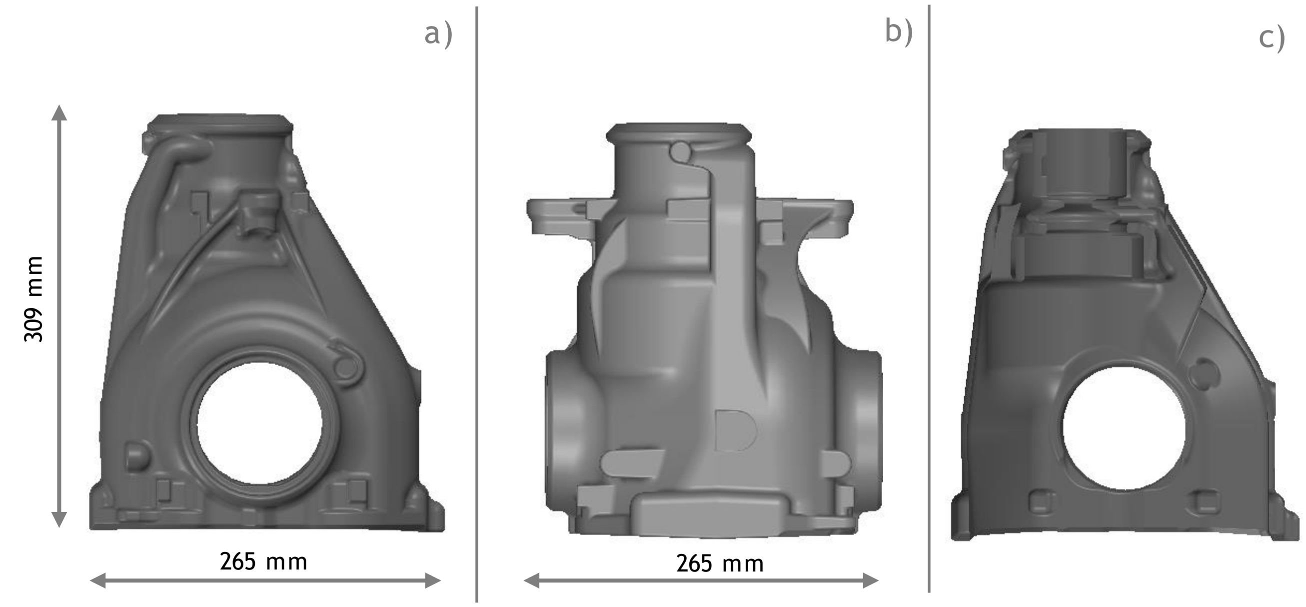

Figure 8: Hollow thin-walled engine component produced by SAKTHI Portugal a) front view; b) left view; c) cut section

Table 1: Reference base target chemical composition of the used alloy

Element	C	Si	Mn	P	S	Mg	Cu
Content (%)	3.54	2.56	0.399	0.014	0.006	0.032	0.117

3.1. GATING SYSTEM DESIGN

For the gating system design, in the first instance, the pouring time t was calculated using the equation (1), where K represents the fluidity, calculated through equation (2), T is the average thickness (in inches) and W is the casting weight (in pounds) [17]. Equation (2), Tp represents the pouring temperature and CE is the carbon equivalent calculated through equation (3), where $\%C$ represents the alloy's carbon content, $\%Si$ is the silicon content and $\%P$ is the phosphorus content [3, 17].

$$t = K \times (0.95 + \frac{T}{0.853}) \times \sqrt{W} \tag{1}$$

$$K = \frac{(14.9 \times CE + 0.05 \times Tp - 155)}{40} \tag{2}$$

$$CE = \%C + \frac{\%Si + \%P}{3} \tag{3}$$

Firstly, for the gating system calculation was calculated the choke area through equation (4). Here, c represents the loss coefficient of the gating system, t is pouring time, g represents the gravity acceleration (9.81 $m.s^{-2}$), mdrag and mcope represent, respectively, the drag mass and the cope mass, h is the cope height and, finally, hc represents the height of casting above parting plane including feeders. This equation is only applicable in those cases where casting is placed in both parts of the mold, i.e., in drag and cope [23].

$$A = \frac{1}{c \times t \times \sqrt{2g}} \times \left[\frac{mdrag}{\sqrt{h}} + \frac{1.5 \times hc \times mcope}{\sqrt{h^3} - \sqrt{(h-hc)^3}}\right], \qquad hc < h \tag{4}$$

The gating system calculations were based in two laws, the continuity law represented at the equation (5) and Torricelli's theorem represented at the equation (6). The continuity law, represented at equation (5), states that the flow rate is the same at all points in the system, where Q represents the flow rate, $V1$ represents the fluid velocity in section 1, $\mathrm{V2}$ is the fluid velocity in section 2 [6, 24]. In the Torricelli's theorem, equation (6), Vi represents the velocity in the section i, g represents the gravity acceleration (9.81 $m.s^{-2}$), and hi represents the height of fluid in the section i above the pouring [6]. To obtain the velocity at the top of the sprue was used the continuity law, based on the zero velocity on the top of the pouring cup. Afterward, the velocity at the choke was obtained using the same methodology, and then the area on the top of the sprue well was achieved.

$$Q = V1 \times A1 = V2 \times A2 \quad (5)$$

$$Vi = (2 \times g \times hi)^{0,5} \quad (6)$$

For the calculation of runner's and gate's area, the already calculated choke area was used referring to the natural pressurized system with the respective relationship of 1: 1.1: 1.2, as explained in section 2.3.1. According to the number of runners and gates was calculated the area of each runner and gate. Afterwards, using the relationship of height/width for runner's area of 1.5 and the gate's area of 0.25 were obtained the respective dimensions [6].

The calculation of yield for the gating and feeding system was done used the equation (7), where $mass\ (casting)$ represents the mass of all produced castings and $mass\ (casting + gating\ system + feeding\ system)$ is the total mass of whole gating and feeding system as well as the casting.

$$Yield\ (\%) = \frac{mass\ (casting)}{mass\ (casting + gating\ system + feeding\ system)} \times 100 \quad (7)$$

In this case, are used some mold cavities per each parting plate. Thus, it is crucial to calculate the pattern yield by equation (8), where $area\ (casting + gating\ system + feeding\ system)$ represents the area filled by the casting as well as gating and feeding system in the pattern, and $area\ (pattern\ plate)$ is the pattern area.

$$Pattern\ yield\ (\%) = \frac{area\ (casting + gating\ system + feeding\ system)}{area\ (pattern\ plate)} \times 100 \quad (8)$$

3.2. CAD MODELING

All the components were designed in *SolidWorks*, a 3D modeling software. The whole gating system was designed as being a *part*. Afterwards, using an *assembly*, all the components, including the casting, gating and feeding system, chills, and insulation sleeves, were placed in their correct position. Here is crucial to get different *parts* for all the components with different materials, because once all the *assembly* is imported to *QuikCAST*, every single part will be assigned with the respective material. Therefore, chills, insulation sleeves, and all the casting should be modeled as separated *parts* in *SolidWorks*. After modeling all parts and join them in an *assembly*, the model should be exported as a *.igs* file or *.stl* file in order to import the geometries to *QuikCAST*.

3.3. SIMULATIONS

3.3.1. THERMAL MODULUS

Feeders should be positioned at the casting hot spots, sections with higher thermal modulus. To have a notion of their values in order to determine the localization of feeders was carried out a solidification simulation of the casting isolated in the mold. All the assigned preprocessing parameters, boundary condition, and simulation control parameters are represented in table 2. Figure 9 represents the casting and the mold after meshing.

Table 2: Preprocessing parameters defined in *QuikCAST* in solidification simulation to obtain the thermal diagram of the casting

Preprocessing parameters		
Gravity vector magnitude	$9.80\ m.s^{-2}$	
Mesh size	Casting	1.7 mm
	Mold	2 mm
Material	Casting	EN-GJS-500-7
	Mold	green sand
Initial Temperature	Casting	1390°C
	Mold	20°C
Graphite precipitation degree	0.75	
Boundary conditions		
External temperature	20°C	
Simulation control parameters		
Convection time step acceleration factor	3	
All the remaining simulation control parameters were kept as default		

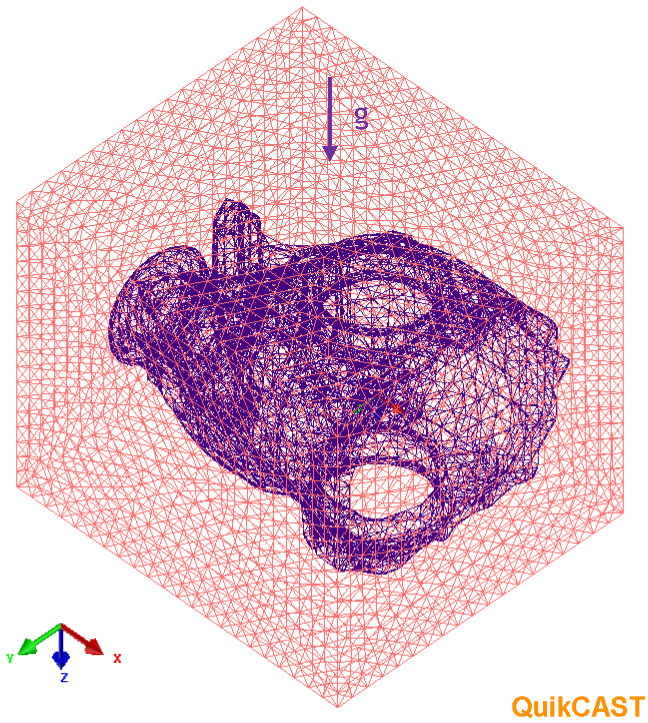

Figure 9: Casting and the mold after meshing in QuikCAST, with the gravity vector used to evaluate solidification modulus of casting

3.3.2. MOLD FILLING AND SOLIDIFICATION SIMULATIONS

To simulate the casting with its gating and feeding system were made seven different approaches for two mold cavities pattern plate, and five different approaches were carried out to three mold cavities pattern plate, as represented in table 3. Apart from these simulations, were done additionally three mold filling and solidification simulations to evaluate the difference between system A and B and the effect of pouring temperature on the predicted porosity. According to the whole developed and discussed work in chapter 4, in total, fifteen mold filling and solidification simulations were carried out. All the considered process conditions were always the same, as explained afterward in this section.

Table 3: Representation of all carried out mold filling and solidification simulations

Mold cavities	**2**							**3**				
Approach number	1	2	3	4	5	6	7	1	2	3	4	5

Firstly, all the elements were meshed, as shown in figure 10, with the imposed direction of gravity vector with a magnitude of 9.80 m.s^{-2}. The defined mesh size was 1.7 mm for the casting and the gating and feeding system. For the mold, was defined a mesh size with 2 mm. For all the remaining elements, a 1 mm mesh size was imposed.

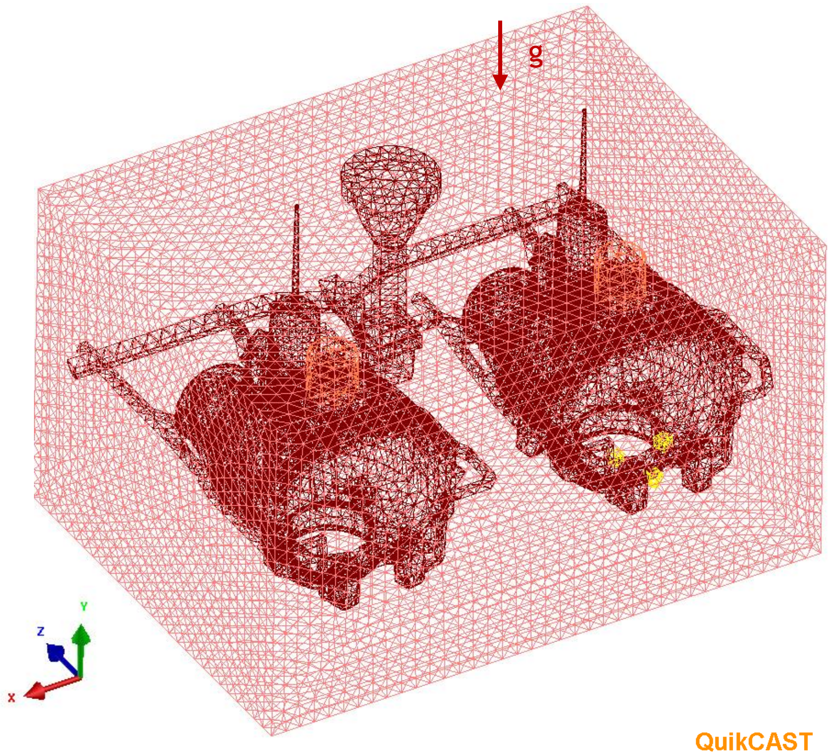

Figure 10: Gating system, feeding system, and castings in two mold cavities pattern plate design after meshing in QuikCAST, as well as the gravity vector

The casting material was spheroidal graphite cast iron EN-GJS-500-7, as in the previous simulation. Furthermore, in this step was considered the graphite precipitation degree of 0.75. For the insulation sleeves was established *Foseco* brand ones. Green sand was imposed to the molding material. In that simulation where chills were used, the defined material was the same as for the casting, spheroidal graphite cast iron EN-GJS-500-7. The initial temperature defined for all the materials was 20°C. The initial filling percentage for the casting as well as the feeding and gating systems was 0% since at this point the mold cavities are empty. For the mold, insulation sleeves and chills, a 100% filling percentage was imposed. All these conditions are shown in figure 11. Afterwards, for thermal process conditions, only the exterior mold boundary was defined with a temperature of 20°C. The fluid flow process conditions were the inlet, permeability, and roughness. The inlet was defined at the top of the pouring cup. In order to the *QuikCAST* calculate the mass flow rate, as shown in figure 12, a pouring time of 10 s (according to the result obtained in section 3.1) and the lowest pouring temperature of 1375ºC were used. The selection of the pouring temperature is explained in section 4.2.4. The permeability condition was defined for all the surfaces in contact with the mold by using the green sand permeability. The roughness condition was imposed for the same surfaces as average, since being green sand. For the grid definition, was imposed a three-dimensional one automatically (XYZ) with the average cell size of 4.55 mm. The convection time step accelerator factor was kept with a factor of 3. Then, a flow and thermal simulation with standard calculation was carried out with the remaining processes kept as default by the *QuikCAST*.

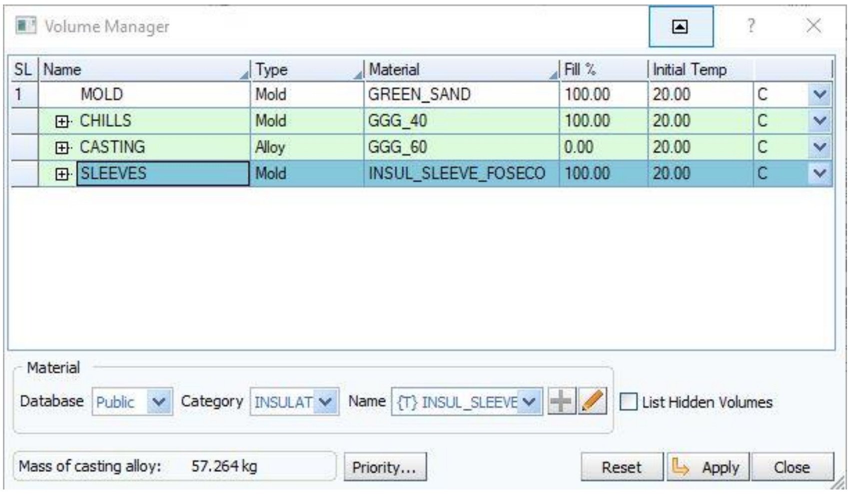

Figure 11: Volume manager conditions imposed for all the present elements

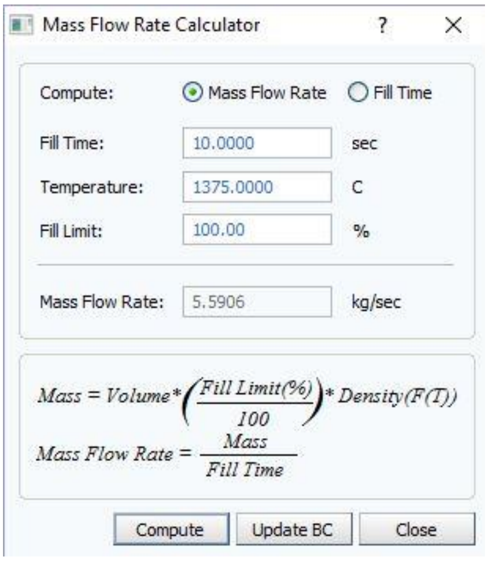

Figure 12: Mass flow rate calculator according to the imposed filling time and pouring temperature

3.3.3. CORE BLOWING SIMULATIONS

The core, its dimensions, as well as core prints, is represented in figure 13. Here, the represented core prints are used in practice to hold the core in the required position in the mold cavity during its filling. This core is used to make the hollow part of the casting represented in figure 8.

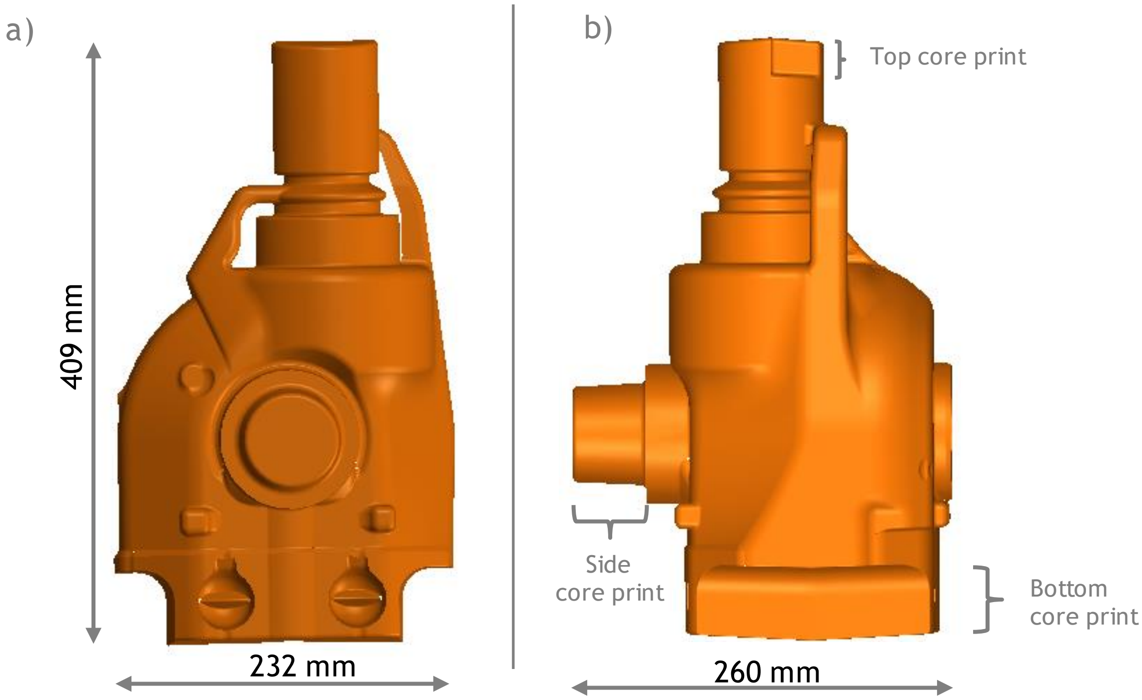

Figure 13: Sand core produced by SAKTHI Portugal

For the core blowing simulations, two shooting pressures, several nozzles configurations and distinct vent proportion were used. In total were made sixteen simulations, according to table 4. In these simulations, according to those used in practice by the company, were used the minimum pressure of 44 kPa, and the maximum pressure of 294 kPa. There were six distinct nozzles with different dimensions, according to the figure 14, named as D_1, D_2 and H. Here, D_1 is the upper nozzle diameter, D_2 is the bottom diameter, and H is the height of the nozzle's bottom part. The variation in such dimensions in each nozzle is represented in table 5. For vents proportion variation, were used 100%, 50% and 0%. Furthermore, were made two simulations without any nozzle, using the minimum and the maximum pressure.

Table 4: Representation of different conditions used for all core blowing simulations

Nozzle	**1**				**2**		**3**		**4**		**5**		**6**	
Pressure (kPa)	44			294	44	294	44	294	44	294	44	294	44	294
Vents proportions (%)	0	50	100	100	100	100	100	100	100	100	100	100	100	100

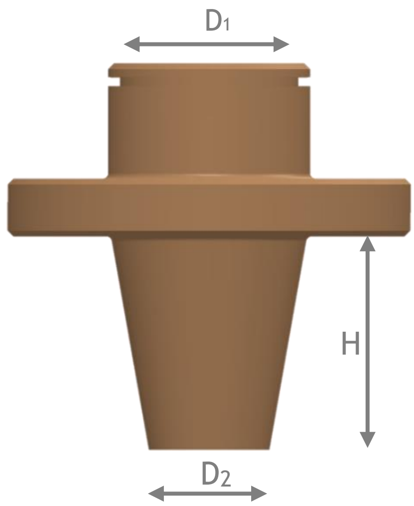

Figure 14: Representation of different dimensions of all used nozzles

Table 5: Values of different dimensions for all the used nozzles

Nozzle Dimensions	1	2	3	4	5	6
D_1 (mm)	22	22	22	22	22	25
D_2 (mm)	12	12	18	18	22	25
H (mm)	37	42	37	42	31	37

All the elements were imported to *QuikCAST* as *.igs* file. In the first instance, the core, as well as the nozzle, were meshed with a mesh size of 1 mm. Then, the inlet was built 10 mm above the top of the nozzle with the same mesh size as the previous elements. Figure 15 shows all the elements meshed as well as the direction of the gravity vector imposed with a magnitude of 9.80 $m.s^{-2}$. The initial temperature defined for the core, inlet, and nozzle was 20°C. The initial filled rate for the core was 0%, once the core box is empty at this moment.

On the other hand, for the inlet and nozzle, the initial imposed filled rate was 100%, because these elements are not filled with sand during core blowing. The defined material for all the elements as well as for gas was *Sand1Gas1*, the only one available in *QuikCAST* database. Several fluid flow process conditions were considered, such as pressure, imposed initial fluid, air venting and roughness. The pressure was imposed on the top surface of the inlet. The initial fluid was imposed in the inlet with a fill percentage of 100%. The air venting was defined with a given diameter as well as its position in the core. The core with the implemented in practice air venting spots, as well as their diameters in mm, are shown in figure 16. For the core where 50% of used vents was considered is shown in figure 17. The roughness was defined in the exterior of the core with a roughness index of 0.05 mm. For the grid definition, was imposed a three-dimensional one automatically

(XYZ) with the average cell size of 3.01 mm. Then, the core blowing simulation of the core box was carried out with a convection time step accelerator factor of 1 considering a sand core simulation type. For the stop criteria, was defined the maximum time of 60 s. The blowing calculation option was assigned. The thermal calculation during core blowing was deactivated because this parameter does not have the interest to be evaluated in this type of simulations. All the remaining simulation parameters were kept as default. It is important to point out that some differences from the core blowing tutorial were made in order to be able to proceed with the simulation (see Annex I).

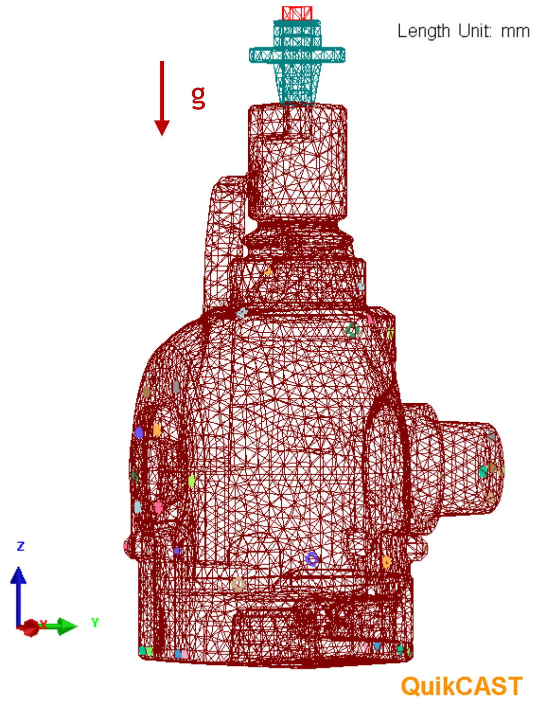

Figure 15: Core, nozzle, and inlet after meshing in QuikCAST, as well as the gravity vector

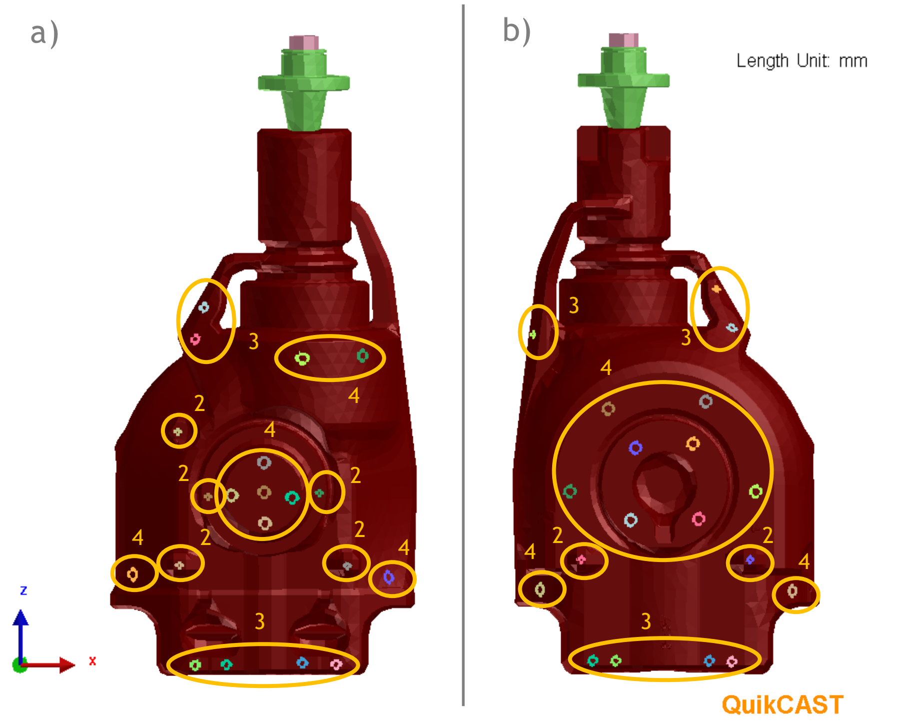

Figure 16: Core with the used vents position in SAKTHI Portugal as well as the imposed diameters in mm

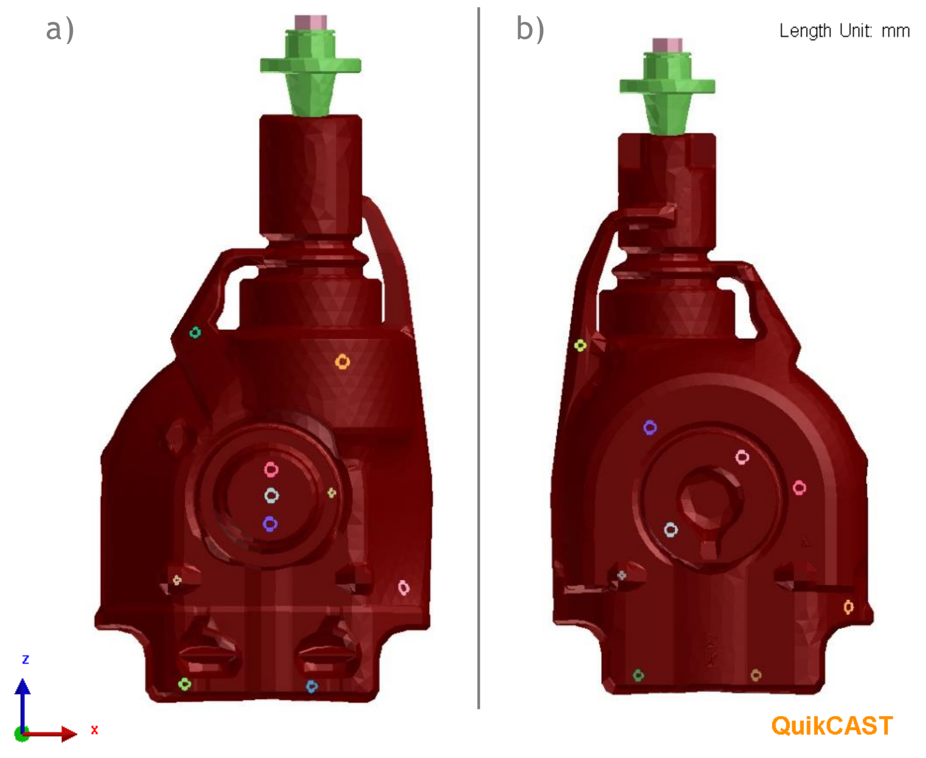

Figure 17: Core with 50% of the currently used vents in SAKTHI Portugal

4. RESULTS AND DISCUSSION

In this chapter is presented the development and optimization of the whole work. In the first instance, is presented and discussed the design and improvement of the gating and feeding system, for two and three molding cavities pattern plate, according to the results obtained in the mold filling and solidification simulation in *QuikCAST*. Further ahead, the results of core blowing simulations and the influence of the used shooting pressure, the nozzle's dimensions and the vents proportion on the obtained voids density are presented and discussed.

4.1. THERMAL MODULUS

Firstly, was obtained the thermal diagram of the component represented in figure 18. The red spot represents the section with the largest thermal modulus of 1.00 cm. This spot denotes the predicted last section of the whole casting to be solidified. So, these sections represent the place where the shrinkage porosity may appear if no feeder is used.

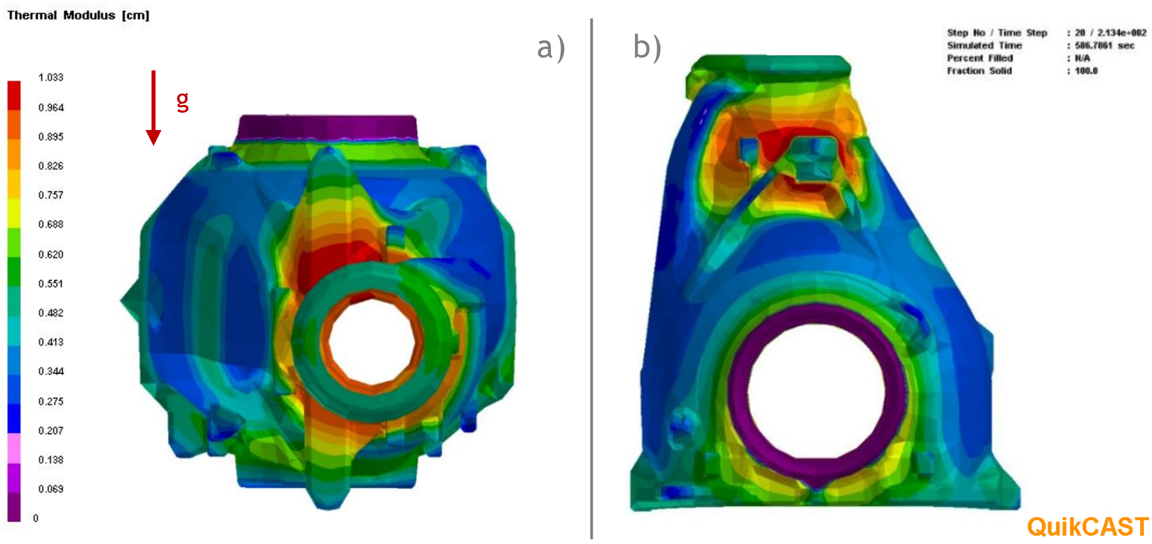

Figure 18: Thermal modulus distribution for the analyzed component after solidification simulation

4.2. DEVELOPMENT OF GATING AND FEEDING SYSTEM FOR TWO MOLD CAVITIES PATTERN PLATE

4.2.1. DEVELOPMENT OF GATING SYSTEM A

Once done the calculations for the design of the gating system, described in section 3.1, all its components were modeled. Here, it was essential to consider the draft angle in order to ensure pattern removing without damaging the mold. For sand casting, this angle should be between 0.5° and 2° [28]. In this case, an angle of 2° was considered.

For the first approach of the gating system design for two mold cavities pattern plate, was considered the thickness of gates in contact with the casting after solidification. This thickness must be lower than the average thickness of the casting section in order to allow, in a shakeout, the breaking of the gating system from the casting without damaging it. Otherwise, if the average thickness of the casting is lower, instead of breaking in the junction of the gate to the casting, it will crack at the casting itself. So, the first approach, represented in figure 19 a), consider the gate's height of 3 mm. Another way to guarantee the breaking of the junction is to include a notch in the gate, close to it, with a lower thickness than in the casting (figure 19 b)). Here, a notch with 3 mm height was considered, increasing up to 4.5 mm in the junction area. The drawback of this approach, in comparison with the previous one, is that here an additional deburring operation is required. However, the chosen approach was the second one because it avoids in practice the fracture in the casting.

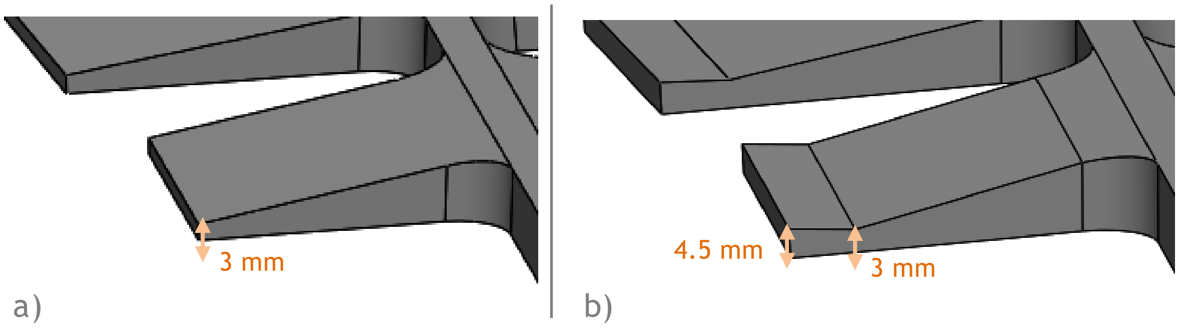

Figure 19: Representation of the proposed gates a) with a section of 3 mm and b) with a notch of 3 mm

For the first suggested feeding system, the configuration and localization of the used feeders in mold cavities were the same as used in practice by SAKTHI, represented as system B (figure 22). The difference was in the thermal efficiency of the feeders since in this system they were used as cold feeders and the company use it as hot ones, this last increases their thermal efficiency.

The result of the first simulation shows that the liquid metal front, at the ingates of the mold cavities, achieves velocities higher than the critical 0.5 $m.s^{-1}$, around 1.2 $m.s^{-1}$. In order to decrease this velocity, the width of the gate section was increased up to 50 mm. Thus, the velocity reduction was achieved, as represented in figure 20. The CAD model of the suggested gating and feeding system A is shown in figure 21.

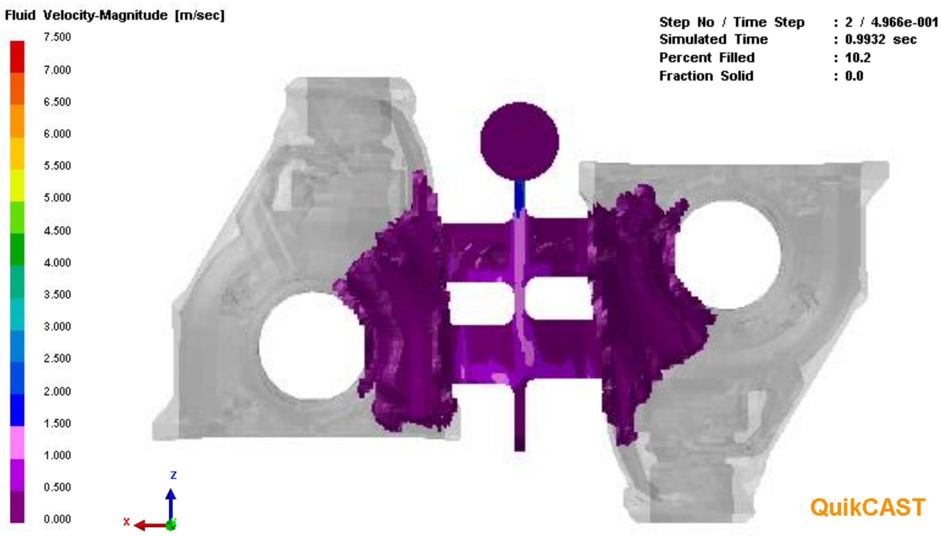

Figure 20: Fluid velocity of the system A at 10% of filling volume. Here the velocity of the front of molten metal achieves speeds below 0.5m.s^{-1}at the ingate of mold cavities

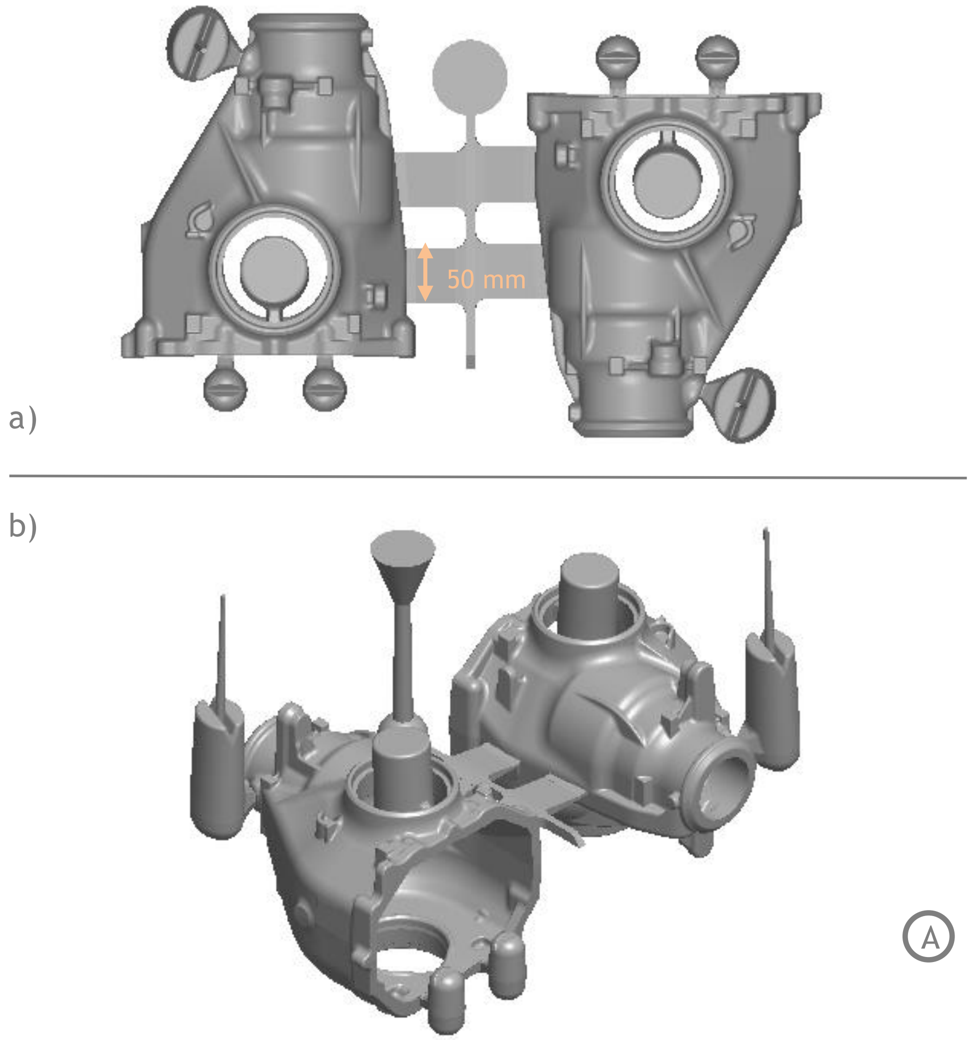

Figure 21: a) top view; b) isometric view of the proposed gating system (system A) with the used feeding system in SAKTHI Portugal for two mold cavities

The approach of this gating system was to provide liquid metal through the gates only in one side of each mold cavity. In order to achieve the same thermal gradient in both mold cavities, the gates were placed on the same side of each one. However, this approach means that, in practice, the placement of the cores in each mold cavity, in comparison with the system B (represented in the next section), should be done in opposite positions.

4.2.2. Gating system used in practice (System B)

In contrast to the developed gating system A, in the currently used one in SAKTHI Portugal, represented as system B and shown in figure 22, each mold cavity is filled by both sides (eight gates per each mold cavity). The mold filling and solidification simulation of the gating and feeding system A shows that the fluid velocity at the entrance of the mold cavities is below critical 0.5 $m.s^{-1}$. Each mold cavity has four feeders, three of them (feeder 1, feeder 2 and feeder 4) are side feeders, and the feeder 3 is a top one. All of them are hot feeders, which allows the increasing of their thermal efficiency.

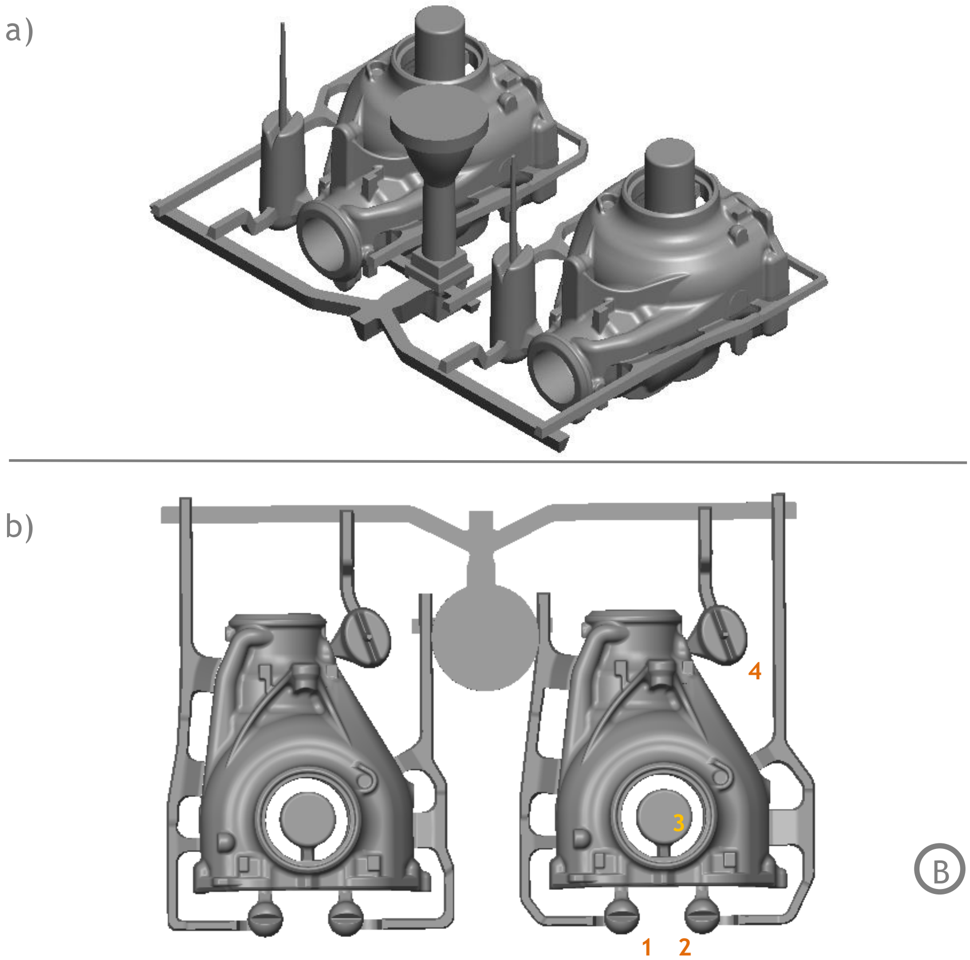

Figure 22: a) isometric view; b) top view of the gating and feeding system used in SAKTHI Portugal (system

4.2.3. COMPARISON BETWEEN THE GATING SYSTEM A AND B

After the simulation of the proposed gating system A (figure 21) and the used one B (figure 22), was analyzed the thermal gradients as well as the formed porosity in both ones. Thermal gradients should be directed from the first to the last portion of the casting to solidify. Thermal gradients obtained in the gating system A and B and represented in figure 23, show that system B presents a thermal gradients distribution that promotes the directional solidification from the middle of the casting to its borders. On the other hand, in the system A, the directional solidification is done from the right side to the left side of the casting. The direction of the solidification is important in order to guarantee the same microstructure and, therefore, the same properties throughout the whole casting. Beyond that, it is important to guarantee that the last casting sections to solidify are those that might be fed. The gating system A presents a thermal distribution within the casting that may produce different microstructures according to the side of the casting, which is more disadvantageous in comparison with system B, that presents a directional solidification from the middle of the casting to its borders. So, displace the gates only in one side of each mold cavity is unfavorable to the thermal gradients obtained in each mold cavity after filling.

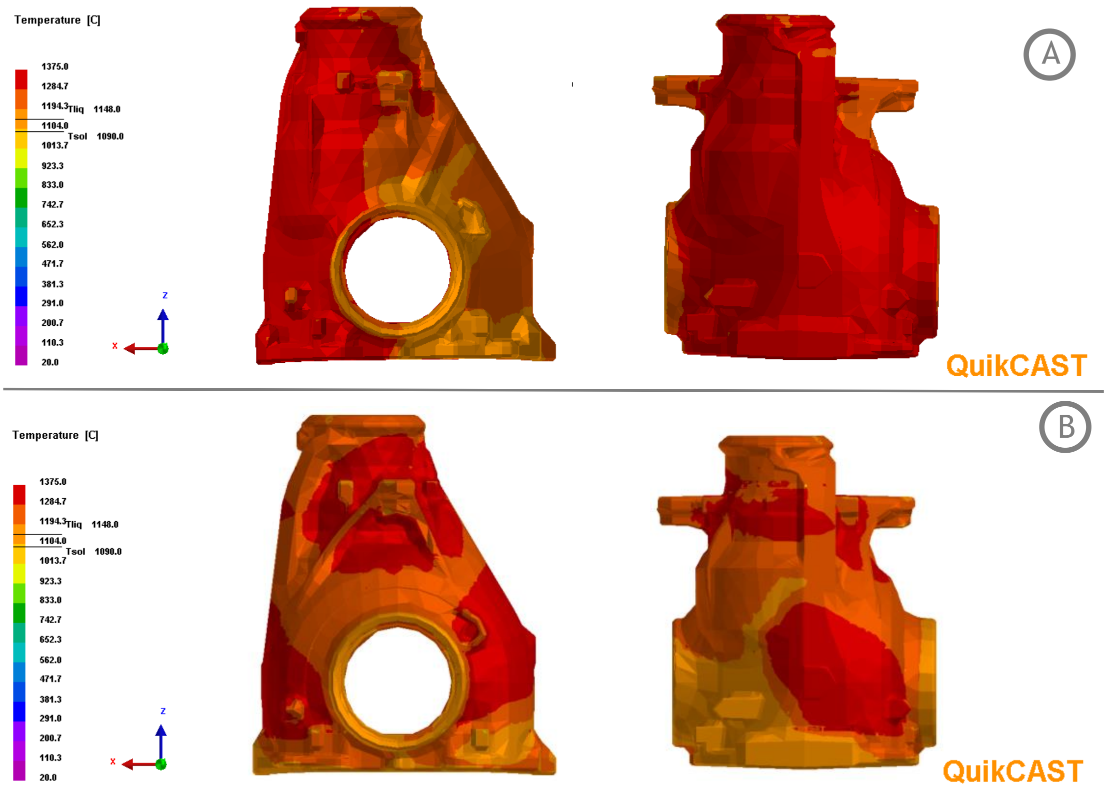

Figure 23: Thermal gradients of 100% filled mold cavities obtained in system A and system B

In the obtained porosity model for both gating systems, shown in figure 24, the differences are not meaningful. In both cases, there are some porosities present in one model, which is absent in the other and vice-versa.

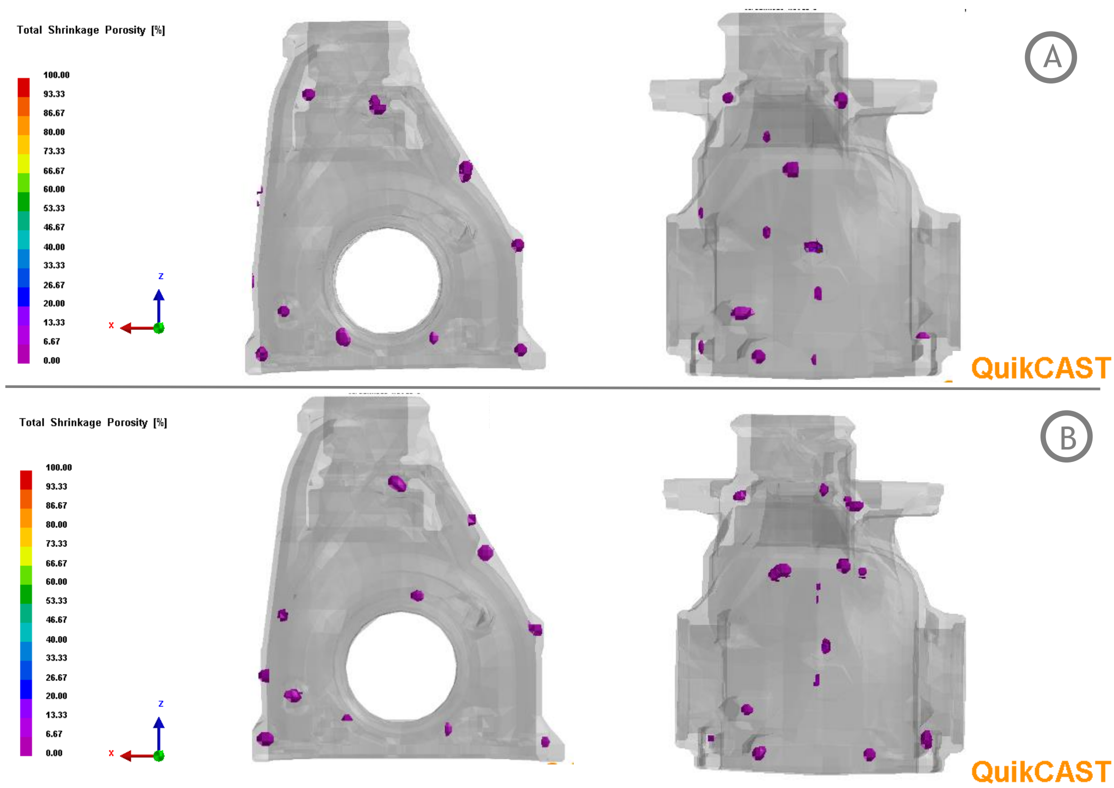

Figure 24: Obtained porosity after solidification in system A and system B, where no significant difference is visible

Summing-up, due to a more homogeneous thermal gradients distribution obtained with the gating system B, all the subsequent modifications in the gating and feeding system were made using this one.

4.2.4. Effect of pouring temperature on the predicted porosity

In order to evaluate the effect of the pouring temperature in the obtained porosity, expressed in figure 25, was used the gating system B to proceed with two simulations, using the minimum and the maximum pouring temperatures. One simulation was made using the minimum (1375°C) and another one using the maximum pouring temperature (1400°C). The porosity values, represented in this figure, were obtained by cutting of the given sections, which is represented in Annex II.

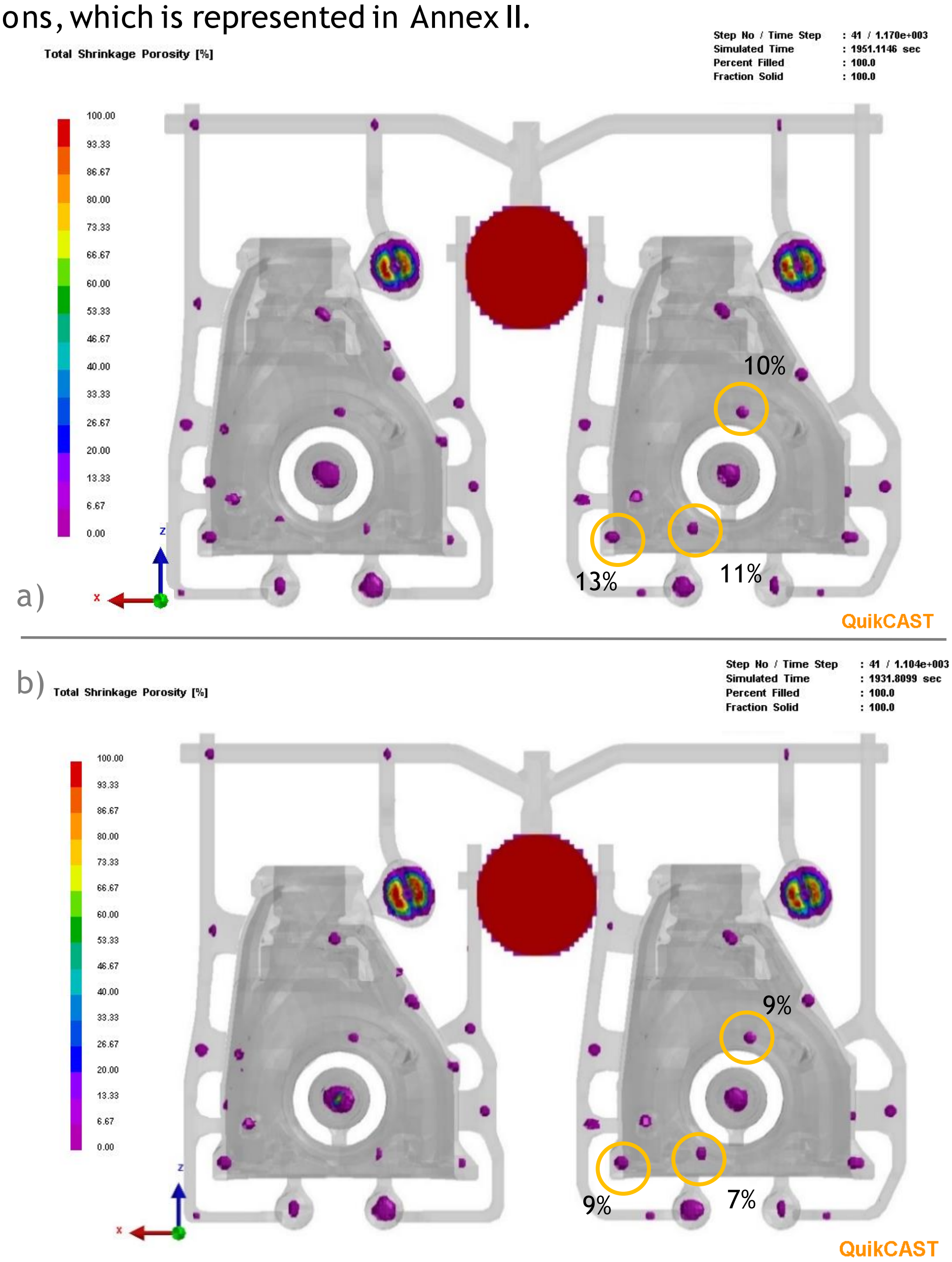

Figure 25: Obtained porosity after solidification using a) the lowest pouring temperature (1375°C); b) the highest pouring temperature (1400°C). Using the highest pouring temperature (1400°C), the produced porosity is lower than using the lowest pouring temperature (1375°C)

According to figure 25, the obtained porosity in both lower (1375ºC) and higher (1400ºC) pouring temperatures is not significantly different. However, when a cutting section is done, it is found that the porosity values are different (see Annex II). With the lowest pouring temperature, a greater porosity is predicted. Therefore, all the simulation was done using the lowest pouring temperature in order to evaluate the greatest possible porosity and make all the modification in order to obtain, in simulation, 0061 sound casting.

4.2.5. Shrinkage porosity in the casting

Once the porosity shown in *QuikCAST* does not represent exactly the reality, the obtained porosity after simulation should be compared with the obtained porosity in practice. It is essential to point out that in every casting processes simulation software, the obtained results do not correspond exactly to the porosity obtained in practice. Thus, it is crucial to work on the adjustments of the software's preprocessing parameters until the obtained porosity corresponds as similar as possible to the obtained in practice. Nevertheless, this represents a different work from the current one.

Figure 26 shows the predicted porosity after mold filling and solidification simulation of the component with the currently used gating system in SAKTHI (system B) using the lowest pouring temperature (1375ºC). The highlighted porosity represents the most critical macroshrinkage obtained in practice. So, all the subsequent changes in gating and feeding system were made in order to avoid the presence of porosity in those sections. It is important to stress that there are some porosities represented in simulation, that do not occur in practice, as represented in figure 26.

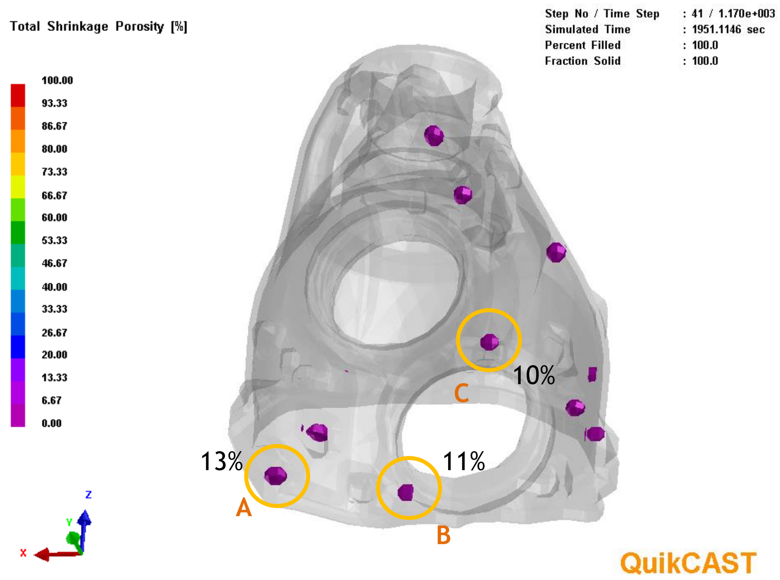

Figure 26: Predicted porosity after mold filling and solidification simulatin using the gating system B and the porosity obtained in practice (highlighted)

4.2.6. APPROACH 1

The first approach was to move both feeders 1 and 2 from the bottom part to the parting plane, represented in figure 27 as feeders 5 and 6. Comparing the predicted porosity with the used gating and feeding system B represented in figure 26, the obtained porosity in this first approach, represented in figure 28, enlarged the initial porosity B from 11% up to 40% and produce another one, porosity D, with 5%. On the other hand, the porosity C of 10% is diminished up to 1.5% by the displacement of both feeders. Furthermore, the porosity A of 13% is removed with this approach.

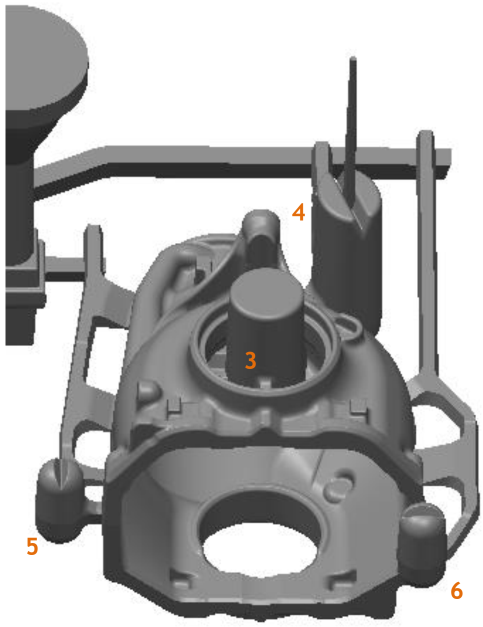

Figure 27: First approach, with the displacement of the feeders 1 and 2 in the bottom part to the parting plane to the feeder 5 and feeder 6

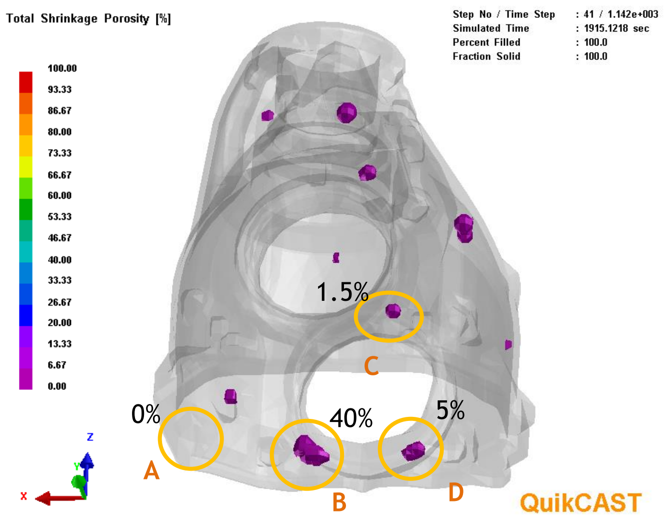

Figure 28: Predicted porosity in the first approach

The increase of the porosity B and D on the bottom part of the casting means that the feeders 1 and 2 are crucial to keep the soundness of the casting in that section. So, to remove the porosity B and D, it was decided to introduce to the current used feeders 5 and 6, the feeders 1 and 2 in the next approach. This approach was done because in the current one was found that the absence of feeders 1 and 2 produce an extra porosity (porosity C) and increase of the porosity B in 29%. Also, this feeder's displacement causes a reduction in porosity C up to 1.5%. So, in the next approach, the feeder 5 and 6 were also kept.

4.2.7. APPROACH 2

The second approach was to place the bottom feeders 1 and 2 in addition to the used ones 5 and 6 in approach 1, as shown in figure 29. The predicted porosity of this simulation is represented in figure 30.

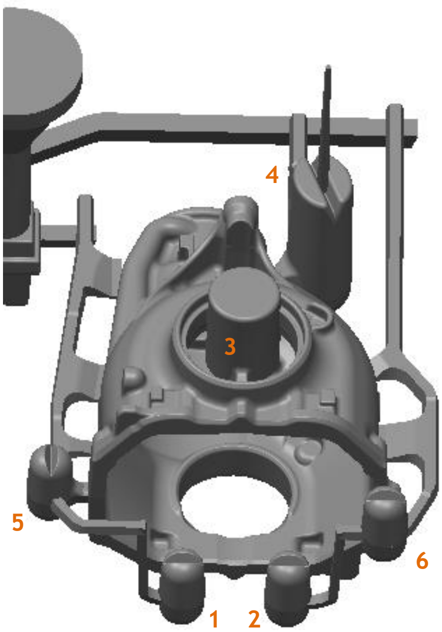

Figure 29: Second approach with the use of four feeders in the bottom part of the mold cavity 1, 2, 5 and 6

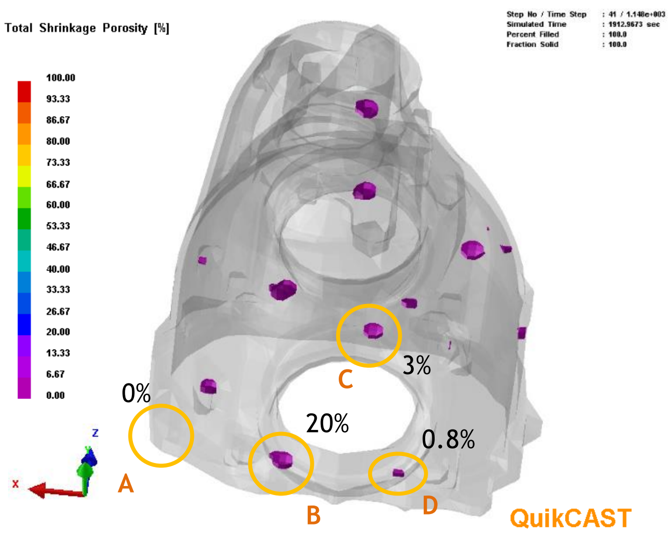

Figure 30: Predicted porosity in the second approach

Comparing with the previous approach, porosity B was reduced from 40% up to 20%, and porosity D was reduced from 5% up to 0.8%. The porosity A remains as being zero, and the porosity C increased in 1.5%. However, considering the original system B, porosity B of 5% increased up to 20%. So, the use of four side feeders does not reduce this porosity. Furthermore, this approach induces another porosity, porosity D of 0.8%. Nevertheless, the initial porosity C of 10% is reduced up to 3% with this modification, and the initial porosity A of 13% was removed.

4.2.8. APPROACH 3

In order to remove the predicted porosity B and D in the second approach, was tested the volume increase on the feeder 1. The volume increase was made according to the volume requirement discussed in section 2.4.3., with an increase in 15 mm of the diameter of feeder 1, as shown in Annex III. The results after simulation, represented in the same Annex, show that the porosity C of 3% persists. Nevertheless, porosity A remains as being zero, porosity B of 20% in the latter approach is reduced up to 1.4%, and the porosity D of 0.8% in the approach 2 was reduced up to 0.5%. This third approach, in comparison with the previous one, aids in porosity reduction of porosity B in 18.6%. However, the porosity B remains. The subsequent approaches were made without considering this volume increasing since it decreases the system yield and does not play an important role in the porosity reduction.

4.2.9. APPROACH 4

For the fourth modification, shown in figure 31, was suggested not to consider the feeder 6, since the use of four feeders decreases the yield of the current system. Thus, to increase the system's yield and, in order to see the effect of the absence of this feeder, was simulated the same approach as the second one, but without the feeder 6 (figure 31).

In comparison with the second approach, in the current one porosity B of 20% is diminished up to 4% and the porosity D of 0.8% is removed (as shown in figure 32). Nevertheless, the absence of the feeder 6 results in an increase of the porosity C of 3% up to 17%. Therefore, it is deduced that this feeder is crucial to avoid porosity in this section. However, in comparison with the initial porosity B in system B of 11%, in the current approach, it is still present as 4%. In order to understand the formation of this porosity, other postprocessing simulation parameter must be analyzed.

Solidification time was studied in order to evaluate if the feeders solidify later than the casting itself as it should be, in line with section 2.4.2. According to the solidification time in this approach, represented in figure 33, it is found that the solidification time for the bottom part of the casting is higher than the average solidification time in the feeders 1 and 2. This effect indicates that these feeders solidify before the solidification of the bottom part of the cast, which strongly suggests the possible generation of the porosity in this part of the casting. According to the heat transfer requirement, represented in section 2.4.2., the feeder should solidify later than the casting itself, which in this case it is not fulfilled. The problem source was found out. So, in order to promote the solidification towards to feeders 1 and 2, solidification aids, such as chills, might be helpful.

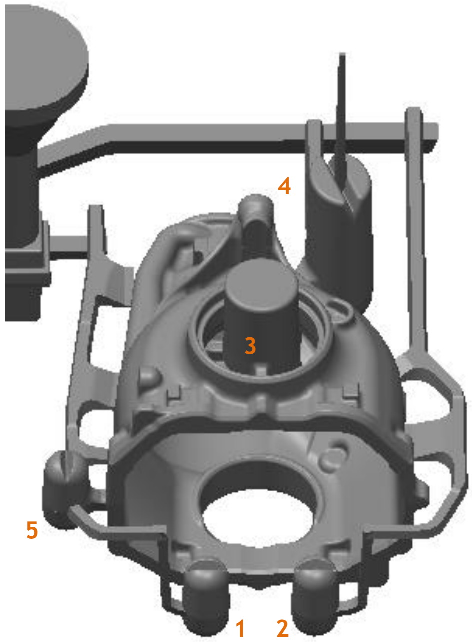

Figure 31: Fourth approach with the use of three feeders (1, 2 and 5) in the bottom part of the mold cavity

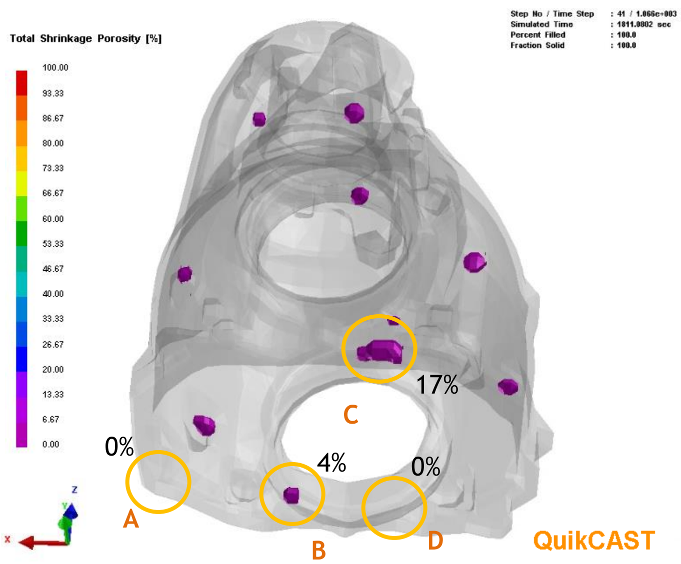

Figure 32: Predicted porosity in the fourth approach

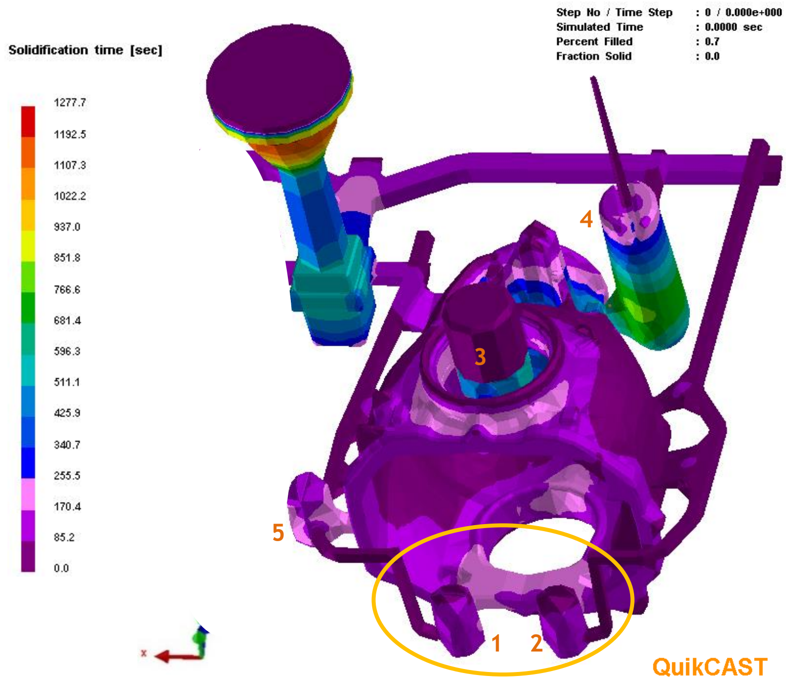

Figure 33: Predicted solidification time in the fourth used approach, where it is visible that the feeders 1 and 2 solidify before the highlighted section of the casting

4.2.10. APPROACH 5

In the fifth approach, one internal chill was introduced to the initial system B in order to see its effect on the promotion of local solidification, as discussed in section 2.3.5 and, consequently, if it avoids the porosity B of 4% in the bottom part of the casting. In terms of porosity, shown in Annex IV, the initial porosity A in the system B of 13% was reduced up to 10%. The initial porosity B of 11% was diminished up to 3%. Finally, the initial porosity C of 10% decreases up to 3%. Therefore, a placement of the chill in the bottom part of the core promotes a reduction of porosity A, B, and C. However, it is not enough to delete it, so in the next approach, three intern chills were used.

The drawback of using chills is the requirement for placing the internal chills in each core before fitting it in the mold cavity. Nevertheless, this was the suggestion to remove the porosity of the bottom part of the casting, since previous approaches do not allow this porosity removal.

4.2.11. APPROACH 6

As verified in the previous approach, one internal chill aids in the local solidification and, therefore, diminished all the initial porosities A, B, and C. However, it is not enough to remove them. So, to evaluate the effect of more internal chills were added three internal ones in the bottom part of the mold cavity and a mold filling and solidification simulation were done using the system B (see Annex V). This approach removes the predicted porosity B and D. Nevertheless, the initial porosity A of 13% only is reduced up to 10%. So, it is deduced that the side feeder 5 is required to remove this porosity, as supported by approach 1, 2, 3 and 4.

4.2.12. APPROACH 7

The seventh approach, represented in figure 34, was based on the fourth approach with the placement of three internal chills, according to the results of the previous approach. The predicted porosity is shown in figure 35. Here, in comparison with the initial system B, the porosity A and B are removed. However, the initial porosity C of 10% is increased up to 20%.

Looking at the solidification time represented in figure 36, the directional solidification towards feeders 1 and 2 is promoted by chills. Thus, these feeders solidify later than the bottom section a) of the casting, as it should be, which leads to the absence of porosity B. In the same figure it is verified that chills promote a higher solidification time on the highlighted spot b), which leads to the increase of porosity C in this casting section. In comparison with the previous approach, porosity A was removed thanks to adding of the feeder 5. So, adding an extra feeder 5 and three internal chills, the obtained porosity in practice A and B is not detected in simulated results.

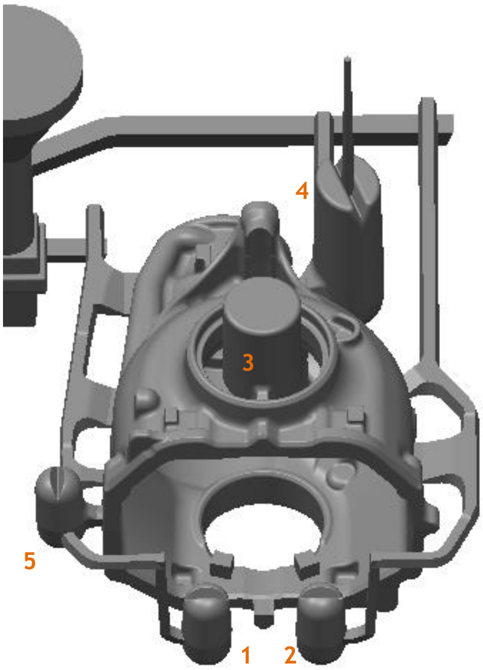

Figure 34: Seventh approach with the used of three internal chills and three side feeders in the bottom part of the mold cavity (feeder 1, feeder 2 and feeder 5)

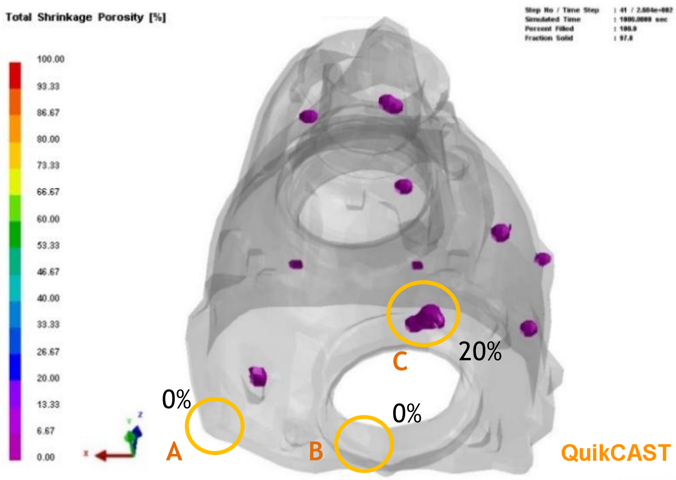

Figure 35: Predicted porosity in the seventh approach

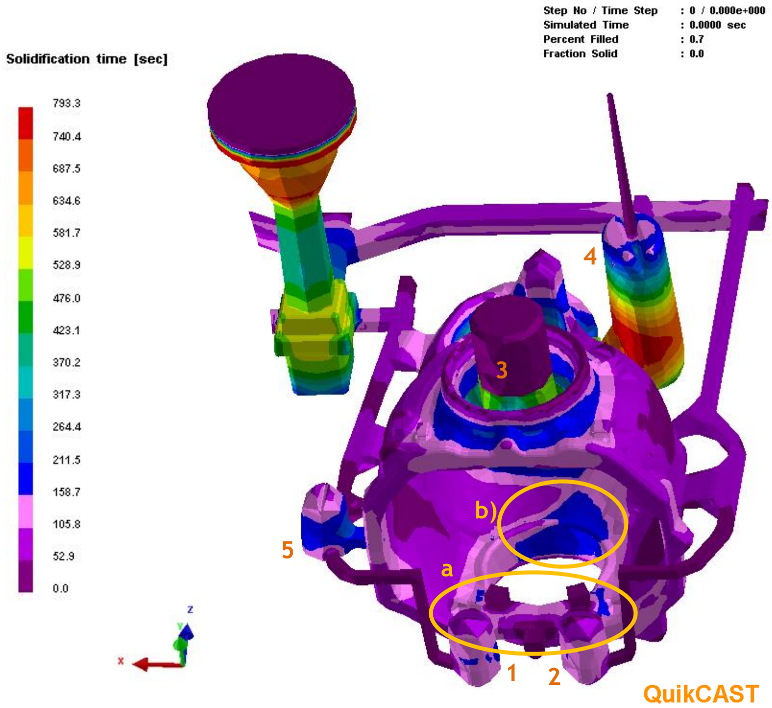

Figure 36: Predicted solidification time of the seventh approach. The use of three chills promotes an earlier solidification of the feeders 1 and 2 in comparison with the section a) of the casting.

Table 6 summarizes the development of the achieved porosity in the course of the whole gating and feeding system optimization, starting at system B. It is visible in comparison with the initial system B, in the seventh approach the porosity A and B was totally removed, as well as the porosity D that appeared in some previous approaches. Nevertheless, the initial porosity C was increased in 10%. So, to eliminate the porosity C for future simulations two approaches may be tested. One of them is the displacement of some chills to the section b) represented in figure 36. The other one is the use of feeder 6, since its use in approach 1 and 2, diminished the porosity C up to 1.5%.

Table 6: Development of the obtained porosity, in the course of the optimizations of the gating and feeding system for two mold cavities pattern plate, from the system B to the last approach

Porosity	A	B	C	D
System B	**13%**	**11%**	**10%**	**0%**
Approach 1	0%	40%	1.5%	5%
Approach 2	0%	20%	3%	0.8%
Approach 3	0%	1.4%	3%	0.5%
Approach 4	0%	4%	17%	0%
Approach 5	10%	3%	3%	3%
Approach 6	10%	0%	4%	0%
Approach 7	**0%**	**0%**	**20%**	**0%**

4.3. DEVELOPMENT OF GATING AND FEEDING SYSTEM FOR THREE MOLD CAVITIES PATTERN PLATE

According to the obtained gating system dimensions, based on the calculation of section 3.1, all the elements were modeled. Were assumed six gates per each mold cavity (to fill it on both sides) and four runners for all gating system. The draft angle was also 2° as in section 4.2.

4.3.1. DISPOSITION OF THREE MOLD CAVITIES ON THE PATTERN PLATE

To design the gating and feeding system for three mold cavities pattern plate, firstly, their placement on the parting plate was tested to fit them all. Here, it is crucial to consider the useful area of the parting plate by excluding 50 mm of each side in order to guarantee the integrity of the green sand on the boundaries of the mold. Once the use of current core prints does not allow the arrangement of three mold cavities on this parting pattern, the bottom core prints length, as represented in figure 18, was considered being 32 mm instead of currently used 58 mm. Three possibilities of mold cavities arrangement were found. However, the possibility that allows better space exploitation to fit the gating, as well as the feeding system is represented in figure 37. This arrangement was used. Here, the disposition of the mold cavities has one of them (mold cavity A) reverted in relation to the other two, which are placed as used in system B. Each mold cavity has the same position of the feeders (for feeders 1, 2, 3 and 4) as used for two mold cavities pattern plate in system B. The main hindrance was to fit the feeder 4, represented in figure 37, in each mold cavity because here the current position does not allow, the disposition of the gating system. In order to enable the layout of three mold cavities as well as feeding and gating system, the first approach was to reduce the neck's length of the feeder 4 in 9 mm. Nevertheless, this reduction was not an option because even so space is not enough to fit the runners and ensure the integrity of the sand between them and mold cavities.

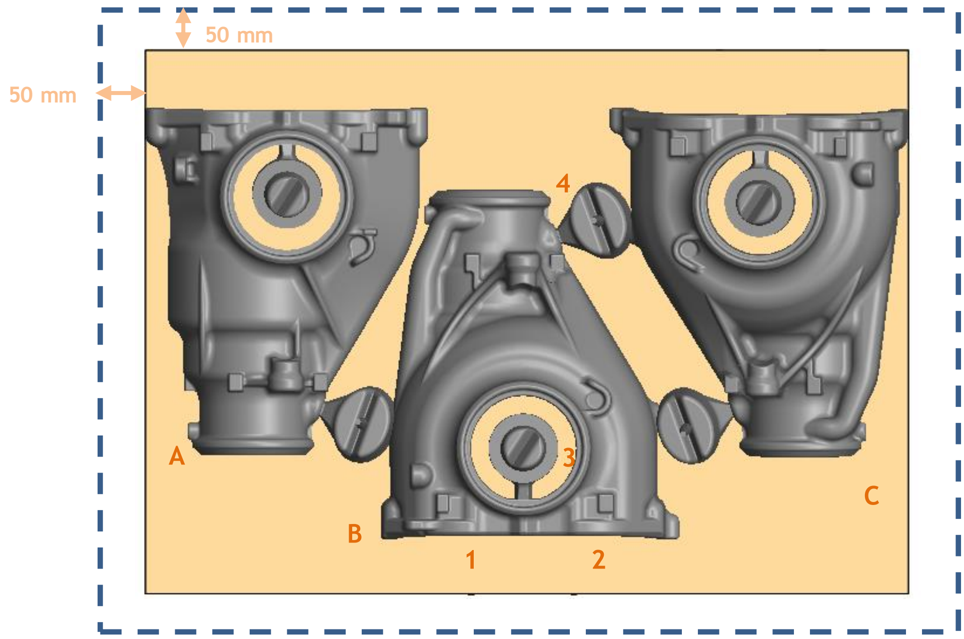

Figure 37: Used disposition of three mold cavities with the feeding system on the useful pattern plate area

As the reduction of feeder's neck was not a solution, another disposition was required. Thus, in order to find a different position of feeder 4, a thermal diagram was used (figure 18). As described in section 2.4.1, the hot spot presents the greatest thermal modulus, represented as the red section, and represents the last section to be solidified. In order to promote the solidification at the feeder before the solidifications of the casting itself, the feeder should be placed as near as possible to that spot. Although the current feeder disposition being the best, since being the closest place from the hot spot, it does not enable to three mold cavities fit in the parting plate with the gating and feeding systems. Therefore, it is required to find another spot to place it. The first suggestion was to place a top feeder at the top of the casting close to the hot spot. However, according to the volume requirement, the volume that it is needed to the feeder does not allow its placement there due to lack of space. So, another alternative was to find a different position, even knowing that there the feeder will be not so efficient as it is in the current one. According to the thermal diagram in figure 18, one of the latest casting sections to solidify is represented as a green spot with a thermal modulus of 0.55 cm. Thus, it was suggested to place the feeder 4 on this section. There are only two ways to arrange this feeder on this position. The first way is to reduce the core prints stability by cutting the intersected area with the feeder from the core. The second way is to cut this intersected area from the feeder, ensuring the same stability for core prints (see Annex VI).

4.3.2. APPROACH 1

For the design of the gating system, the purpose was to fill at the same place each mold cavity on both sides in order to homogenize thermal gradients all over the mold cavities after their filling. The first approach is shown in figure 38. Here, was considered to use all the side feeders as hot ones in order to increase their thermal efficiency. However, the disposition of the feeder 1, feeder 2 and feeder 4 was changed. To ensure core print stability, was cut the intersected area of the feeder 4 with the core print from the feeder itself.

Feeders 1 and 2 were placed in the pattern plane as represented in figure 38 b) in order to allow the fitting of the core print with a length of 32 mm, as discussed in the previous section. In order to reduce the velocity loss of the liquid metal through the runners, all the flow direction changes were smoothed with the use of fillets. However, the highlighted runner section in figure 38 is over-dimensioned, which reduces the velocity of liquid metal and the yield of the system, and provides a colder liquid metal to the subsequent runner's section of the mold cavity A. To evaluate the effect of internal chills, were placed three ones in the bottom part of the mold cavity B and cavity C, as was done in section 4.2.11. The mold cavity A remains without them. In Annex VII it is visible that the obtained porosity in mold cavity A, which does not have internal chills, is much higher than in the others (which is below 1%). At first sight, it is concluded that internal chills are required to avoid the porosity in the bottom section of the mold cavities. However, even with the use of internal chills, the obtained porosity in the bottom section of mold cavity A reversed in relation to the others, does not lead to the removal of the porosity (verified forward in approach 3).

The obtained thermal gradients are represented in figure 39. It is verified in figure 39 a) that at 40% percent filled of the whole system, the mold cavity C is already filled with liquid metal, and the runner section and gate that should provide it, do not provide the liquid metal. The mold cavity C instead of being filled with the liquid metal through the highlighted gate in figure 39 a), this last portion is filled through the mold cavity itself. Beyond that, in the same section, the feeder 4 does not act as a hot feeder by providing a liquid metal to the mold cavity, but it is filled by the mold cavity itself. Figure 39 b) suggests that the thermal gradients in all mold cavities are not equivalent, which may lead to different microstructure and, subsequently, to distinct mechanical properties, as discussed in section 2.2.2.3. The mold cavity A and mold cavity C have similar thermal gradient due to being filled with a hotter liquid metal at the same place, at the bottom part. However, the mold cavity B presents distinct thermal gradients, where the hotter liquid metal is provided at its top part.

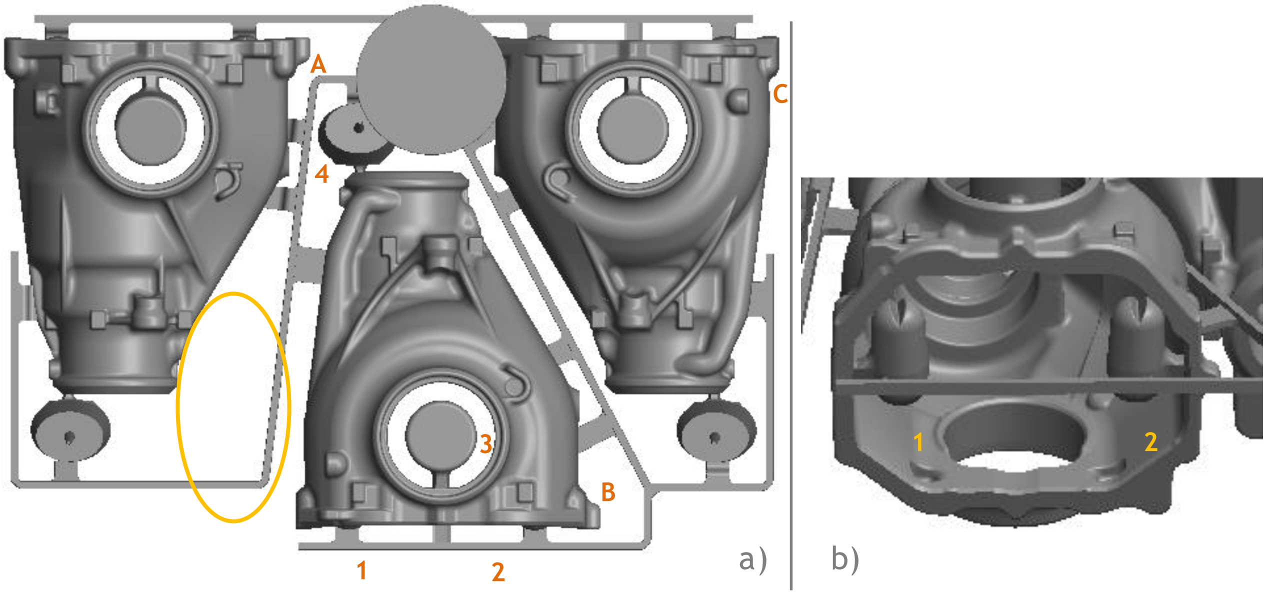

Figure 38: a) top view; b) view with the chosen disposition of feeder 1 and feeder 2 of the first suggested design of a gating and feeding system of three mold cavities pattern plate

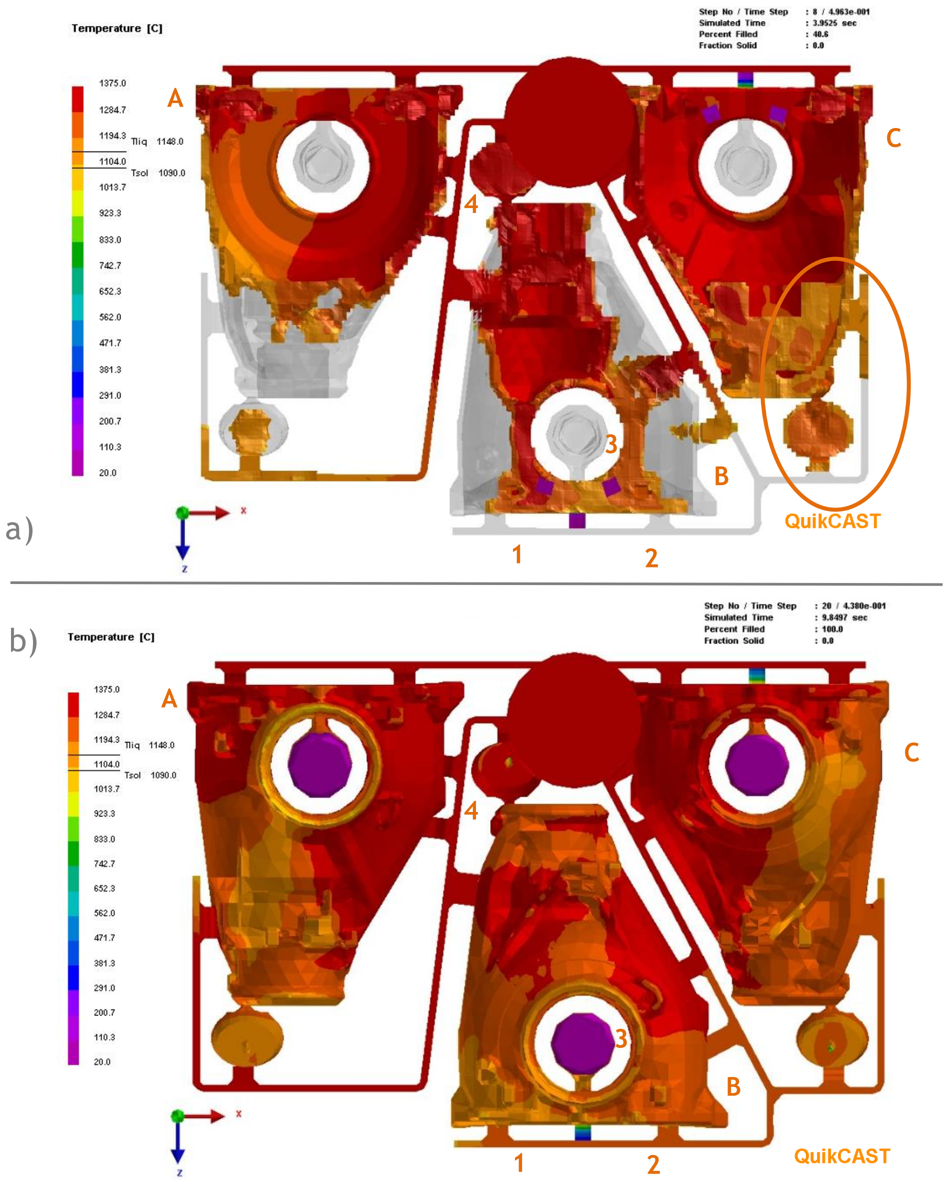

Figure 39: Thermal gradients obtained in the first approach for three mold cavities pattern plate design at a) 41% of filling volume, where the highlighted runner section does not fill the mold cavity C; b) for 100% of filling volume, where the thermal gradients obtained after filling are not equivalent for all the mold cavities

4.3.3. APPROACH 2

In order to fill the drawbacks of the previous gating system a second suggestion was developed by introducing several changes: (1) the over-dimensioned runner section, highlighted in figure 38, was reduced in order to provide a hotter liquid metal to that mold cavity and, at the same time, increase systems yield. Furthermore, (2) the runner's sections were increased.

Evaluating the fluid flow throughout the current gating system, represented in figure 40, it is visible that the velocity of the liquid metal front at the entrance of mold cavity A and cavity C in the highlighted gates is higher than the critical 0.5 m.s^{-1}, which can induce fluid turbulence described in the section 2.3.1. So, in the next approach, some changes were done to reduce this liquid metal front velocity.

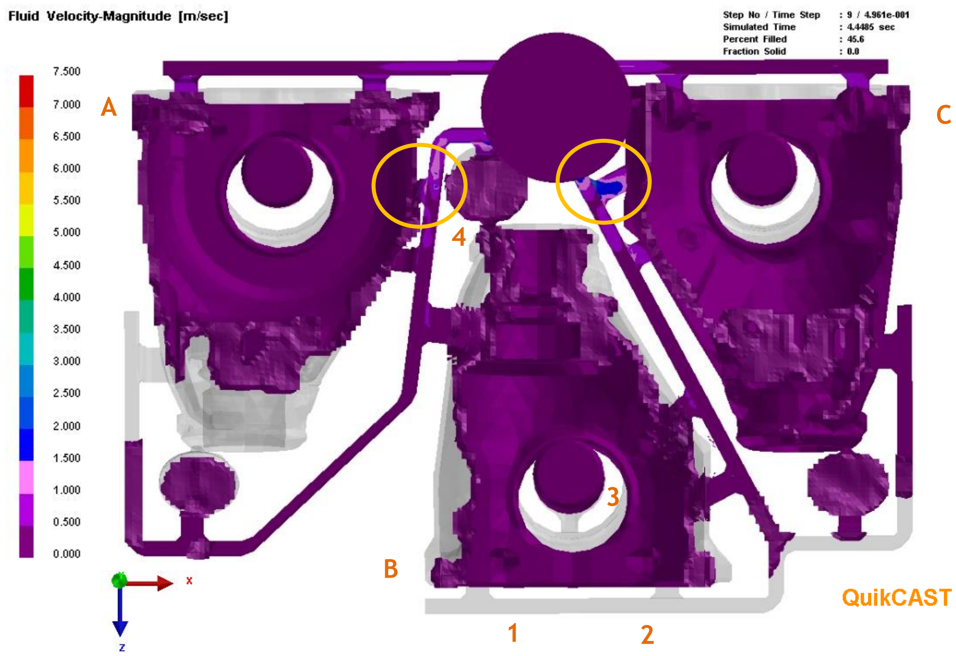

Figure 40: Fluid velocity resulted from the second suggestion of three mold cavities pattern plate design with a filling rate of 45%, which suggests that the liquid metal front may exceed the critical velocity of 0.5 m.s^{-1} in the highlighted gates of mold cavity A and mold cavity C

4.3.4. APPROACH 3

In the third approach, represented in figure 41, several changes were done: (1) feeders 1 and 2 were kept as cold due to the impossibility, in practice, of used them as hot.

Furthermore, (2) by adding three internal chills in the bottom part of the mold cavity A was verified that porosity a), shown in figure 42, was removed. Nevertheless, the porosity c) in the mold cavity A is increased up to 55%. So, internal chills that were placed in this mold cavity do not displace the porosity to the feeders 1 and 2, but only shift its position from a) to c). Therefore, in order to avoid porosity in this section several changes may be tested. The first one is the use of another spot to place the chills and the second one is to compensate the noticeable contraction on these spots, increase the dimensions of feeders 1 and 2, according to the volume requirement discussed in section 2.4.3.

Beyond that, (3) the gate's dimensions were increased in order to decrease the fluid velocity in the ingates of every mold cavity, and trying to allow the filling of the mold cavity C in the highlighted gate in figure 39 a). However, this last purpose was not fulfilled because even increasing the runner's and the gate's sections, the liquid metal is not able to fill this mold cavity, as shown in Annex VIII.

According to the hydraulic requirement explained succinctly in section 2.4, in order to avoid the porosity b) in figure 42, (4) the height of side feeders was increased. This change decreases the porosity b) in mold cavity A in 8%.

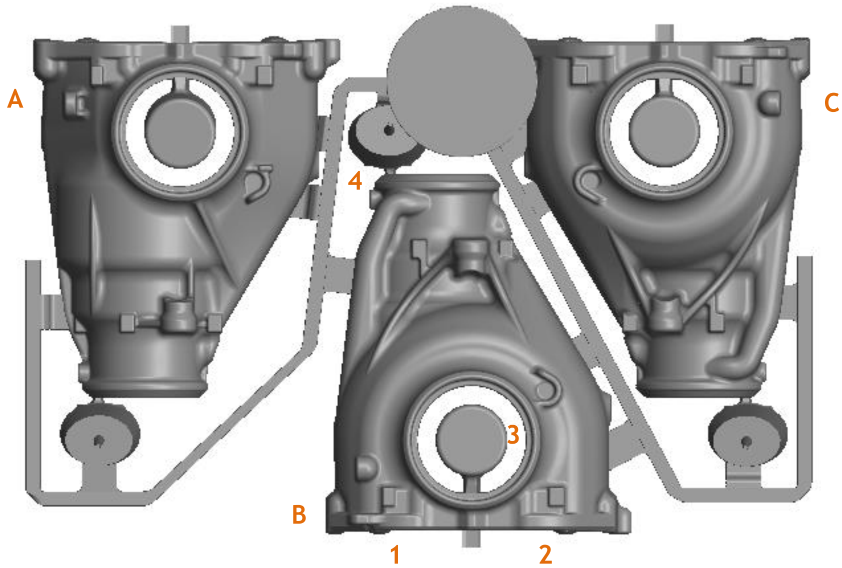

Figure 41: Third approach of gating and feeding system for three mold cavities pattern plate design

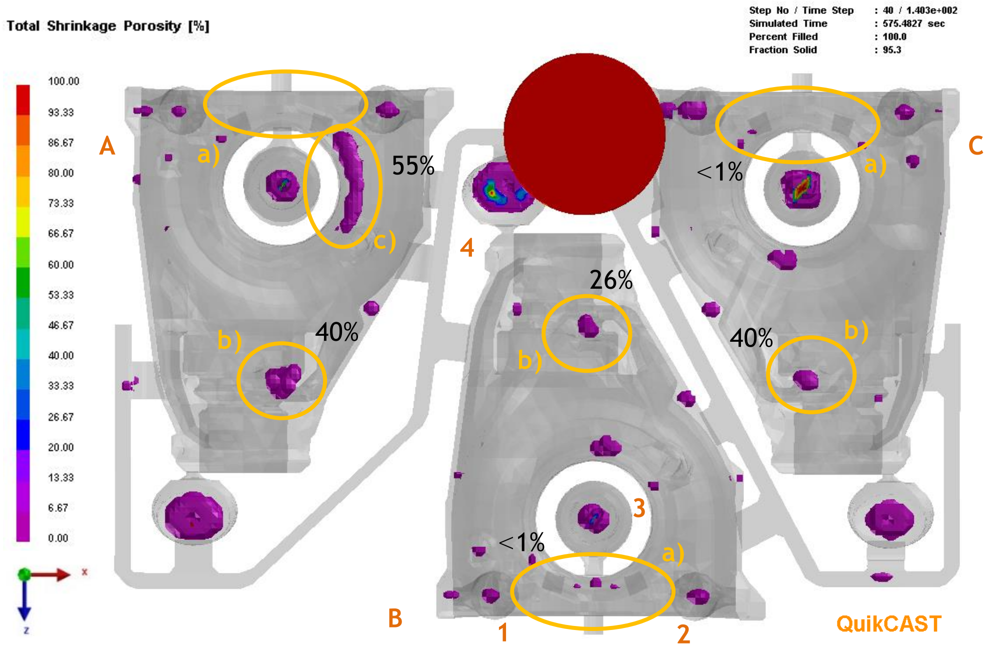

Figure 42: Predicted porosity in the third approach of three mold cavities pattern plate design. Three internal chills placed in section a) promotes a porosity reduction in this area, increasing the porosity in section c) in mold cavity A

4.3.5. APPROACH 4

To test the effect of the presence of feeder 4 was done a simulation with its absence in the mold cavity A. As expected by thermal modulus distribution in figure 18, the obtained porosity was 100%, which make it possible to conclude that this feeder is needed in that section (see Annex IX). Beyond that, one internal chill was added near to the hot spot in the mold cavity C in order to decrease the highlighted porosity b) in figure 42. However, in comparison with 30% of porosity reached with the previous approach, a porosity increasing of around 14% was achieved (see Annex IX). Therefore, it is concluded that, in this case, an internal chill in this position does not play an important role in terms of prevention of porosity in the hot spot.

4.3.6. APPROACH 5

Since changes done in the approach 4 did not improve the predicted porosity, the current approach was the same as the third one, but without the highlighted runners section in mold cavity C (figure 39 a), once it is not filling the mold cavities and, at the same time, decreases system yield. The obtained thermal gradients are represented in figure 43, which are similar to those obtained with the third approach. So, it is concluded that this gate does not play an important role in the obtained thermal gradients and, thus, it is not needed. Beyond that, the obtained porosity is the same as in approach 3. For this last suggestion for three mold cavities pattern plate, the achieved system yield was around 69%, and the pattern yield was around 22%. Table 7 shows the main achievements and conclusions taken in each done approach for the optimization of the gating and feeding system of three mold cavities pattern plate.

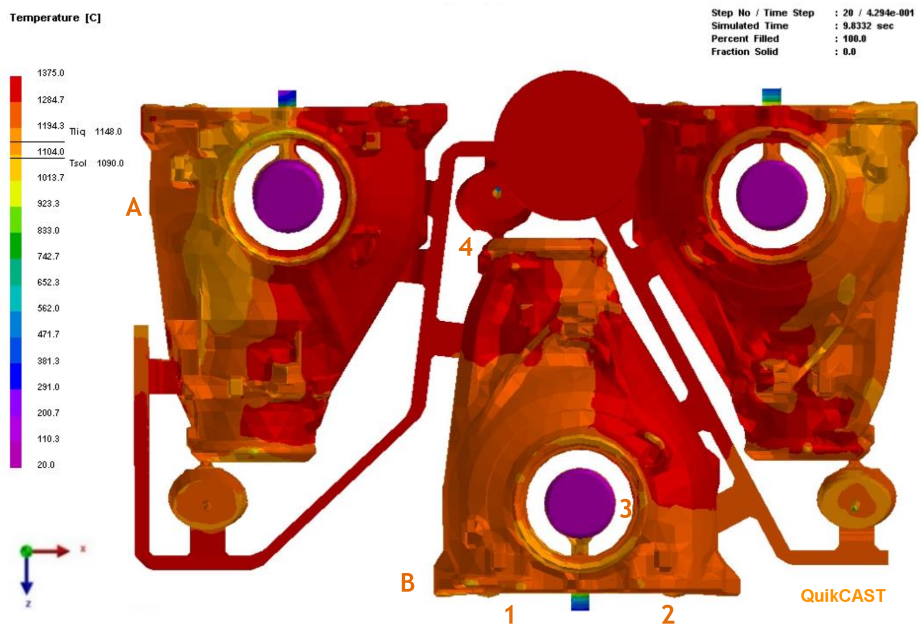

Figure 43: Resulted thermal gradient for 100% filled mold cavities of the fifth approach of three mold cavities pattern plate design. Here, the eliminated the gate of mold cavity C does not play an important role in the thermal gradients imposed in this mold cavity in comparison with the others

Table 7: Main achievements/conclusions of the carried out work of the gating and feeding system design for three mold cavities pattern plate according to the executed approaches

Approach	Achievements/Conclusions
2	• Was provided a hotter liquid metal to mold cavities and increased system yield by decreasing the over-dimensioned section of runners;
3	• Was decreased porosity b) in mold cavity A; • Was uniformized thermal gradients in all mold cavities; • Was decreased the velocity of the liquid metal front at the entrance of mold cavities;
4	• Side feeder 4 is needed because otherwise a 100% porosity is achieved; • Chills do not play an important role to decrease porosity b);
5	• Was increase system yield by reducing one gate and runner section of mold cavity C, which does not interfere with the obtained thermal gradients

4.4. CORE BLOWING SIMULATIONS

Once all the 16 core blowing simulations were done according to the methodologies carried out in section 3.3.3, was analyzed of the simulation results in postprocessing parameters. In this section, the effect of H, D_2, shooting pressure and vents proportions on the obtained voids density, as well as the effect of the use of a nozzle on the fill time are analyzed. The effect of D_1 nozzle dimension may not be evaluated since there are no nozzles with the same dimensions of D_2 and H, except D_1.

On these simulations, it is evaluated the presence of voids in each core after core blowing simulation. In *QuikCAST*, voids represent the last core portion to be filled, which has more probability of getting low density in comparison with the rest core portions. This effect reduces the soundness of the produced core, as explained in section 2.5, which may be evaluated by hardness tests of the core after core blowing.

4.4.1. EFFECT OF THE USE OF NOZZLES ON THE PREDICTED FILLING TIME

In the first instance, it is important to evaluate, according to the results obtained in core blowing simulations, if the use of the nozzle interfere or not with the obtained results because it is the component that connects the core making tool with the core shooting equipment. Thus, using the minimum pressure, one simulation without using any nozzle and another one with the nozzle on the top of the core were carried out. The fill time obtained in both simulations is presented in figure 44. The last filled portions in both simulations differ. Since the last filled portion represents the lowest density sections, it means that the voids prediction is completely distinct as well. Thus, it is very important to use nozzles in the core blowing simulation because, otherwise, the prediction is quite different. So, the use of a nozzle is crucial to obtain reliable results.

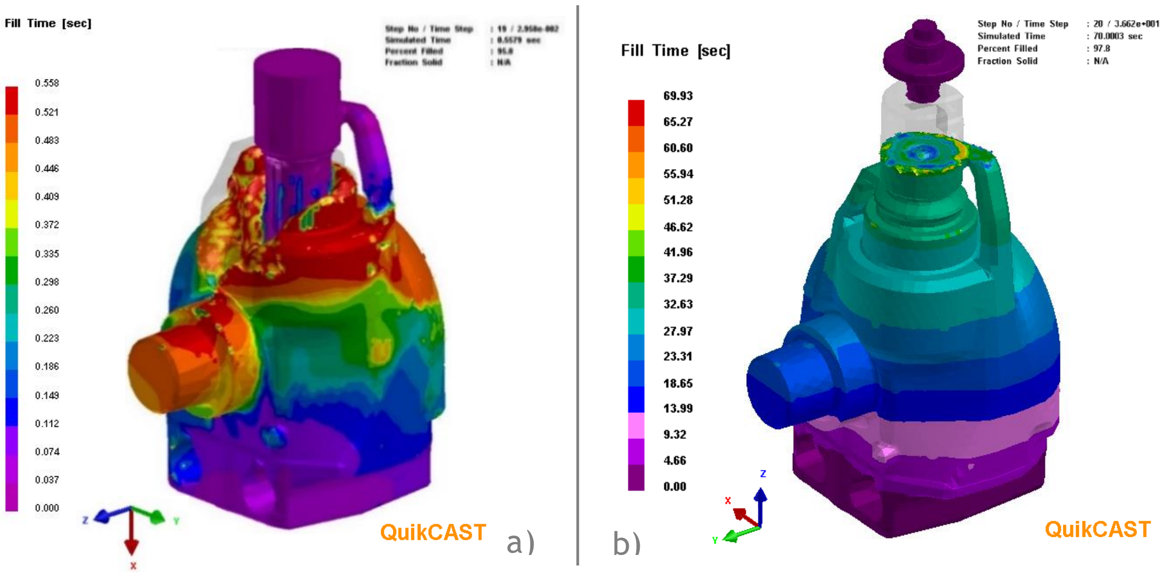

Figure 44: Resulted fill time after core blowing simulation usign a) no nozzle; b) nozzle 5

4.4.2. EFFECT OF H ON THE PREDICTED VOIDS

The effect of height (H) is analyzed using the nozzles 3 and 4 with, respectively, H of 37 mm and 42 mm, keeping the other dimensions the same (D_1 and D_2). Figure 45 represents the predicted voids in the cores with the nozzles 3 and 4 after the core blowing simulation using the minimum pressure. The same effect with the maximum pressure is represented in figure 46. It is visible that increasing H, for both minimum and maximum pressures, the proportion of voids increases. This increase of the height H is harmful to the soundness of the core. Comparing the minimum pressure with the maximum pressure, due to a bigger difference between the density of the voids in both nozzles, the effect of H is more pronounced in the second case. Thus, it is concluded that for the same pressure, increasing the height H, the density of the voids is increased. On the other hand, increasing pressure and keep the H the same, the voids density increases as well, but in a greater proportion.

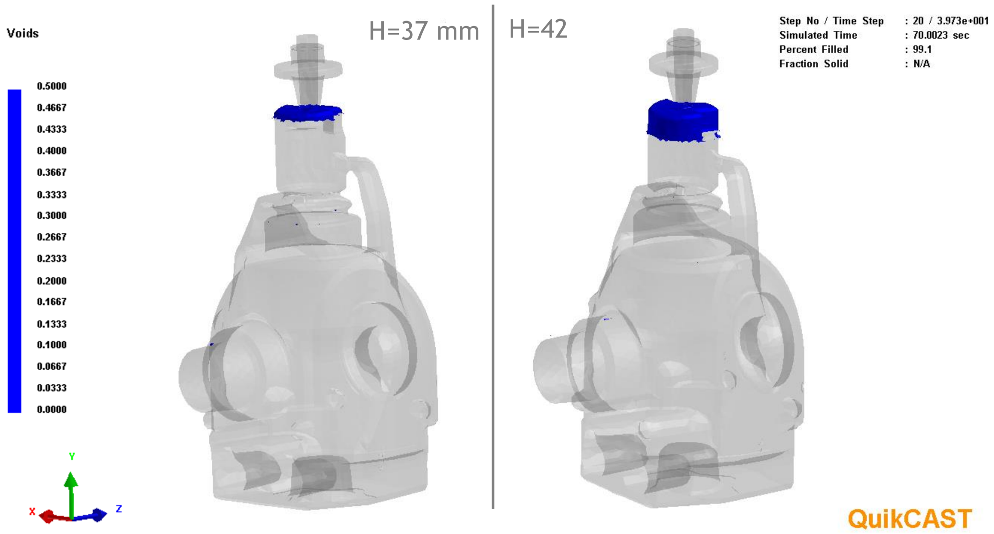

Figure 45: Predicted voids after core blowing simulation obtained with the lowest pressure using the nozzle 3 with H of 37 mm and the nozzle 4 with H of 42 mm. Using a higher H, the voids density increases

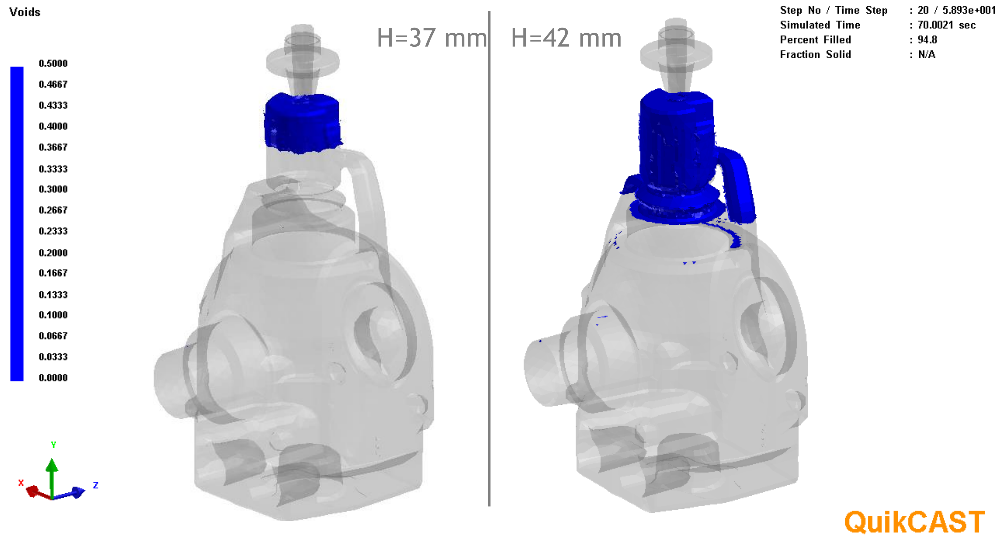

Figure 46: Predicted voids after core blowing simulation obtained with the highest pressure using the nozzle 3 with H of 37 mm and the nozzle 4 with H of 42 mm. Using a higher H, the voids increases extensively in comparison with the lowest pressure

4.4.3. Effect of D_2 on the predicted voids

To analyze the effect of diameter D_2, were selected the nozzle 2 and 4 with, respectively, D_2 of 12 mm and 18 mm. Both nozzles have the same H and D_1. Figure 47 represents the predicted voids after the core blowing simulation with nozzle 2 and nozzle 4 with minimum pressure. Here it is verified that the differences between both are not substantial, despite nozzle 2 presents a greater voids proportion in comparison with the nozzle 4. Figure 48 shows the effect of the same dimension D_2 using the higher pressure for both nozzles. In this case, using higher pressure, the effect of voids is more significant. Thus, in comparison with the minimum pressure, it is obtained a much greater voids density in the core 2 when the maximum pressure is used.

Summing up, increasing D_2 decrease the density of the void. This effect is extensively enhanced when the used shooting pressure is increased. These results are consistent with the results obtained in practice.

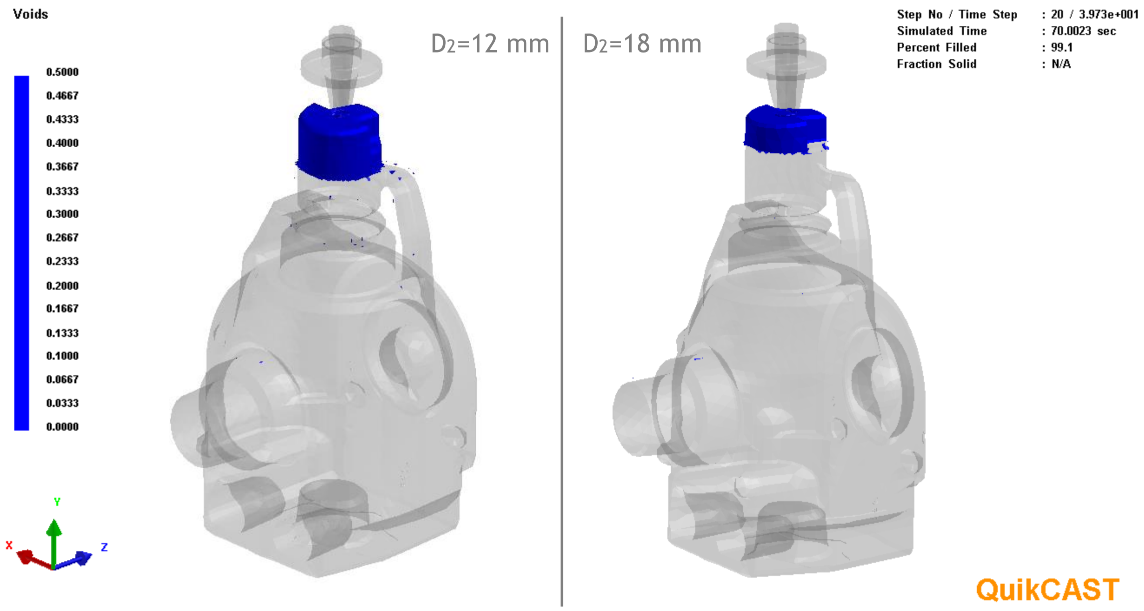

Figure 47: Predicted voids after core blowing simulation obtained with the lowest pressure using the nozzle 2 with D_2 of 12 mm and using the nozzle 4 with D_2 of 18 mm. The effect of voids density increase using a nozzle with lower D_2 is not significant

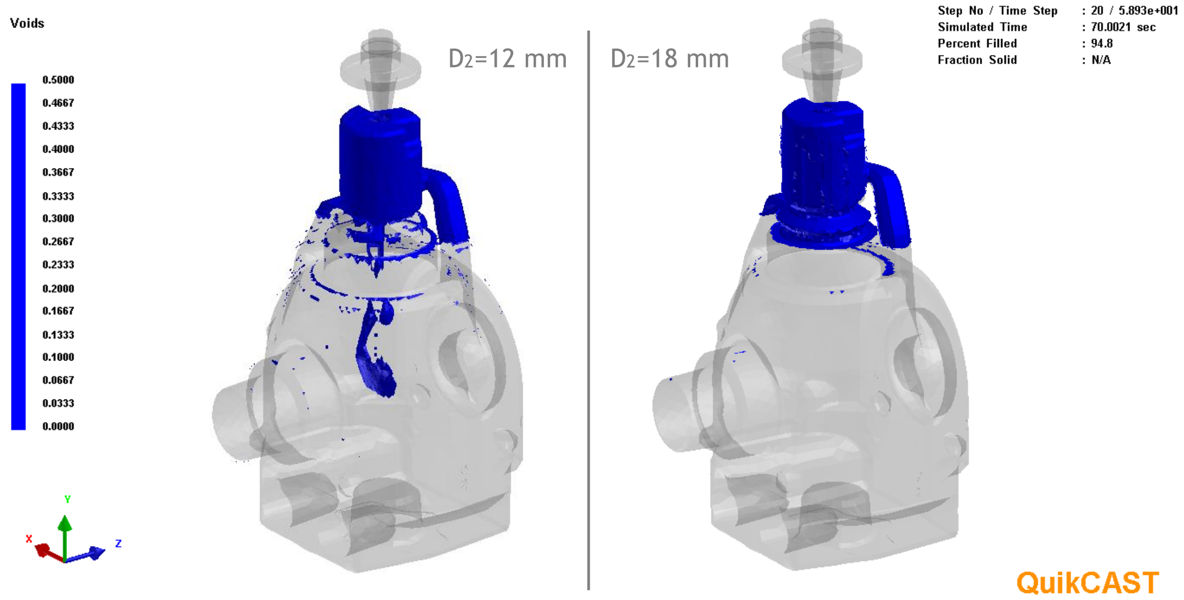

Figure 48: Predicted voids after core blowing simulation obtained with the highest pressure using the nozzle 2 with D_2 of 12 mm and the nozzle 4 with D_2 of 18 mm. Using a lower D_2, the voids proportion increases extensively

4.4.4. EFFECT OF SHOOTING PRESSURE ON THE PREDICTED VOIDS

In order to evaluate the effect of used shooting pressure in the soundness of core, it is analyzed for the same nozzle, the produced voids density after using the minimum and the maximum pressure. In figures 47 a) and 48 a) for nozzle 2, it is observed that the increase of shooting pressure produces an increase in the density of the formed voids. Nevertheless, the same considerable effect is not visible in nozzles with a bigger D_2, such as nozzle 3 represented in figures 45 a) and 46 a), nozzle 4 represented in figures 45 b) and 46 b), and for nozzles with bigger D_2, like 5 and 6 (see Annex X). Therefore, it is concluded that the effect of increasing the shooting pressure is much more significant using nozzles with a D_2 dimension of 12 mm.

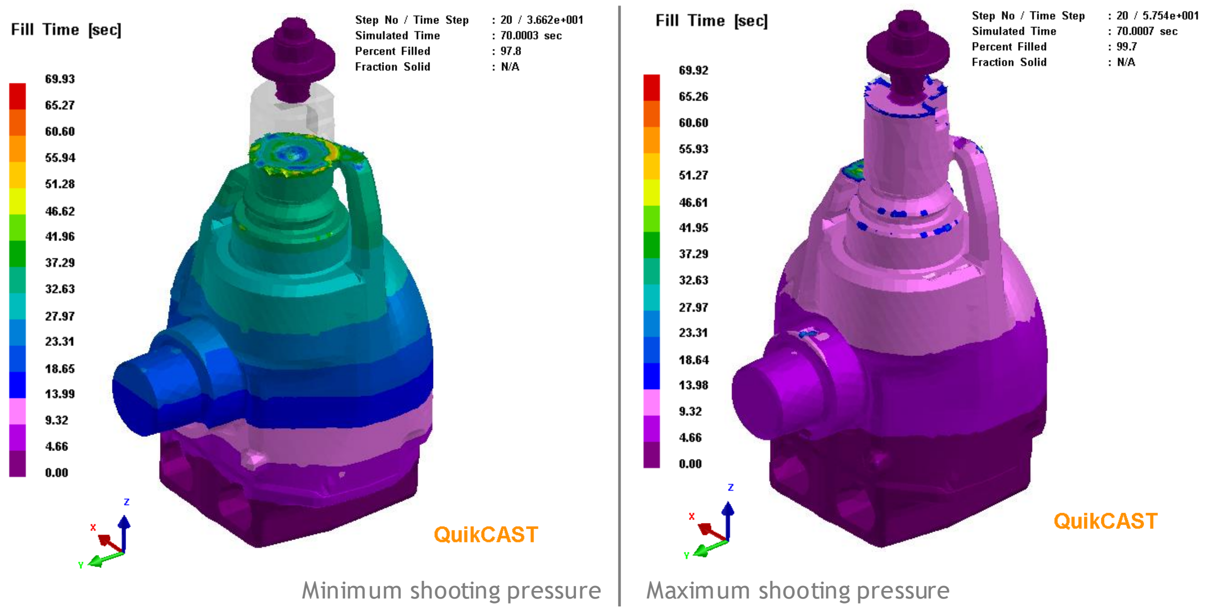

Figure 49: Filling time using nozzle 5 with the lowest pressure and the 294 kPa

4.4.5. EFFECT OF VENTS PROPORTION ON THE PREDICTED VOIDS

To assess the effect of vents proportion in the density of the voids after core blowing simulation, figure 50 shows the effect of the used vents in practice (representing 100%), 50% and 0% of them, using nozzle 5 and the minimum pressure. It is verified that there is not a linear tendency in the density of the formed voids by decreasing vents proportion. However, it is noticeable that the most significant voids proportion is achieved when no vents were used. The filling time reached with 100%, 50% and 0% of voids proportions is, respectively, 33 s, 40 s, and 45 s. Accordingly, fill time increases with a decrease in vents proportions.

Nevertheless, gas behavior cannot be evaluated by the core blowing simulation. Thus, a gassing simulation is suggested in order to enable the visualization of potential inadequate cured areas and, therefore, remove them through the modification of the process, such as vents proportions. Since the process profit also depends on the used vent proportion, it is crucial to determine their optimum number, using the minimum vents density that can provide the best core integrity and minimize defects formation.

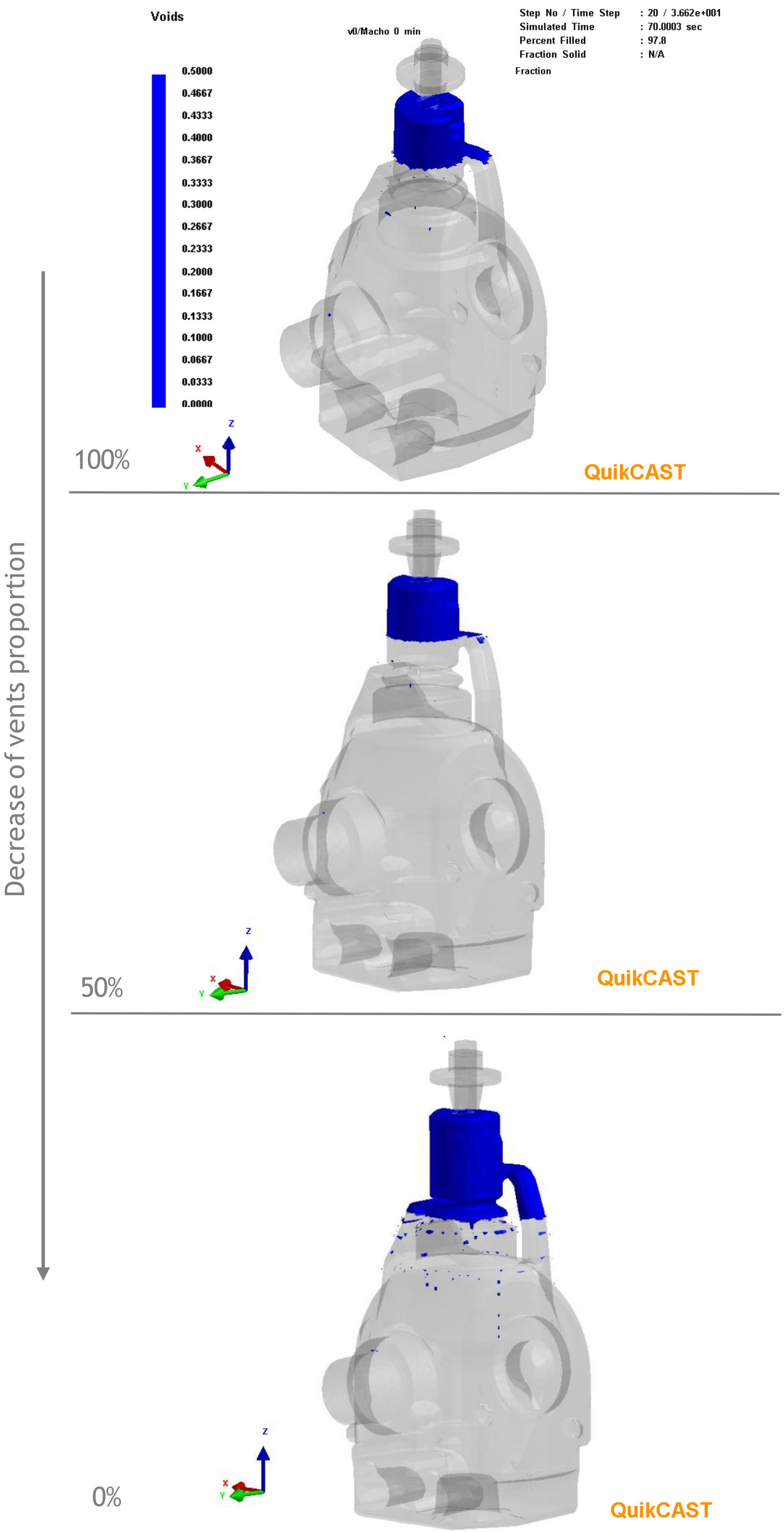

Figure 50: Predicted voids density produced in core blowing simulation according to the vents proportions. The biggest voids proportion is achieved when no vents are used

5. CONCLUSIONS AND FUTURE DEVELOPMENTS

5.1. CONCLUSIONS

All purposes of the present master thesis were achieved. Therefore, the most relevant conclusions of this thesis are:

Two mold cavities pattern plate

1) The directional solidification caused by the displacement of the internal chills, the predicted porosity towards the feeders 1 and 2 and, thus, remove the porosity of 10% which is obtained in practice;
2) The porosity of 13%, obtained in real practice, is removed in simulation by using an extra feeder (feeder 5);
3) With the introducing of these two changes, the obtained system yield was around 58%, against 59% obtained with the used one in practice (system B);
4) The proposal of using internal chills has the drawback, in practice, of introducing them in core before each pouring.

Three mold cavities pattern plate

1) The main hindrance in the design of gating and feeding system for three mold cavities is the limited pattern plate area, which does not allow the best feeders disposition in order to achieve a casting free of porosity;
2) Due to the inversion position of one of three mold cavities (mold cavity A), the porosity is influenced negatively;
3) The suggested position of the feeder 4 requires a reduce of core prints stability by cutting the intersected area with the feeder or a cut the same intersection from the feeder, ensuring the same stability of core prints;
4) Although feeder 4 was displaced to the possible closest section of the hot spot, its efficiency does not allow the porosity removal or, at least, the achievement of the same one obtained with two mold cavities pattern plate;
5) An internal chill close to the hot spot does not play an essential role in the prevention of the porosity in this section;
6) The last right gate of mold cavity C is not required since it does not supply liquid metal to this mold cavity and its absence does not interfere the reached thermal gradients and porosity;
7) The suggested gating and feeding system for three mold cavities achieves a system yield of 69% and a pattern yield of around 22%.

In both mold cavities pattern plate design, a velocity of liquid metal entrance in mold cavity below the critical 0,5 $m.s^{-1}$ was achieved by increasing the section area of gates.

Core blowing simulations

1) The nozzle's dimensions, the shooting pressure, and the vents rate influence the voids ratio present in cores after core blowing simulation;
2) It is crucial to use nozzles in core blowing simulation because the filling process and void prediction is influenced by the presence of the nozzle, not only in terms of inlet diameter (D_2) but also in terms of its height (H);
3) The dimension that influenced the most the obtained voids density after core blowing simulation is D_2;
4) The most critical D_2 dimension is 12 mm, which increases significantly voids density in comparison with nozzles with higher D_2 dimensions. This effect is confirmed by practice;
5) The increase of shooting pressure produces an increase of the predicted voids proportion, which is not consistent with the practice. This predicted effect is more pronounced using nozzles with D_2 of 12 mm;
6) The vents rate does not affect, linearly, the voids proportions produced after core blowing simulation. However, the most significant voids proportion is achieved when no vents are used.

5.2. FUTURE DEVELOPMENTS

Several possibilities may be done in future development, among others:

1) The proposed gating and feeding system for two mold cavities pattern plate increases porosity C in 10% at the machined area of the casting. This porosity increase may be solved by adding an internal chill in this spot or by adding the feeder 6 in the bottom part of the mold cavity;
2) By adding three internal chills in the bottom part of the mold cavity A, in three mold cavities pattern plate, it was verified that porosity a) was removed. Nevertheless, the porosity c) increased up to 55%. Thus, in order to avoid porosity in this section may be tested the use of another spot to place the chills or the increase the dimensions of feeders 1 and 2, to compensate the noticeable contraction at the hot spot according to the volume requirement;
3) To determine the minimum vents density that can minimize defects formation is suggested a gassing simulation.

REFERENCES

1. Jiyang, Z., *Colour Metallography of Cast Iron*. 2010, CHINA FOUNDRY: China.
2. *Modeling of Casting, Welding and Advanced Solidification Processes* Vol. VIII. 1998, United States of America: The Metals & Materials Society.
3. International, A., *Handbook Cast Irons*, ed. D.J. R. 1996, United States of America: ASM International.
4. Yu Yun, H.J., Li Xiaoping, *The Sensibility of Mold Dilation and Graphite Precipitation for the Simulated Porosity in Ductile Cast Iron*. Applied Mechanics and Materials, 2012: p. 1455-1459.
5. Hernando, J.C., *Morphological Characterization of Primary Austenite in Cast Iron*, in *Department of Materials and Manufacturing* 2017, SCHOOL OF ENGINEERING, JÖNKÖPING UNIVERSITY: Jönköping, Sweden.
6. Campbell, J., *Complete Casting Handbook - Metal Casting Processes, Metallurgy, Techniques and Design*. First Edition ed. 2011, United Kingdom: Elsevier.
7. *Modeling of Casting, Welding and Advanced Solidification Processes*. Vol. VII. 1995, United States of America: The Mineral, Metals & Materials Society
8. Group, E. *ProCAST / QuikCAST*. 2019; Available from: https://www.esi-group.com/pt/solucoes-de-software/fabricacao-virtual/fundicao/procast-quikcast.
9. *Modeling for Casting and Solidification Processing*. 2002, New York - United States of America: Marcel Dekker, Inc.
10. Samonds, M., Guo J., *Modeling of alloy casting solidification*. JOM: the Journal of The Minerals, Metals & Materials Society Vol. 63(7). 2011: p.19-28.
11. Group, E., *Getting ready with QuikCAST*. 2016.
12. Marin-Alvarado, T., *Modelling Scheil Cooling of a Metal Alloy – Thermodynamic and Multiphysics Solidification* in *COMSOL Conference* 2016: Boston, United States of America.
13. Hai-feng WANG, F.L., Kang WANG, Hai-min ZHAI, *Effect of back diffusion on overall solidification kinetics of undercooled single-phase solid-solution alloys*. Transaction of Nonferrous Metals Society of China, Elsevier, Science Press, 2012.
14. Hugh Kind, R.N., Nick Wukovich *Foundry Practices*. American Foundry Society, 2010: p. 177-191.
15. Siavashi, K., *The Effect of Casting Parameters on the Fluidity and Porosity of Aluminium Alloys in the Lost Foam Casting Process* in *School of Metallurgy and Materials*. 2011, Faculty of Engineering of The University of Birmingham United Kingdom.
16. Thomas Borsato, P.F., Filippo Berto, Carlo Carollo, *Effect of Solidification Time on Microstructural, Mechanical and Fatigue Properties of Solution Strengthened Ferritic Ductile Iron*. Metals, 2018.
17. Mahi Sahoo, P.D., Sudhari "Sam" Sahu, Ph.D., *Principles of Metal Casting*. Third Edition ed. 2014, New York, Chicago, San Francisco, Athens, London, Madrid,

Mexico City, Milan, New Delhi, Singapore, Sydney, Toronto: McGraw-Hill Education.
18. Guruswamy, S., *Engineering Properties and Applications of Lead Alloys*, ed. C. Press. 1999.
19. M. Schneider, R.S., *Simulation of the entire core production process* American Foundry Society 2012.
20. Dominique Lefebvre, A.M., Valérie Vidal, Vincent Pavan, Peter M. Haigh, *Development and use of simulation in the design of blown cores and mould, Foundry Trade Journal, vol.179 no.3621 p.17-20, 2008.*
21. Dańko, J.Z., J. Dańko, R. , *Diagnostic methods of technological properties and casting core quality*. Archives of Metallurgy and Materials, 2009. **54**: p. 382-392.
22. WAGNER, J.C.S.A.I., *Real-World Application of Core Simulation for Process Optimization*
23. Stefanescu, D., *Science and Engineering of Casting Solidification*. 2009, Springer US.
24. International, A., *Casting Design and Performance*. 2009: ASM International.

ANNEX I – ADJUSTMENTS AT THE *QUIKCAST* TUTORIAL OF CORE BLOWING SIMULATIONS

Some changes and suggestions were done in the ESI's tutorial for core blowing simulations which are represented in pages 62, 63 and 72. As descried in page 62, a *.igs* file was used to import the core to *QuikCAST* instead of the suggested *.stl* file, which in this case does not allow the right inlet building on the top of the nozzle and, afterwards, originates mesh problems that do not enable the running of the simulation. In page 63, it is noted that the inlet area should not have any fillet in order to extract the correct curve. Page 72 suggested using a maximum time higher than 20s, because of the need for more time to fill the core box when a nozzle is used.

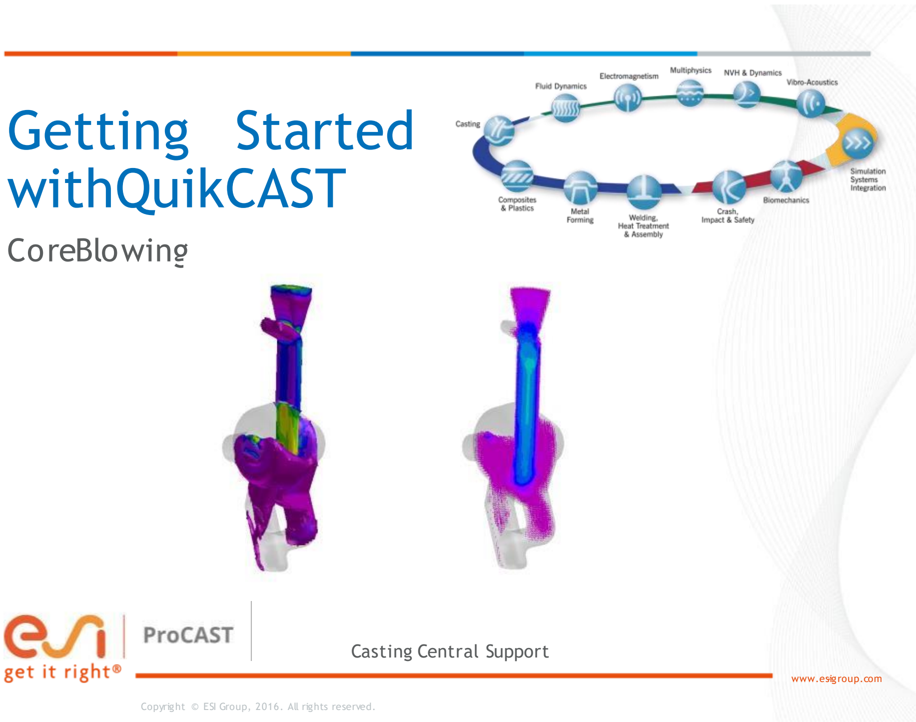

The goal of this tutorial is to show a typical workflow for the setup of a Core Blowing Simulation.

Note 1 : Basic knowledge of the Visual Environment is required

Note : what is shown is one way of using the software. It does not mean that this is the only way of using it.

For the best visualization experience, please run the presentation in Slide Show Mode

get it right®

2

Activating QuikCAST functionalities in Visual Environment

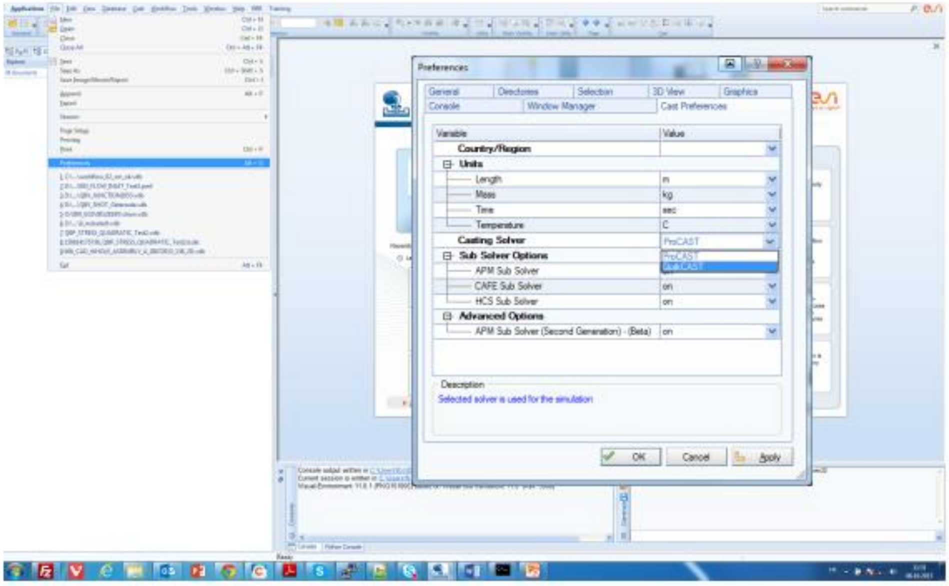

- Go to Files / Preferences
- In Cast Preferences / Casting Solver select QuikCAST

get it right® www.esi-group.com 3

In this case, importing a *.stl* model does not allow the correct mesh execution and, afterward, does not enable the running of simulation. So, an *.igs* model may be an option. However, here a manual meshing is required

Loading Files / Visual-Mesh

1 File / Open

2 Import Core.stl

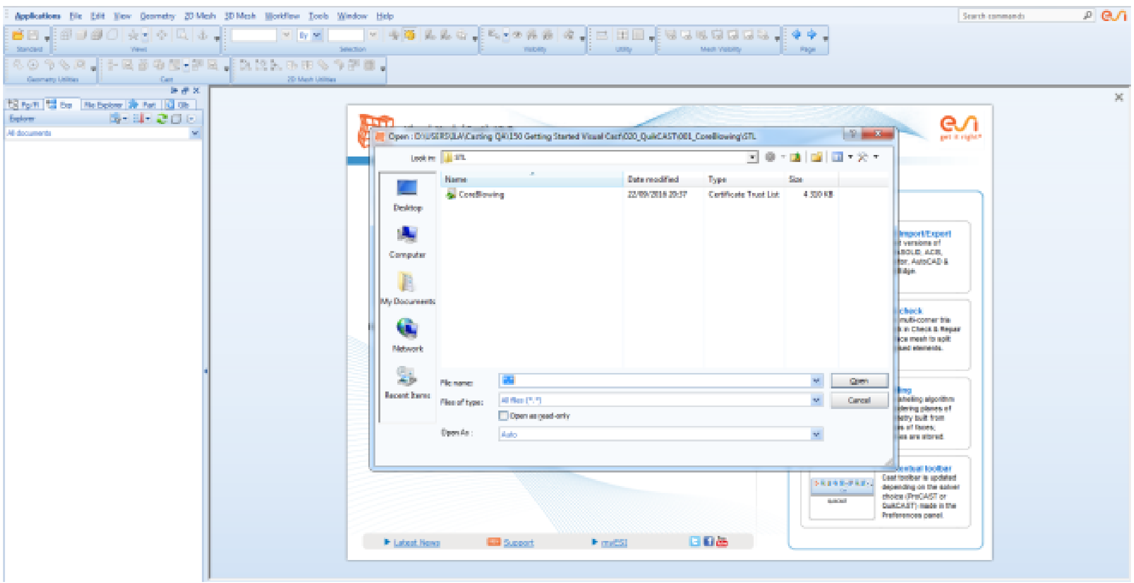

get it right® www.esi-group.com 4

Mesh Repair

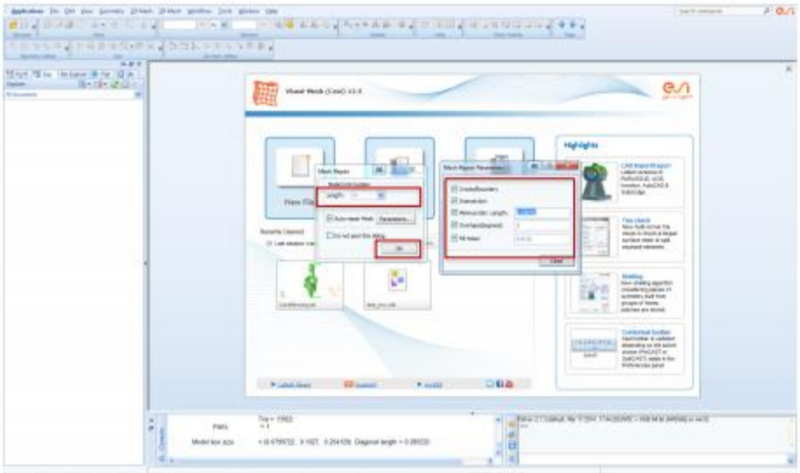

After loading STL file :

- Model Unit System is set to m.
- Automatic check of surface mesh will be performed
- Surface mesh will be corrected after confirmation from the user
- Volumes are computed
- Non-coincident Interfaces are computed

Here it is important to note that to a correct curve extract, the inlet surface should not have any fillet

Inlet creation

1 Go to Geometry > Curve > Extract

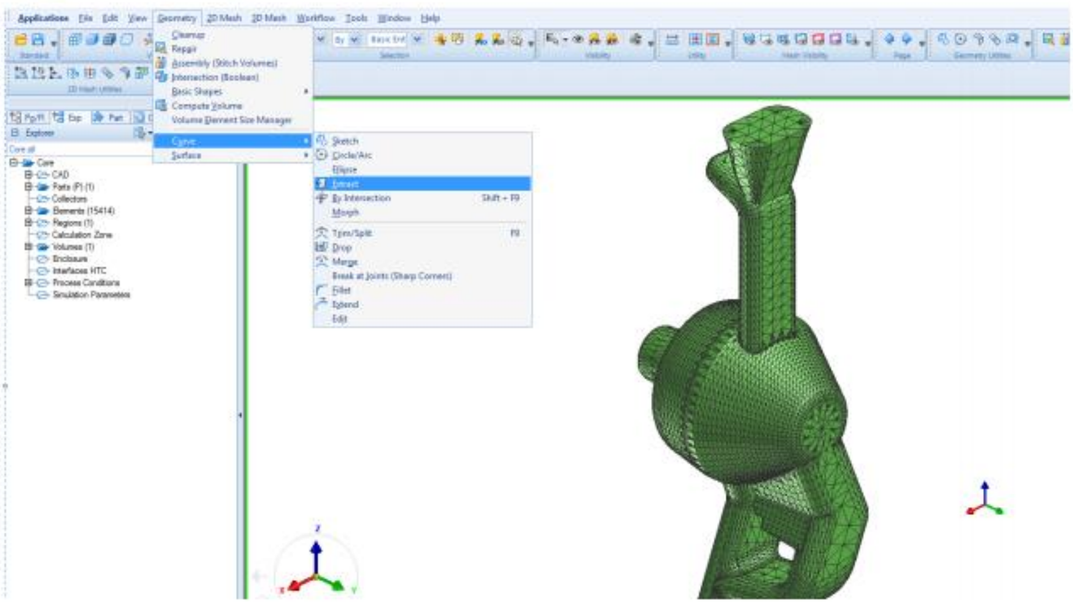

1 Select Element Faces

2 Activate contiguous selection and select this surface

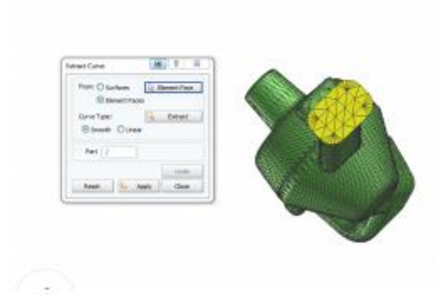

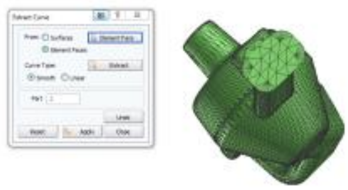

3 Click on Extract then Apply

1 2D Mesh > 2D > Sweep (Drag)

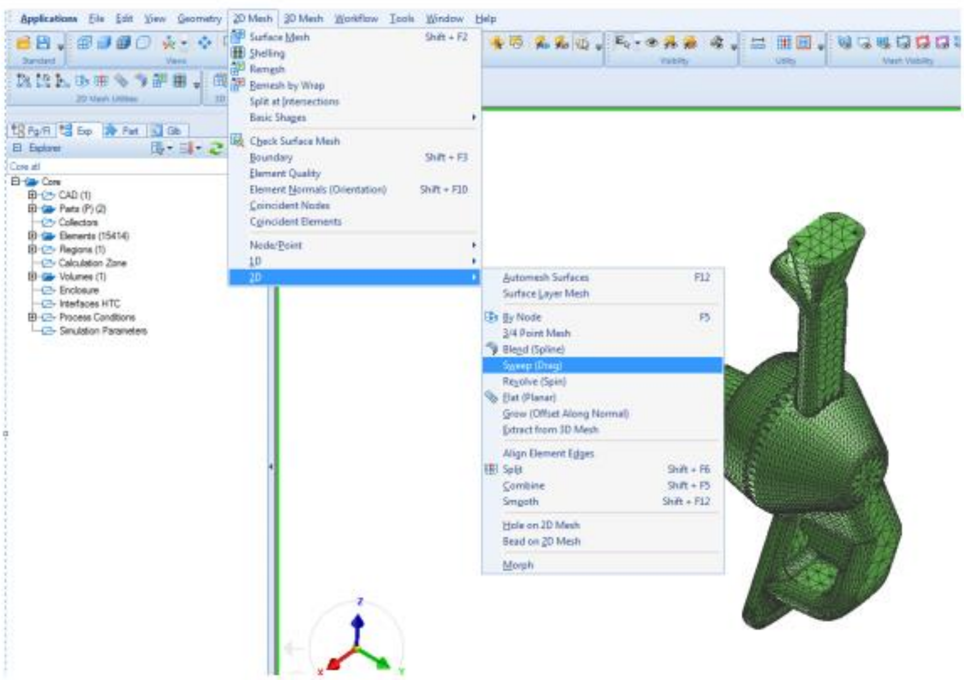

1 Select Multiple curves and pick the curve extracted

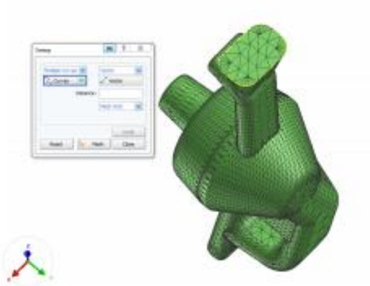

2 Select the element normal then click OK

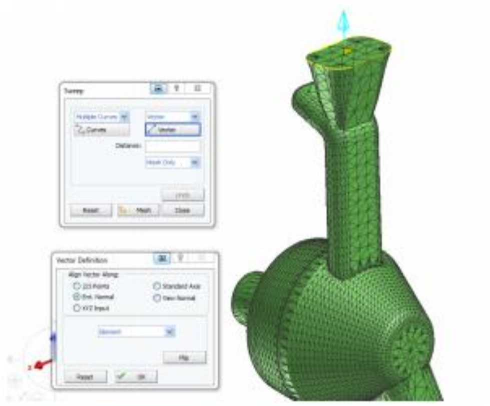

get it right®

1 Set the distance to 0.01 then click on Mesh

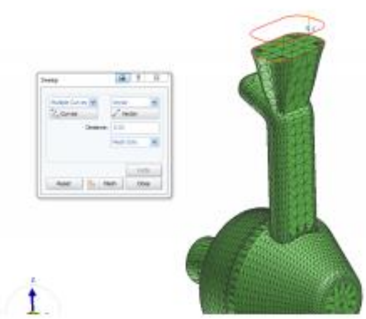

2 Set the element size to 0.01

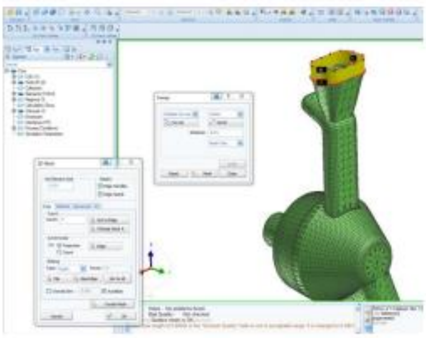

3 Click on Create mesh

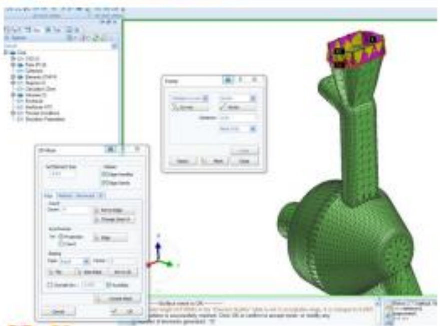

4 Click OK then Close

get it right®

1 Go to Geometry > Curve > Extract

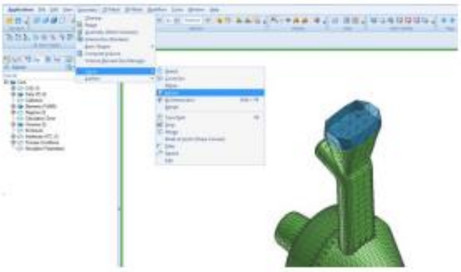

2 Contiguous selection and select the inlet

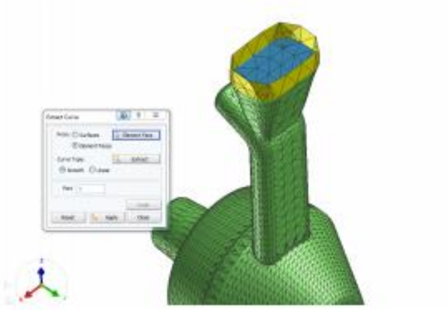

3 Click extract then Apply

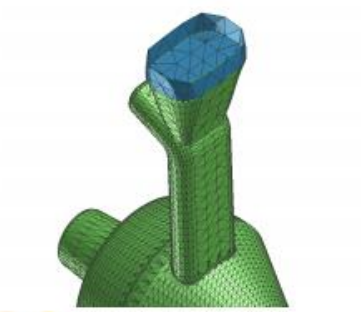

4 2D mesh > 2D > Flat (planar)

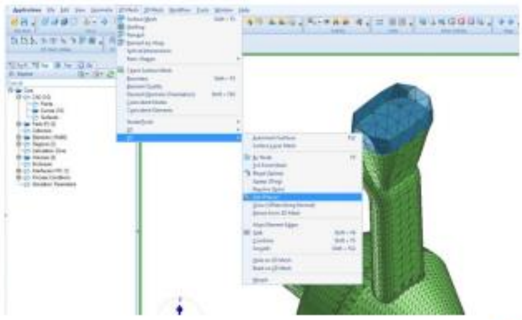

1 Select curves

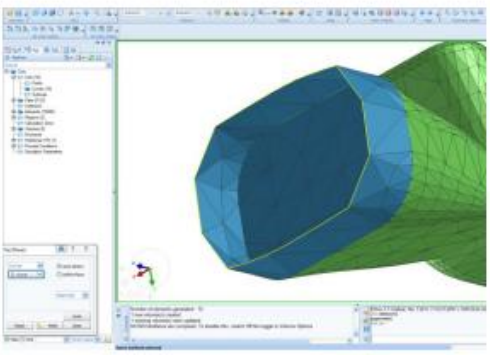

2 Pick the upper curve then confirm

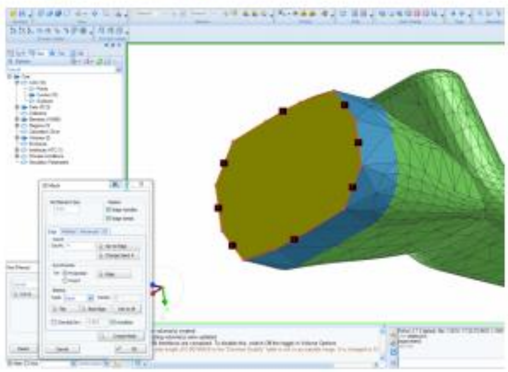

3 Click Create mesh then confirm

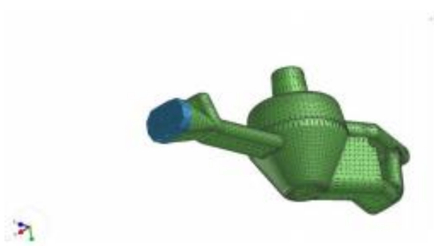

4 Delete the curves

1 Tools > Volume Options

2 Update the volume by clicking on Compute

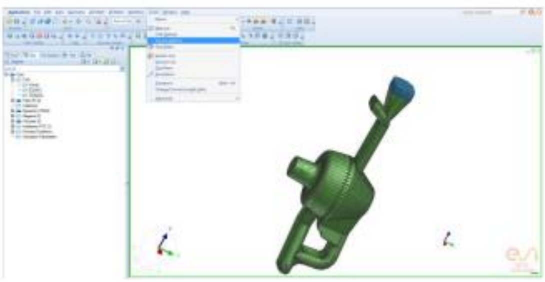

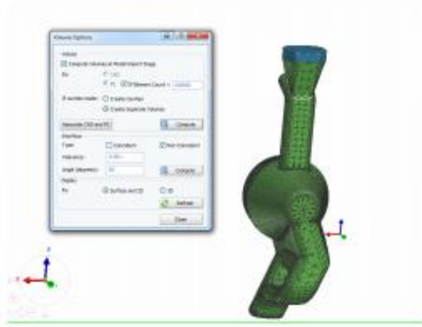

3 Check surface mesh using coarse method

4 Surface mesh is OK

Visual-Cast / Setup

Set Gravity Axis

1 Applications > Cast

2 Set Gravity direction to -Z Axis then Apply and Close

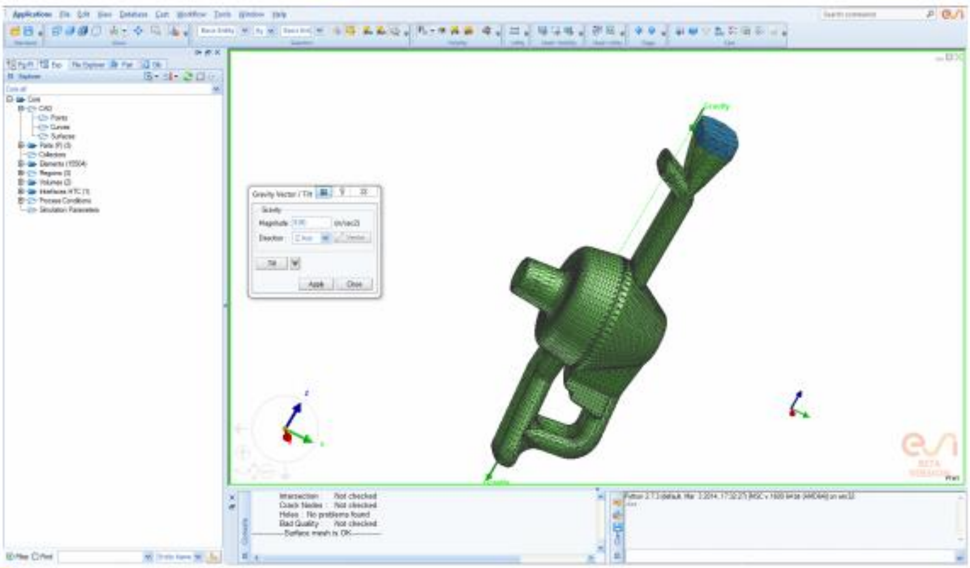

Assign Volumes conditions

1
- Right Click on Volumes
- Edit

2 Rename volumes as shown
- Set the type of both Core and Inlet to « Core Blowing »
- Assign the material from the public DB / Category : CORE
- Put the initial temperature to 20 °C

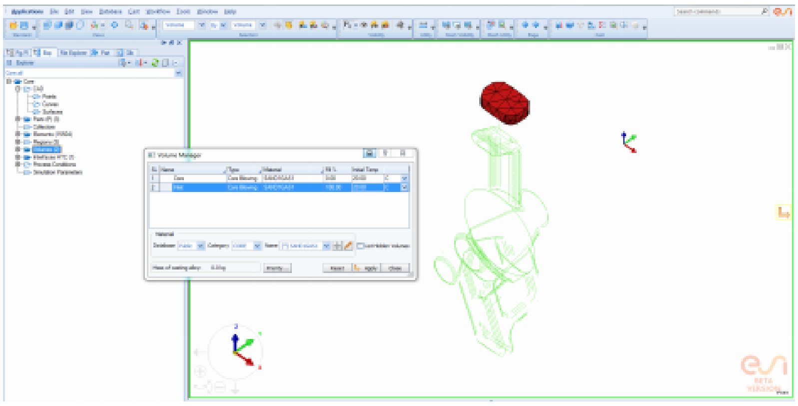

Boundary Conditions – **Pressure**

1 Create a new Pressure BC

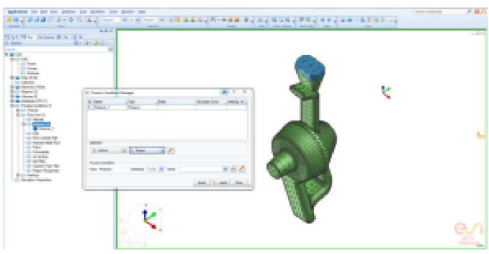

2 Define Region :
Type : Element face
Select the upper surface of the inlet using contiguous selection

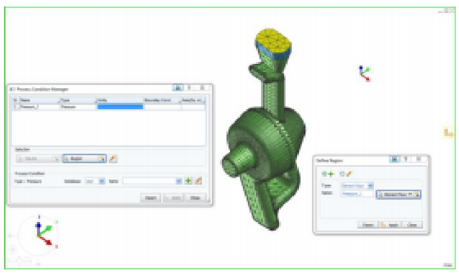

3 Add a pressure process condition :
Pressure : 500000 Pa
Condition Type : Imposed
Save and Close.

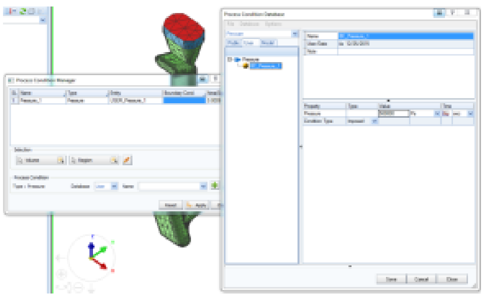

4 Apply and Close

Boundary Conditions – **Imposed Initial Fluid**

1 Create a new Imposed Initial Fluid BC

2 Select the Inlet Volume then confirm

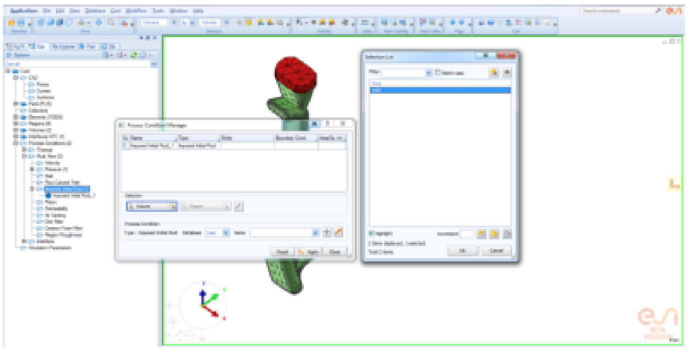

3 Put 100 % for the fill percentage

3 Apply then Close

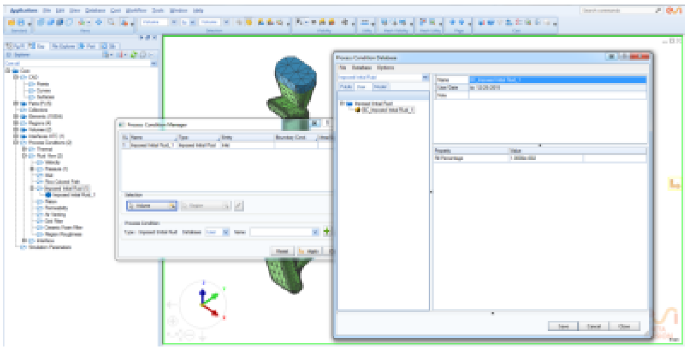

Boundary Conditions – **Air Venting**

1 Create a new Air Venting BC

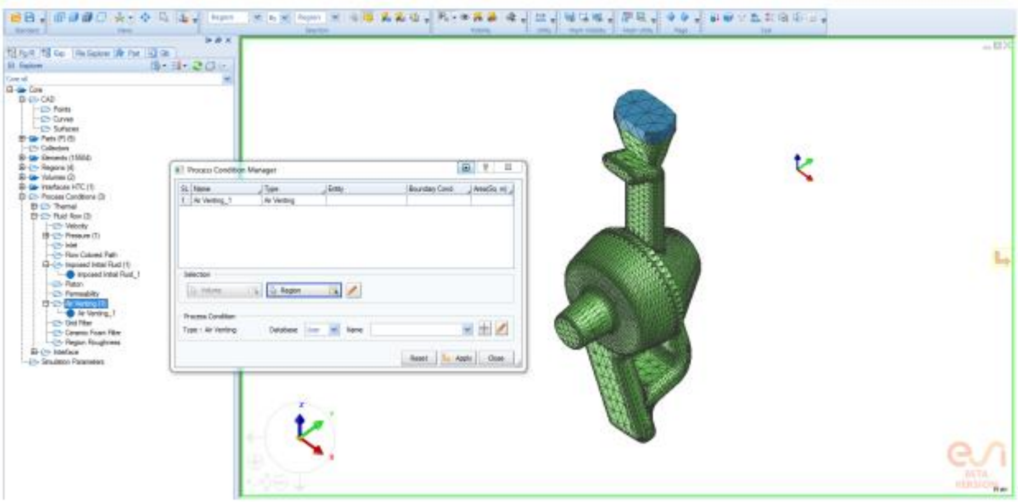

2 Define Region :
Pick venting regions as shown using
Element face selection

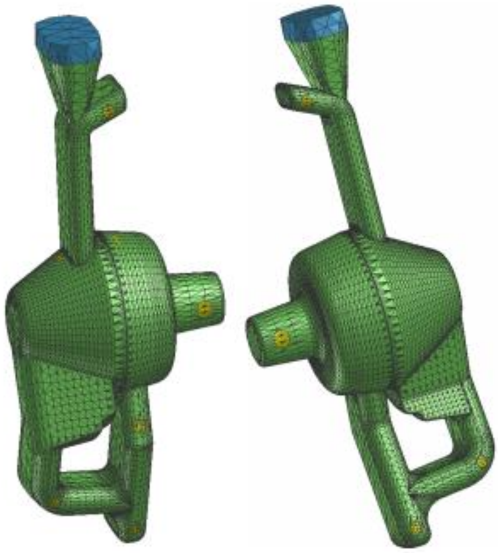

3 Set the Region Weighting factor to 20%

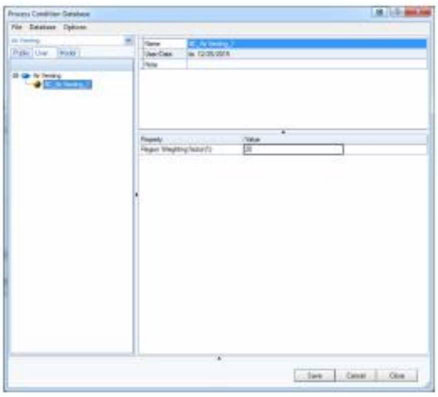

4 Save then Close

5 Click on Yes to apply
the Air venting BC

6 Apply and Close.

Boundary Conditions – **Region Roughness**

1 Create a new Region Roughness BC

2 Select the external core region

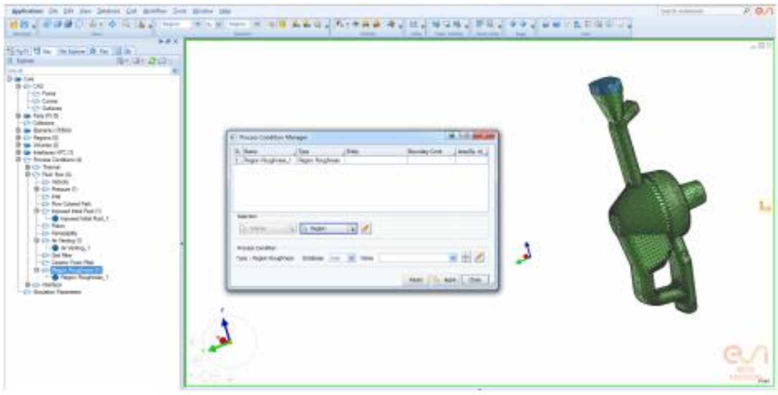

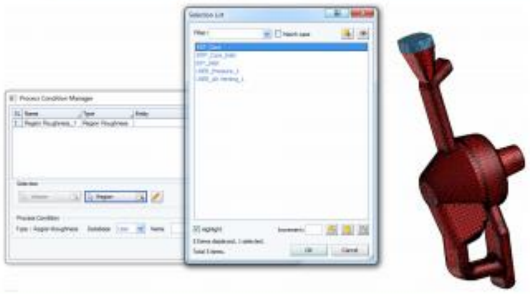

3 Input **0.05** for the roughness index

4 Save then Close

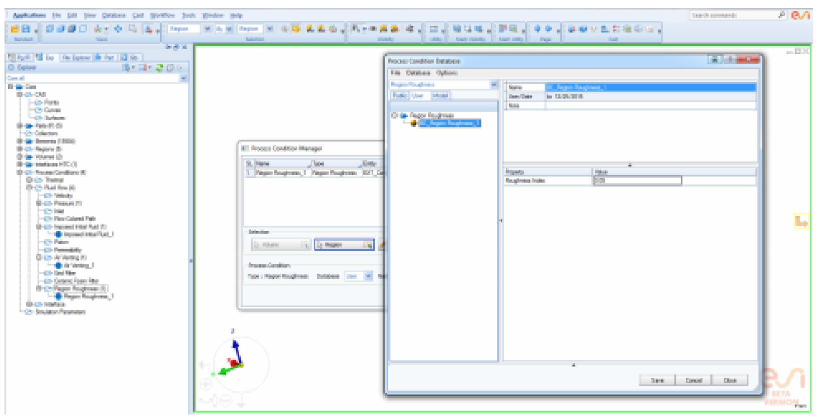

5 Validate the Region Roughness BC

6 Apply and Close.

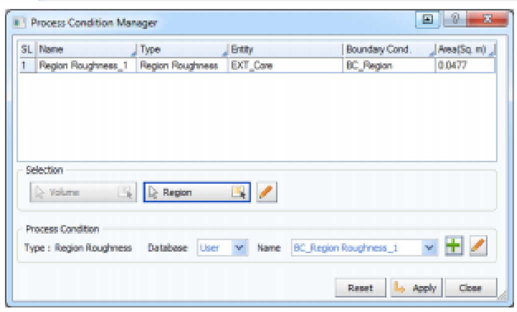

Simulation Parameters

1 Double Click on Simulation Parameters

2 QCA General Parameters :

- Simulation type : Sand Core
- Calculation type : Standard calculation
- Calculation Options : Blowing

3 - Set 1 for the **Convection time step accelerator factor**
- Deactivate the **Thermal calculation during filling**
- Set 1 for the **End of filling criteria**

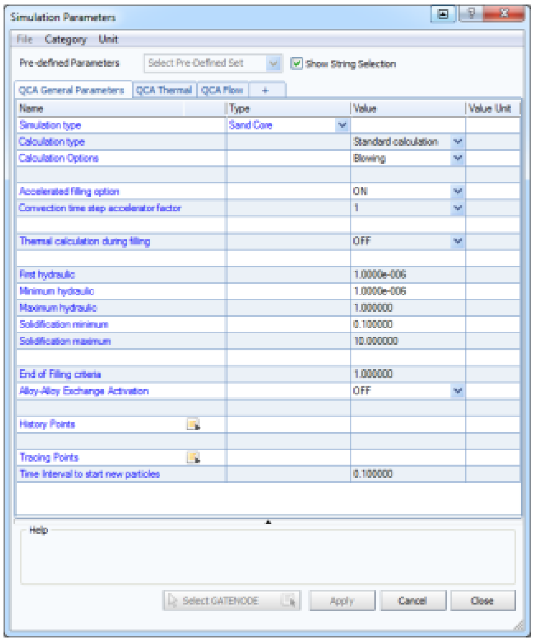

4 QCA Flow :

- Stop criteria : Time and % Fill
- Maximum Time : 20s
- Percent of Cavity filled : 95 %

5 Apply then Close

95% of filling produce some voids that are not visible when a higher value is used

The time may not be enough to fill the whole core box

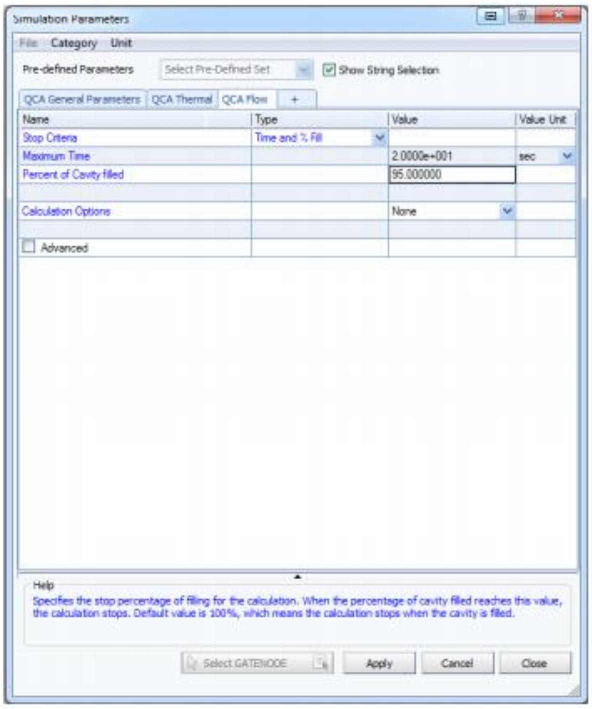

Tools / Grid Definition

1. Activate the advanced method
2. Select all the volumes
3. Set the values of the grid as shown
4. Apply and Close

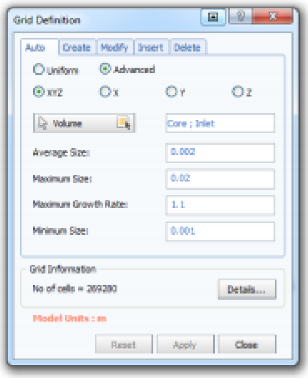

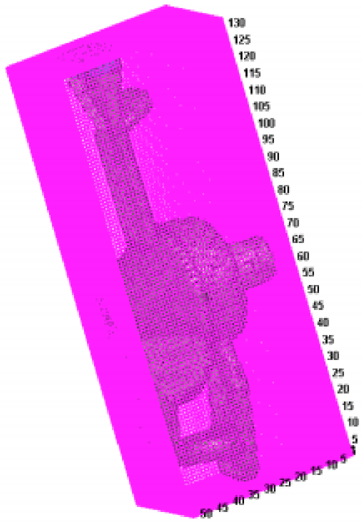

Cast / Start Simulation

1. Press 3D Mesh to generate the mesh
2. Meshing operation successful

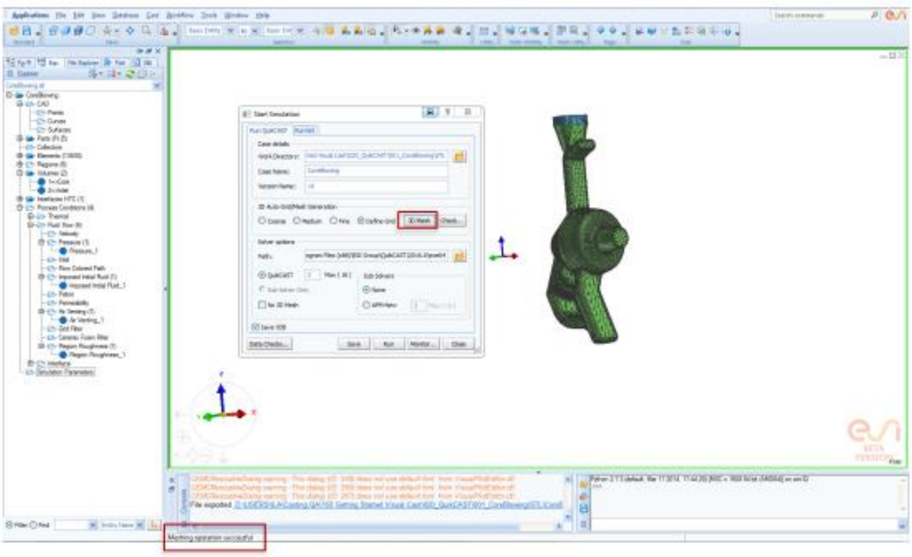

ANNEX II – EFFECT OF POURING TEMPERATURE ON THE OBTAINED POROSITY IN SYSTEMS A AND B

Section cuts of the obtained porosity of system B using a pouring temperature of 1375ºC.

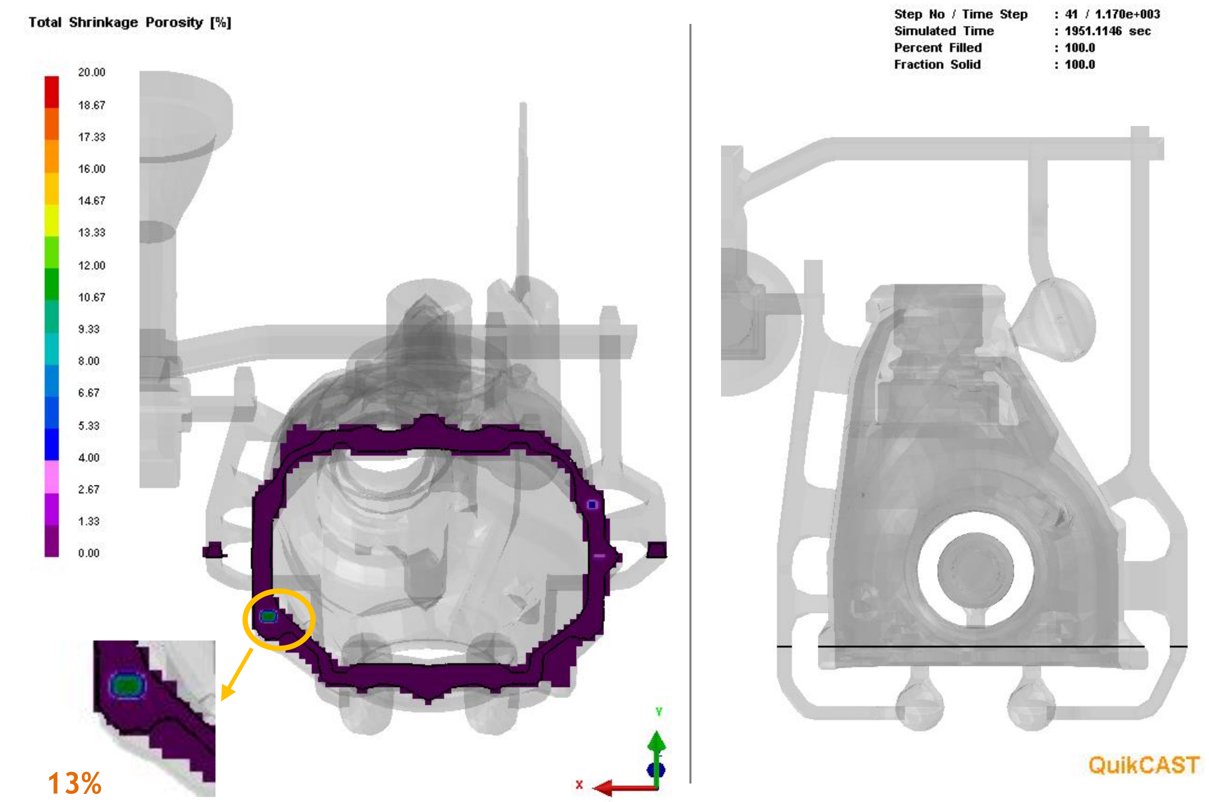

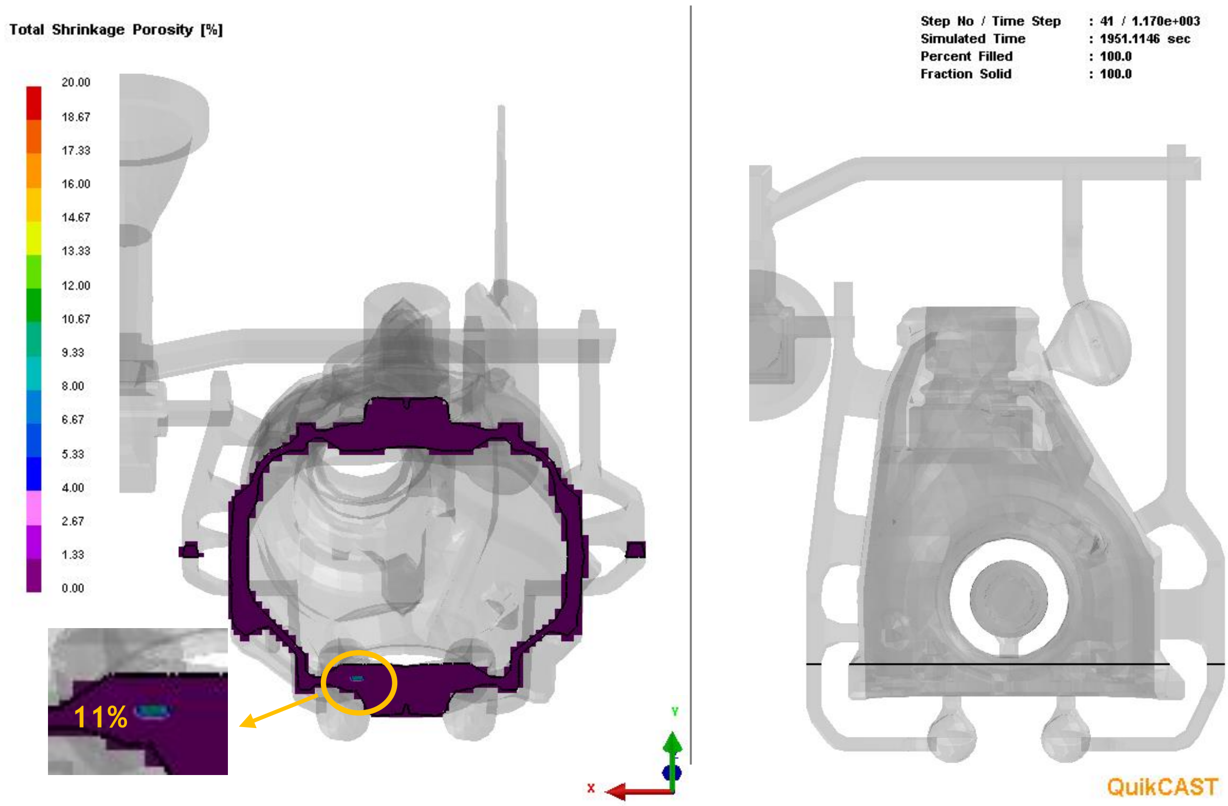

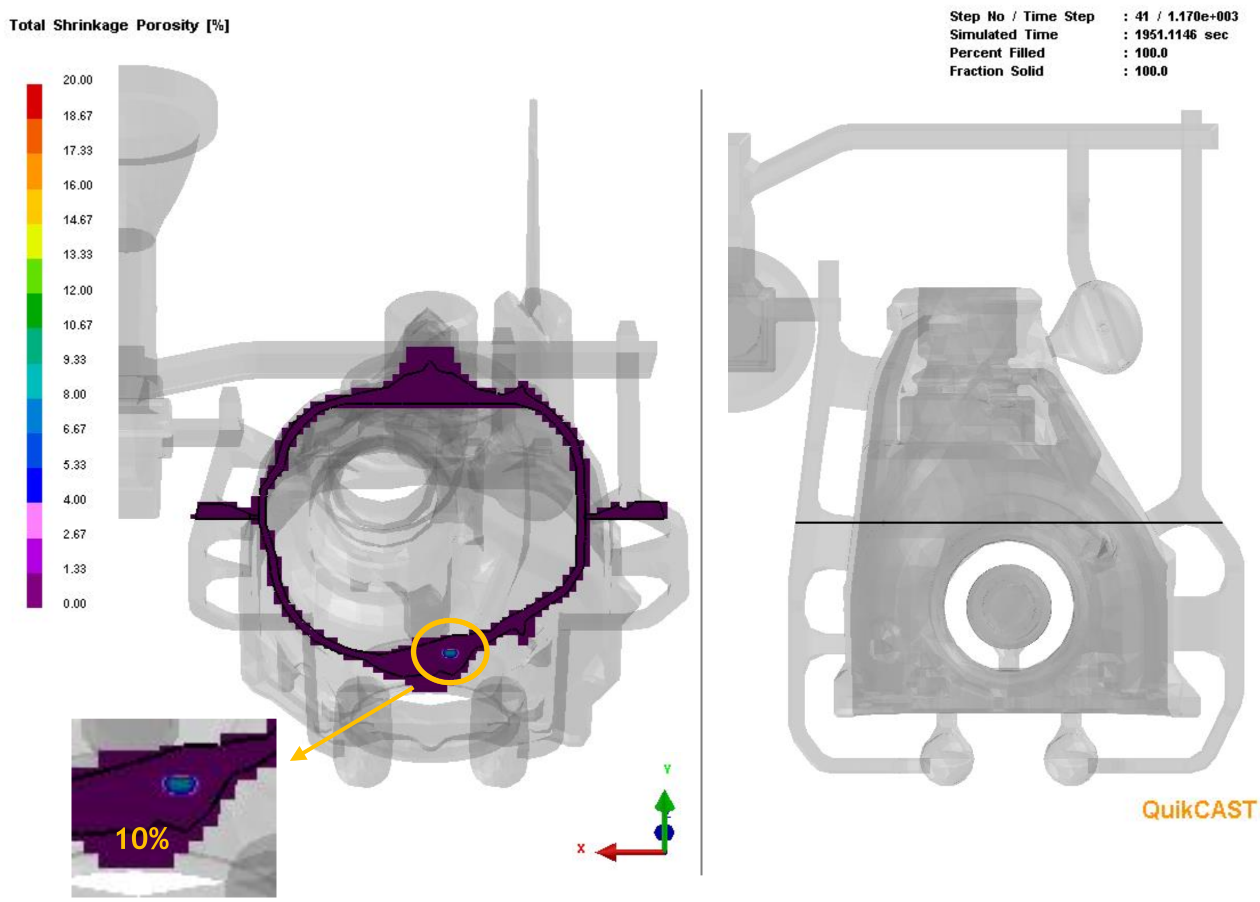

Section cuts of the obtained porosity of system B using a pouring temperature of 1400ºC.

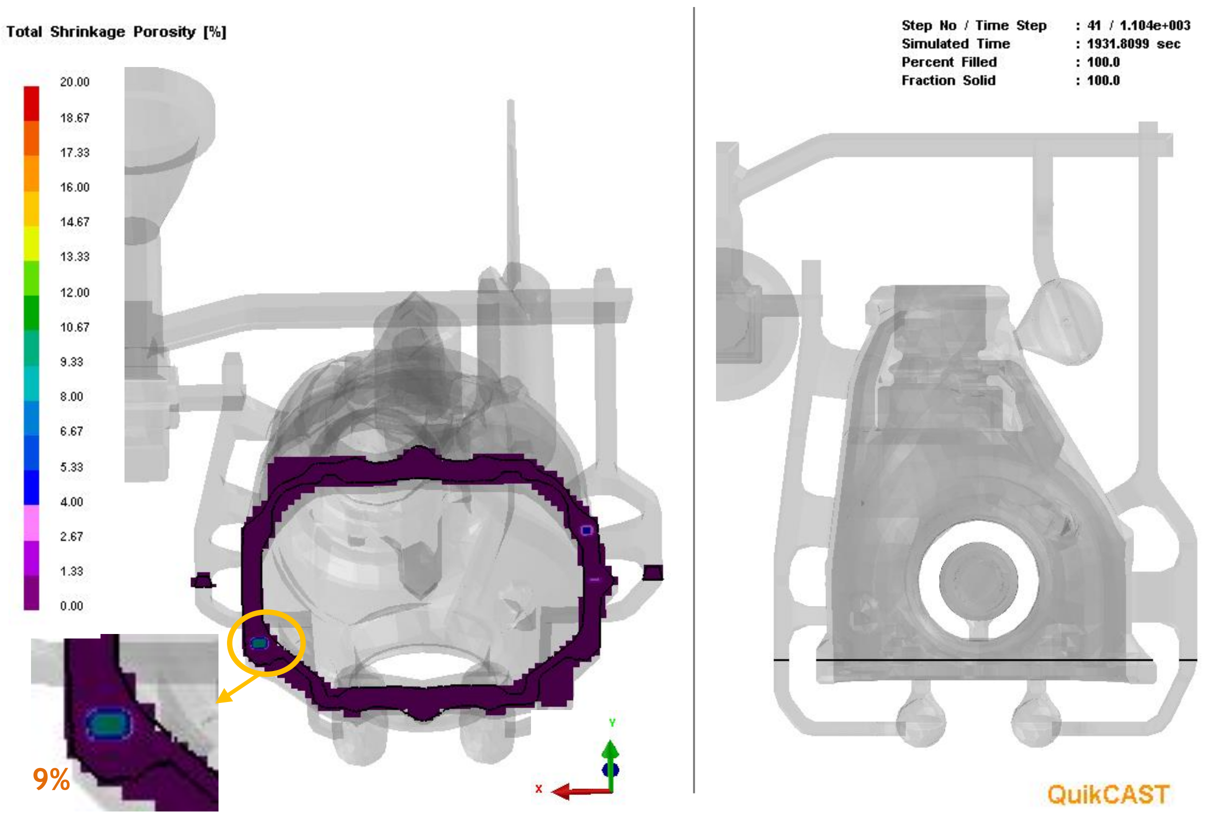

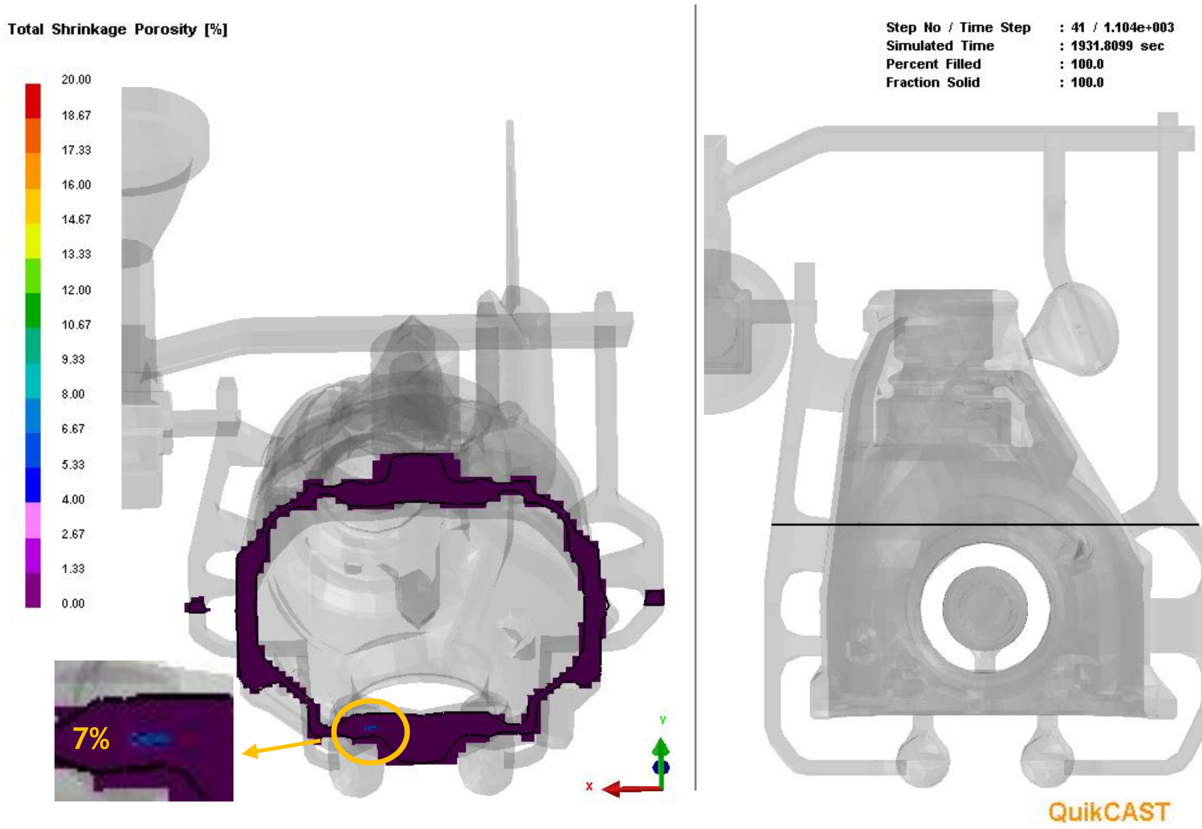
Total Shrinkage Porosity [%]
20.00
18.67
17.33
16.00
14.67
13.33
12.00
10.67
9.33
8.00
6.67
5.33
4.00
2.67
1.33
0.00
7%
Y
X
Step No / Time Step : 41 / 1.104e+003
Simulated Time : 1931.8099 sec
Percent Filled : 100.0
Fraction Solid : 100.0
QuikCAST

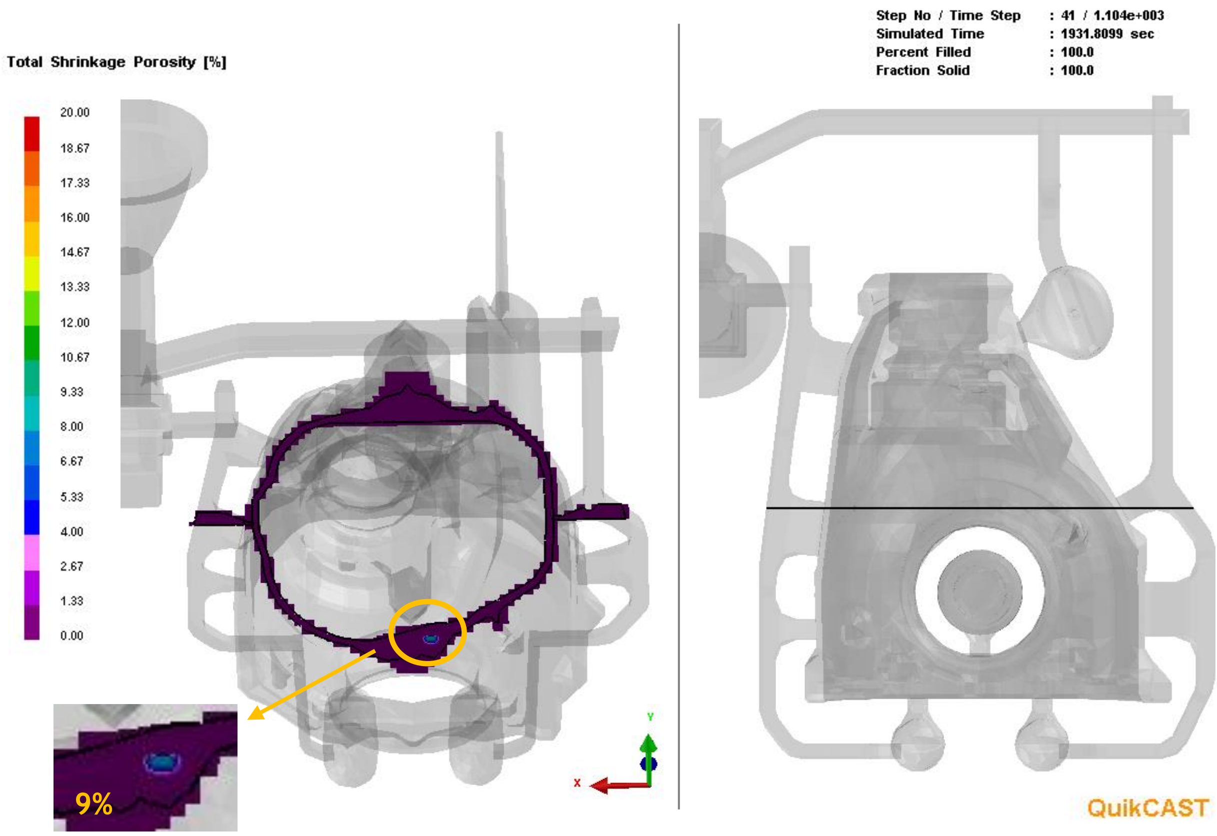
Step No / Time Step : 41 / 1.104e+003
Simulated Time : 1931.8099 sec
Percent Filled : 100.0
Fraction Solid : 100.0
Total Shrinkage Porosity [%]
20.00
18.67
17.33
16.00
14.67
13.33
12.00
10.67
9.33
8.00
6.67
5.33
4.00
2.67
1.33
0.00
9%
Y
X
QuikCAST

ANNEX III – RESULTS OF APPROACH 3 FOR TWO MOLD CAVITIES PATTERN PLATE

Approach 3 of the gating and feeding system for two mold cavities pattern plate, with an increase of 15 mm in the feeder's 1 diameter.

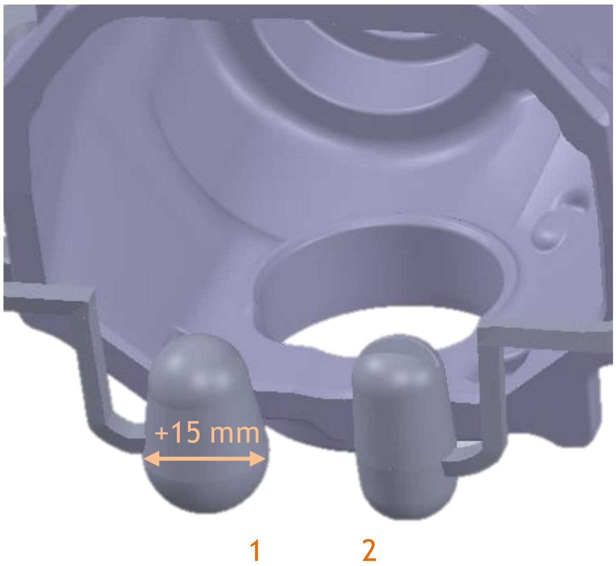

Predicted porosity in approach 3, where it is visible that a reduction of the porosity B up to 1.4% was achieved. The porosity C remains as 3% in the approach 2. The porosity D was reduced only up to 0.5%.

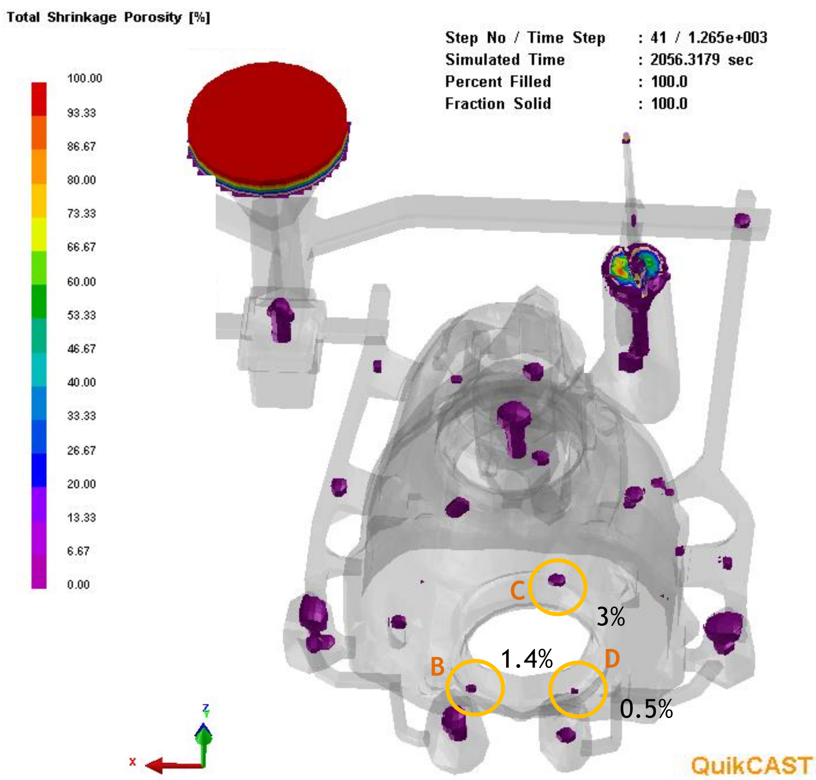

ANNEX IV – RESULTS OF APPROACH 5 FOR TWO MOLD CAVITIES PATTERN PLATE

Approach 5 of the gating and feeding system for two mold cavities pattern plate, where one internal chill was used in the bottom part of the mold cavity. In the spot where the internal chill was added, a decrease of solidification time was achieved and, in comparison with the approach 4, an increase of the solidification time of feeders 1 and 2 was achieved as well. However, it was not enough to avoid porosity B and D.

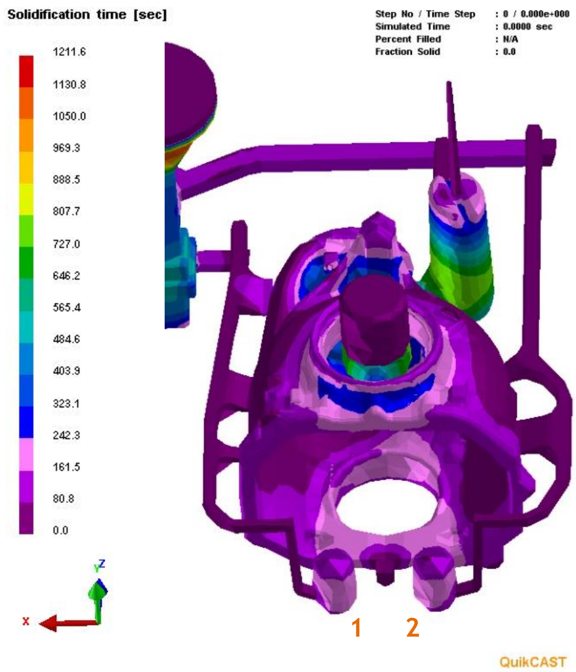

Predicted porosity of approach 5, where a porosity A of 10%, B of 3%, C of 3% and D of 3% were achieved.

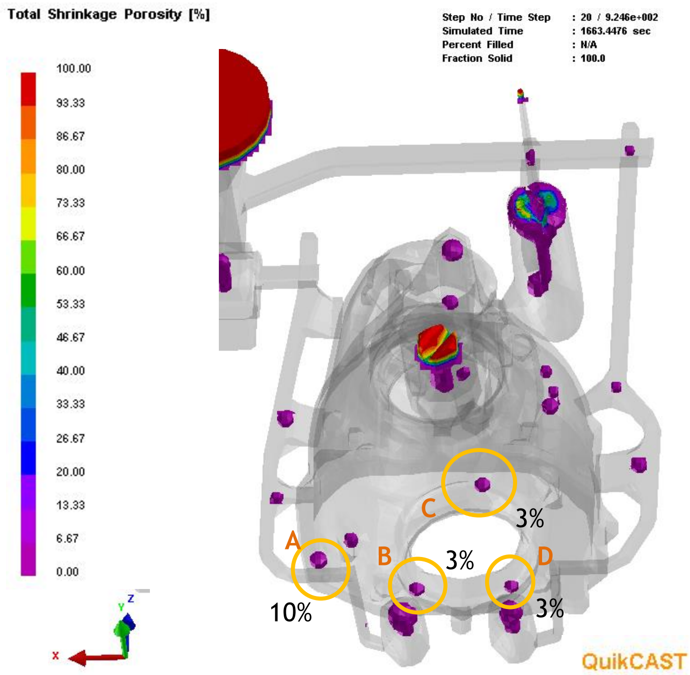

ANNEX V – RESULTS OF APPROACH 6 FOR TWO MOLD CAVITIES PATTERN PLATE

Approach 6 of the gating and feeding system for two mold cavities pattern plate with three internal chills in the bottom part of the mold cavity. In the spot where three internal chills were added, in comparison with the approach 5, the solidification time decreased, and the solidification time of the feeders 1 and 2 remains. Thus, porosity B and D were removed. However, the porosity A remains as being 10% and the porosity C increased up to 4%.

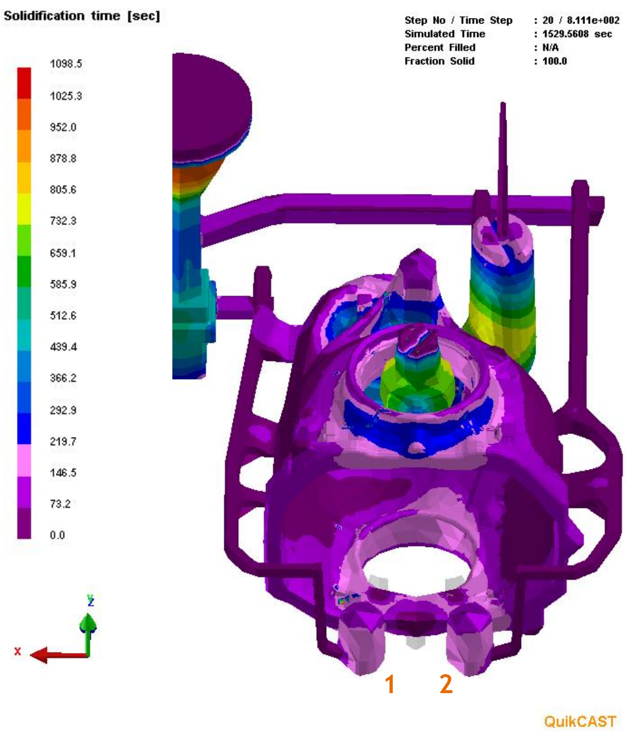

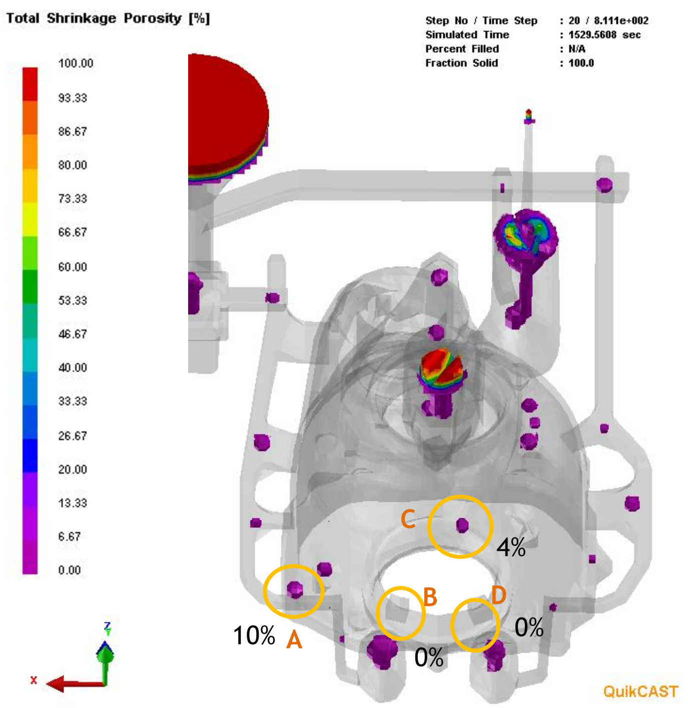

ANNEX VI –INTERSECTED SECTION OF THE FEEDER 4 WITH THE CORE PRINT

Representation of the intersection of the feeder with the top core print in the mold cavity B.

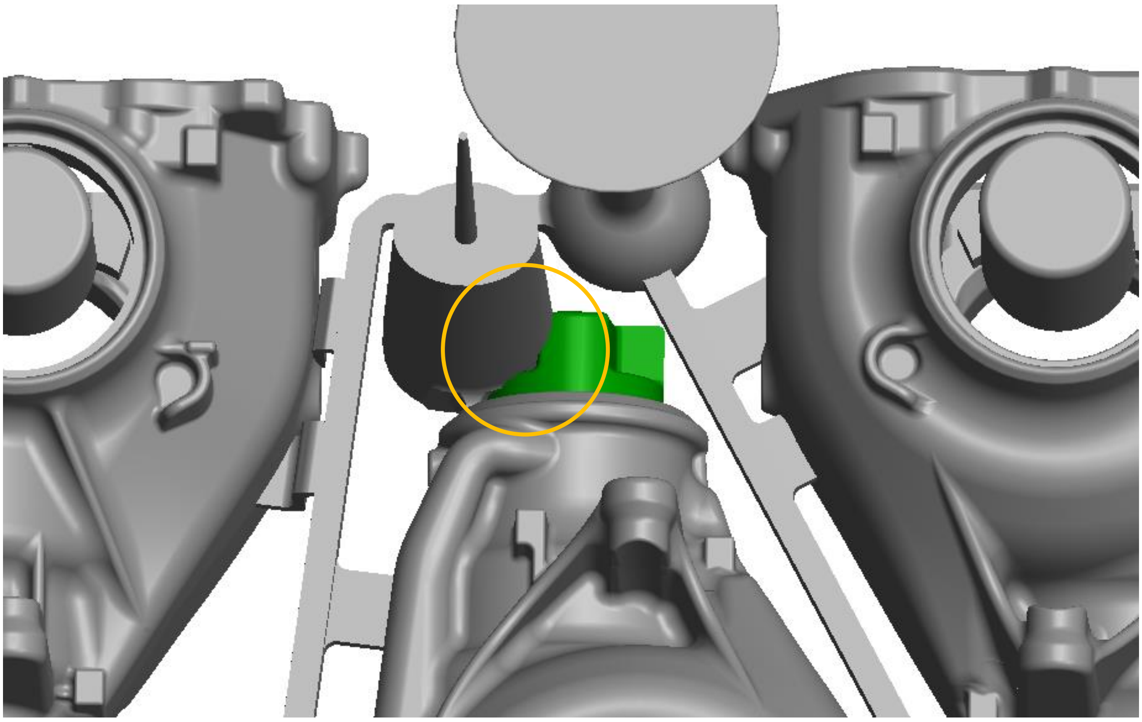

ANNEX VII – RESULTS OF NO USE OF CHILLS IN THE BOTTOM PART OF MOLD CAVITY A (THREE MOLD CAVITIES PATTERN PLATE)

Approach 1 of the gating and feeding system for three mold cavities pattern plate, where three internal chills were placed on the bottom part of mold cavities C and B. The mold cavity A has a total porosity of 100% in the bottom part of the casting, which does not happen in the mold cavities B and C, which have porosities below 1%.

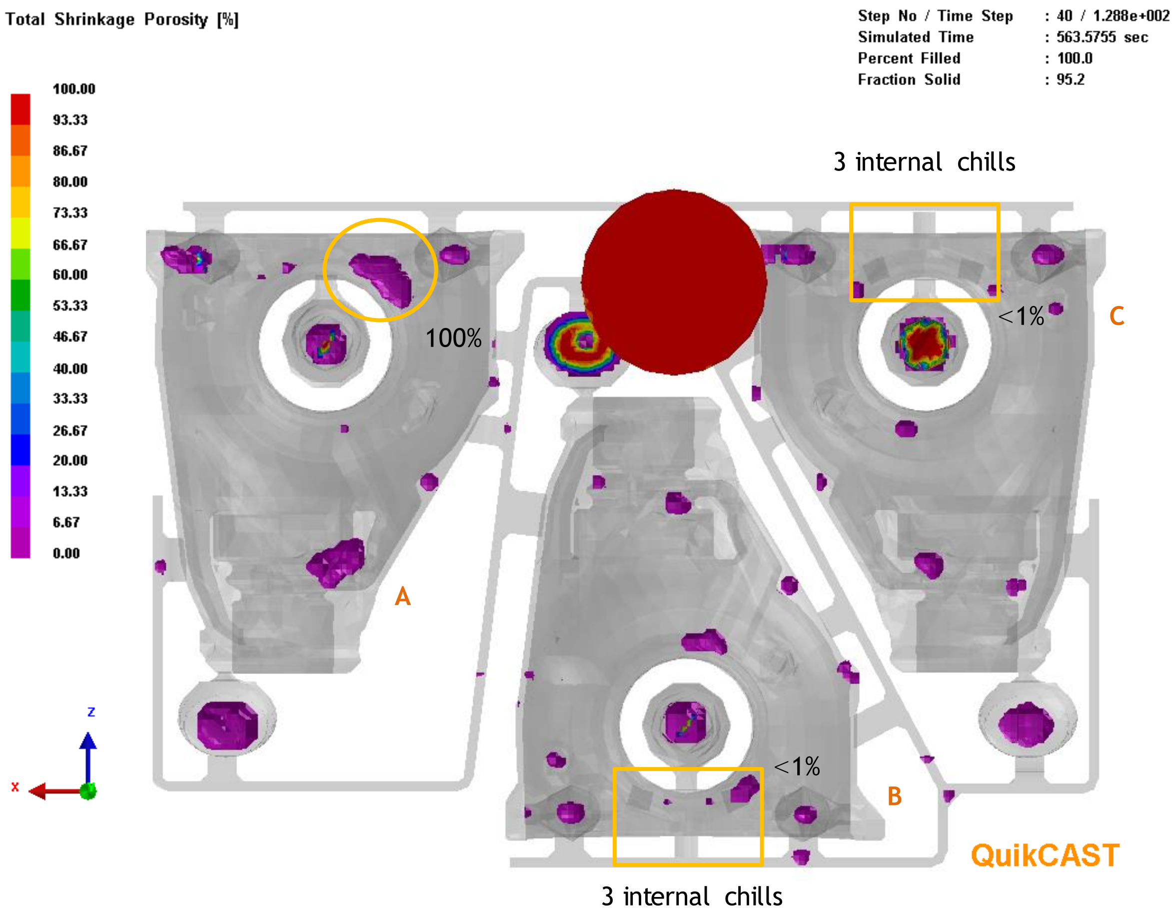

ANNEX VIII – THERMAL GRADIENTS AT MOLD CAVITY C IN APPROACH 3 FOR THREE MOLD CAVITIES PATTERN PLATE

Thermal gradients of approach 3 of the gating and feeding system for three mold cavities pattern plate filled at 45.6%. Here the highlighted runner's and gate's section do not fill the mold cavity C, even with their section increase.

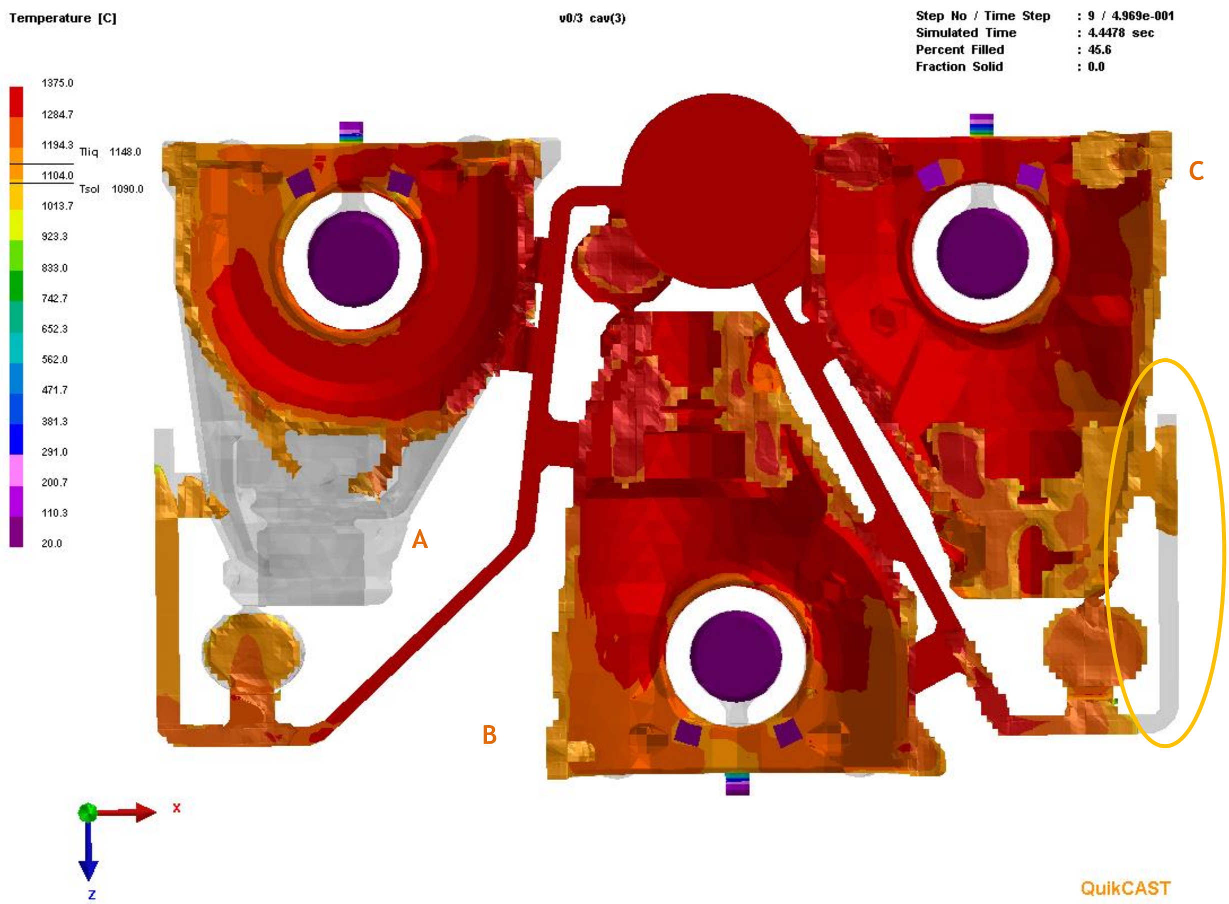

ANNEX IX – RESULTS OF APPROACH 4 FOR THREE MOLD CAVITIES PATTERN PLATE

Predicted porosity of approach 4 of the gating and feeding system for three mold cavities pattern plate. At mold cavity A was added one internal chill, which produce a 44% of porosity. In the mold cavity B, no difference was made in comparison with approach 3, where 30% of porosity was obtained. At mold cavity C, the feeder 4 was not used, where 100% of porosity was reached.

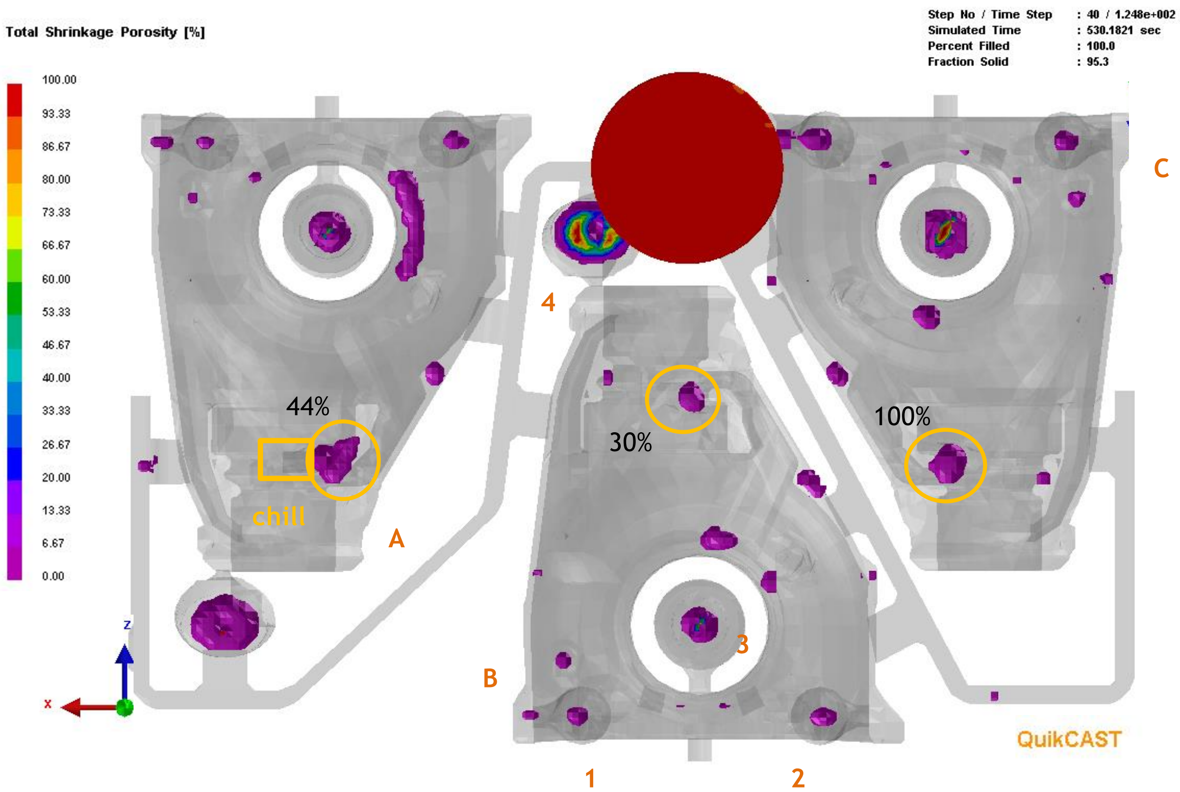

ANNEX X – EFFECT OF SHOOTING PRESSURE ON PREDICTED VOIDS DENSITY AT CORES 5 AND 6

Effect of shooting pressure in the predicted voids after core blowing simulation using nozzle 5.

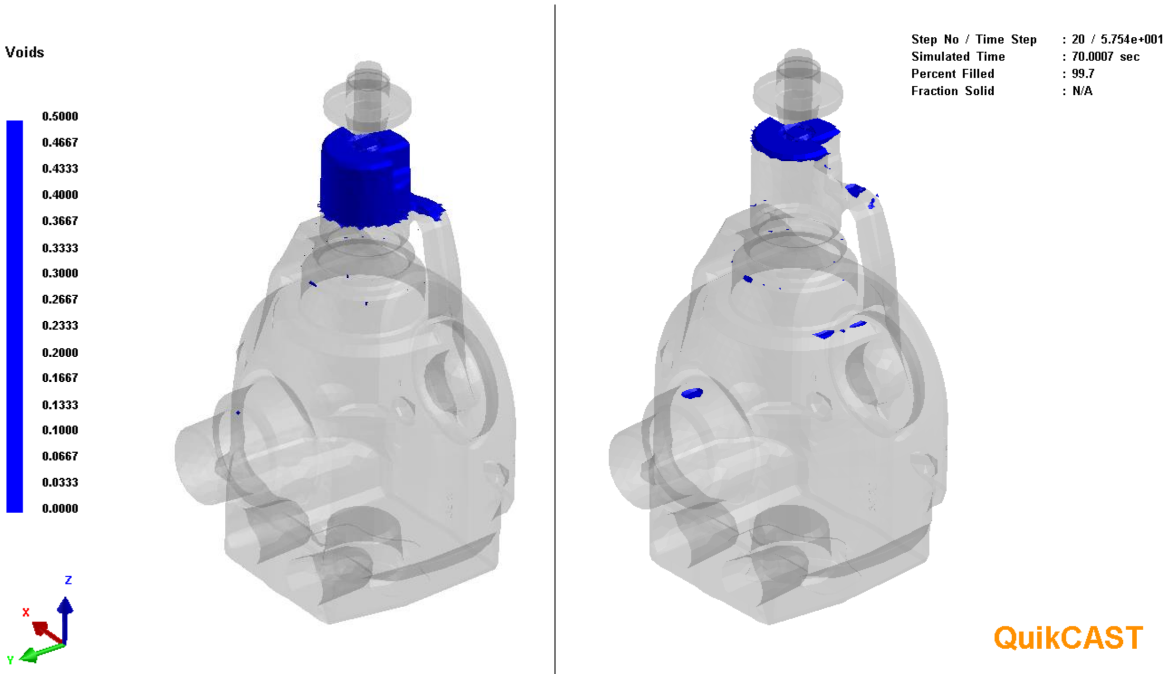

Minimum pressure

Maximum pressure

Effect of shooting pressure in the predicted voids after core blowing simulation using nozzle 6.

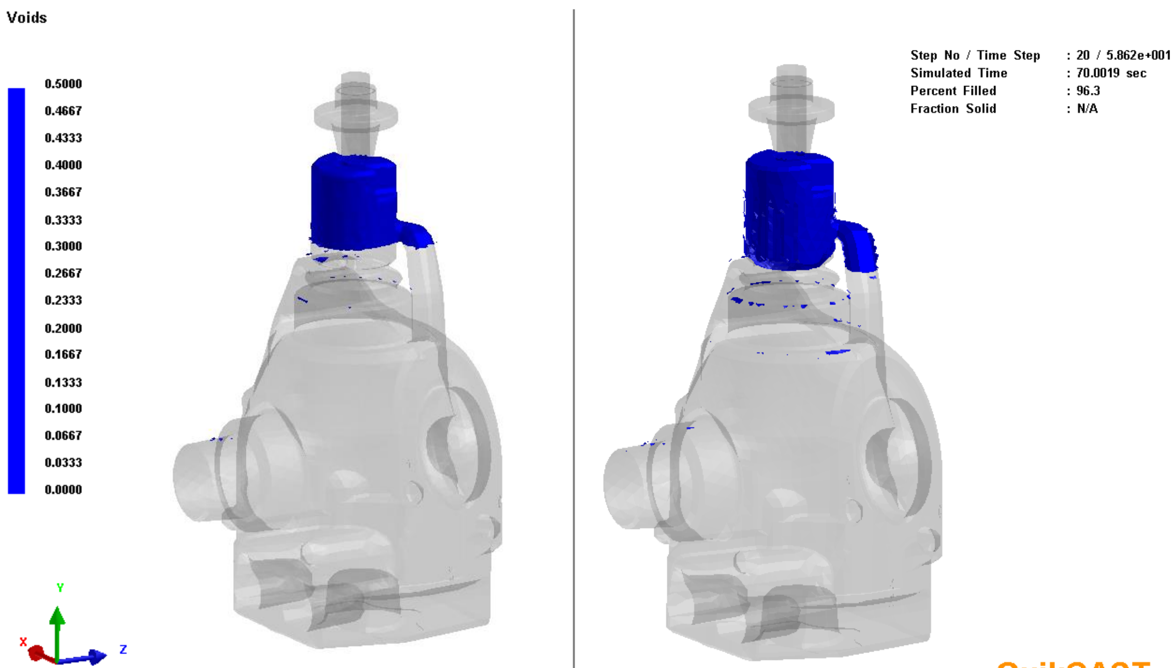

Minimum pressure

Maximum pressure